Auxin-mediated Gravitropism of *Arabidopsis thaliana*

Katelyn Anne Sageman-Furnas

Submitted in accordance with the requirements for the degree of

Doctor of Philosophy

The University of Leeds
School of Biology
Centre for Plant Sciences

September 2016

The candidate confirms that the work submitted is her own and that appropriate credit has been given where has been made to the work of others.

For my father, for teaching me that with enough love and effort, even the simplest ingredients will make a perfect dish. I think you were talking about tomato sauce, but I think that also applies to science.

And finally, for my mother, who does the best she can, always.

Acknowledgements

I feel like I could write a (longer) thesis describing the gratitude I have for everyone who has helped me perform the work here and write this thesis! I am so privileged to have amazing co-workers, friends, and family.

Firstly, I would like to thank Stefan Kepinski for giving me a chance to come to the UK and join his lab. Of course this thesis would have been impossible without your help and advice! I've been very lucky to have such a patient, curious supervisor to guide me along the way.

To everyone else in the Kepinski lab, thanks for all the help! I would like to give so many thanks to Martin for all of your help with everything as usual! I wouldn't know my P5P2s from my P1P5rs without you. I have also enjoyed our interesting political conversations when my plants were being far from phenotypically interesting. Ryan and Rob thank you for helping me while I've been abroad. I would like to thank Séverine for helping with the qPCR experiments in this thesis. Marta, thank you for your sunny disposition and for reading every, single, page of this thesis. Finally, Suruchi, thanks for all of your help in the lab in the beginning and your support from afar towards the end! I would like to thank the undergraduates I worked with, Jess and Lauren with their work on the Arabidopsis shoot experiments and George for the work with other species.

I have been fortunate to work with two other labs during the course of this project. I would like to thank Chris Wolverton for allowing me to use his ROTATO and for all of his useful conversations and humor. I would also like to thank Jiří Friml and Matyáš Fendrych for their help with the *PIN* part of this project and for the (too) many beers.

Also a particular thank you to Tobias Baskin and Heidi Rutschow for giving me a chance to work in your lab so many years ago and for introducing me to plants and Stefan.

I would like to thank my best friends in Leeds and Göttingen. You all have made this California transplant feel at home on this rainy island. Laura Cross, thank you for the so many coffees and late nights! I would like to thank my dear Hugh Xu for being the very best friends to me these past few years. Grace Hoysted, thanks for everything, and I am so glad we went through it together! Sarah Eiteljörge, you and the Göttingen sunshine have definitely saved some of my sanity during the writing process.

And almost finally, so many thanks to my two big sisters and big brother! You have given me a sense of home wherever I am in the world. Mel and Jeffjeff, your practical advice and support has always kept me on track. Ally, thanks for suggesting that perhaps I could aspire to slightly bigger things than being a window washer, as cool as that might be.

And finally, I would like to thank my husband (and my eternal editor) Andrew, whose genuine kindness and humor has made even the days when the PCR just won't work for the 15th time, into gifts.

Abstract

Gravitropism is an important tropic response in plants that allows the ability to respond to changes in orientation and to modify growth to maintain specific patterns of growth with respect to gravity. Gravitropism is controlled by a group of hormones called auxins. There are three steps that contribute to the response: the perception of the gravity signal, the differential flow of auxin, and the transcriptional control of auxin related genes. The so-called sine law of gravitropism states that the magnitude of a plants' gravity response is proportional to the sine of the angle between the organ axis and the vertical. This model has since been described in many species, but the molecular basis of the mechanism remains unclear. Using kinetics experiments, auxin-mediated gravity response in Arabidopsis roots was confirmed to be angle-dependent. The auxin reporter *R2D2* was used to quantify previously unreported angle-dependent auxin asymmetries that likely govern gravity response in primary and lateral roots. The subcellular localisation of auxin efflux carriers, known as PINs, were quantified in the gravity-sensing cells of primary roots. It was found that as the angle of stimulation increases, PINs are targeted more to the basal plasma membrane. Evidence for angle-specific contributions of PINs was also found. Other components of gravity response were also considered. The role of auxin signalling in the gravity-perception and response in Arabidopsis roots and shoots was investigated using gravity-sensing cell- and epidermal cell-specific promoters expressing mutated versions of Aux/IAA and ARF auxin signalling regulators. Gravitropism assays with these transgenic lines indicate that auxin signalling is necessary in the gravity-sensing cells of the primary root, however, its exact role is still unclear.

Table of Contents

List of Tables

List of Figures

Abbreviations

ANOVA – Analysis of variance

ARFs – AUXIN RESPONSE FACTOR

ATS – Arabidopsis thaliana salts

Aux/IAA – AUXIN/INDOLE-3- ACETIC ACID

AuxRe – Auxin response element

cDNA – Complementary DNA

CEZ – Central elongation zone

CIAP – Calf intestinal alkaline phosphatase

DEZ – Distal elongation zone

DNA –Deoxyribonucleic acid

dNTP – Deoxyribonucleotide

DZ – Differentiation zone

EDTA – Ethylene diaminetetraacetic acid

EE – Early endosomes

EZ – Elongation zone

GC – Guanine-cytosine

GFP – Green fluorescent protein

GSA – Gravitropic setpoint angle

H – Hair

HSD – Honest significant difference

IAA – Indole-3-acetic acid

LB – Luria broth

LRC – Lateral root cap

MR – Middle region

NASC – Nottingham Arabidopsis Stock Center

NH – Non-hair

NPA – 1-N- Naphthylphthalamic acid

PAT – Polar auxin transport

PCR – Polymerase chain reaction

PINs – PIN-FORMED proteins

PM – Plasma membrane

QC – Quiescent centre

RT-qPCR – Quantitative Real Time PCR

RC – Root cap

RE – Recycling endosome

RNA – Ribonucleic acid

RPM – Revolutions per minute

SAM – Shoot apical meristem

s.d. – Standard deviation

s.e.m. – Standard error of the mean

TGN – Trans-golgi network

WT – Wild type

Chapter 1
General Introduction

1 General Introduction

A widely conserved trait in plants is the ability to respond to environmental changes through differential growth. These responses, called tropisms, have been formally studied since 1880 when Darwin and his son Francis published *"The power of movement in plants"* (Darwin, 1880). Gravitropism is crucial for establishing the fundamental parameters of the plant form. Plants' ability to grow and respond to their environment is responsible for the universal phenomenon of shoots growing up and roots growing down. Gravitropism has been characterised and studied for over 200 years (Knight, 1806), yet its complex underlying mechanism is still not fully understood. Many advances have been made, and researchers have been able to understand parts of the puzzle with new genetic, microscopy, and imaging tools. The gravitropic response has three parts: sensing the direction of gravity, transmission of the gravity signal, and generation of tropic growth (Morita and Tasaka, 2004). Our current understanding of gravitropism as a whole relies on two theories, the starch-statolith hypothesis and the Cholodny-Went theory.

1.1 Gravity Perception

For a plant to be able to respond to a change in orientation, it must first perceive this change within the gravity field. Two theories have been put forward to explain how plants sense gravity. The gravitational pressure theory for gravity sensing suggests that gravity causes the protoplast to settle within the extracellular matrix, resulting in a differential tension and compression between the plasma membrane and the extracellular matrix at the top and bottom of the cell, respectively. Supposedly, these differential pressures activate the gravireceptors at the top and the bottom of the cell, which are suggested to be integrin like proteins that span the plasma membrane-extracellular matrix junction (Staves et al., 1997). This theory has been based mostly on studies involving the alga, *Chara,* intermodal cells (Staves et al., 1992). Studies in rice involving changing the density of the external medium with impermeant molecules, which should have no effect on statoliths, has shown to reduce the rate of gravitropism (Staves et al., 1997).

The most widely accepted hypothesis explaining how plants sense gravity is the starch-statolith hypothesis. This hypothesis states that dense, starch-filled plastids (amyloplasts) in specialised cells (statocytes) of an organ sediment through the cytoplasm in response to reorientation of the cells (Iversen and Rommelhoff, 1978; Sack et al., 1985). In roots, the statocytes are located in the columella cells of the root tip (Dolan et al., 1993), while the statocytes of the shoot are located in the endodermal of the bundle sheath cells (Fukaki et al., 1998). This theory has been substantiated through genetic, laser ablation, and imaging techniques. Gravitropic responses of starch deficient mutants such as the *phosphoglucomutase mutant (pgm1)* are attenuated (Kiss et al., 1996; Wolverton et al., 2011) (also Figure 7.1). In shoots, an amyloplast-less mutant (endodermal-amyloplast less 1), which contains no intact amyloplasts in the shoot endodermis, but has normal amyloplasts in the columella cells, exhibited normal root gravitropism but defective shoot gravitropism (Fujihira et al., 2000; Saito et al., 2005). Furthermore, laser ablation studies have furthered Darwin's first experiments with root cap removal. Laser ablation of the central columella of the root leads to an attenuated gravity response (Blancaflor et al., 1998). Finally, amyloplasts have been visualised sedimenting in graviresponding maize roots (Sack et al., 1985).

Upon sedimentation of the statoliths, a signal transduction cascade begins within minutes, most of which is not very well understood (Sato et al., 2015). This signalling cascade includes changes in the cytosolic pH of the root cap cells (Fasano et al., 2001; Scott and Allen, 1999), changes in pH following Ca^{2+} waves in the Arabidopsis root elongation zone (Toyota et al., 2013; Monshausen et al., 2010), and dynamic changes in other molecules such as reactive oxygen species (recently reviewed in (Baldwin et al., 2013)).

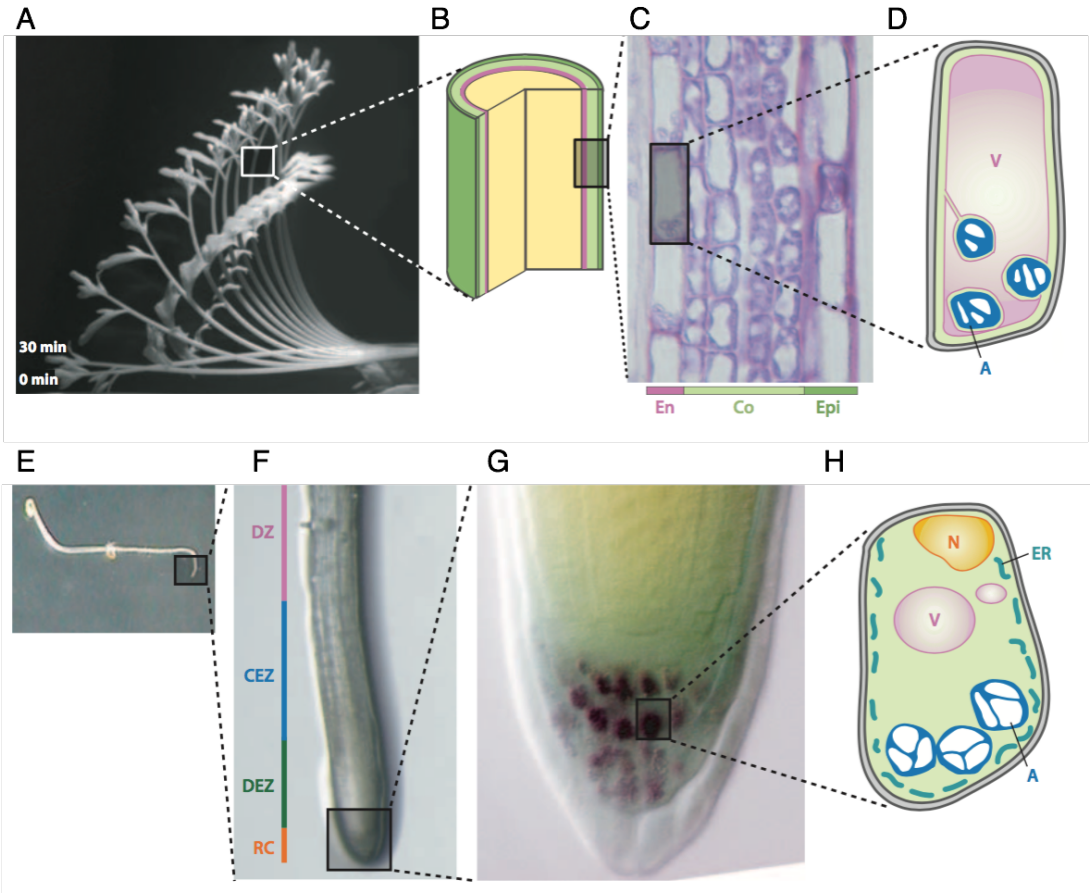

Figure 1.1 Shoot and root structure and statocytes of both organs (adapted from Morita, 2010).
(A) A 5-week-old gravistimulated inflorescence stem (Columbia WT) that was imaged every 10 minutes for 100 minutes. Image shown is composite of those images. (B) Schematic structure of stem tissue, showing the position of the endodermis (pink) (C) Longitudinal section of a stem stained with toluidine blue and observed by microscopy. The epidermis (Epi), cortex (Co), and endodermis (En) are visible. (D) Schematic structure of the endodermal cell, showing the vacuole (V) and amyloplast (A). (E) A three-day-old, gravistimulated dark-grown seedling showing gravity response. (F) Root of a three-day-old seedling dissected from the tip, with the root cap (RC), distal elongation zone (DEZ), central elongation zone (CEZ), and differentiation zone (DZ) visible. (G) Structure of the primary root cap, stained with IKI (iodine-potassium iodide) solution, showing stained amyloplasts. (H) Schematic of the columella structure showing the nucleus (N), vacuole (V), amyloplast (A), and the endoplasmic reticulum (ER).

1.2 The Cholodny-Went Theory

The Cholodny-Went theory of tropic response provides the foundation of the differential growth which changes the organs orientation in the gravity field. The model, first proposed independently by both Cholodny and Went in 1927, states that following a tropic stimulation of a plant organ, the asymmetric lateral transport of the plant hormone auxin is triggered. This leads to the generation of a lateral auxin gradient across the stimulated organ, resulting in tropic curvature (Went and Thimann, 1937). Indeed, when a seedling is placed on its side, auxin is transported to the lower side of the shoot and root. Auxin accumulation promotes growth in the shoot but inhibits growth in the root, resulting in curvature in both organs, but in opposite directions.

Since 1927, this model has been validated in shoots and roots in many plant species. The model was first validated by measuring lateral auxin transport in maize coleoptiles (Lino and Briggs, 1984), and Arabidopsis hypocotyls (Orbovic and Poff, 1993) during phototropic response. More recently, using the auxin response reporter *DR5* (Ottenschläger et al., 2003), lateral auxin gradients have been visualised in live, gravity responding Arabidopsis roots (Ottenschläger et al., 2003) and hypocotyls (Rakusová et al., 2011) using confocal microscopy. *DR5* is a reporter of auxin response, consisting of the synthetic *DR5* promoter (9 inverted repeats of TGTGTCTC) that drives expression of GFP (Ottenschläger et al., 2003).

Gravitropic response can be measured in Arabidopsis roots within 10 minutes of gravistimulation (Mullen et al., 2000). According to the Cholodny-Went theory, before this response can occur, amyloplasts must sediment to the new lower side of the cells, and auxin must be redirected to the lower side of the lateral root cap and epidermis where cell growth must be inhibited in those cells (shown in Figure 1.2). This leads to the root bending downwards, towards the gravity vector.

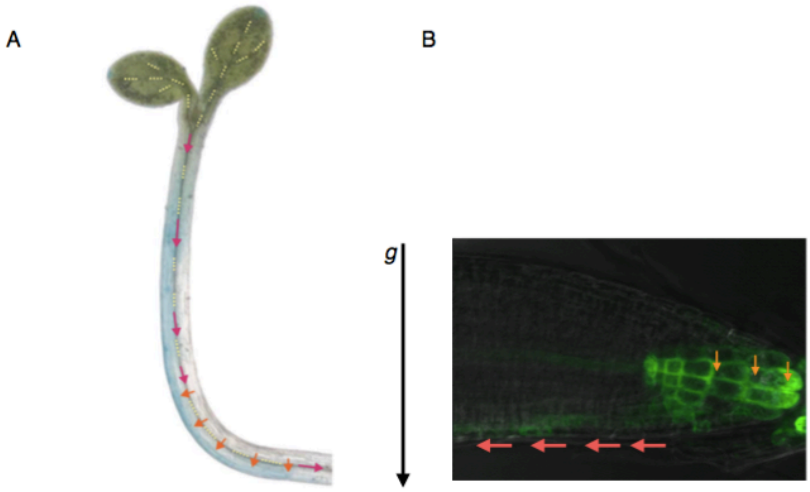

Figure 1.2 The Cholodny-Went theory of gravitropic response.
(A) Upon gravistimulation auxin is moved laterally (orange arrow) to the new lower side of the hypocotyl where auxin is growth promoting (adapted from Friml, 2003). (B) Upon gravistimulation, auxin is transported downwards in the columella (orange arrow) and along lateral root cap cells to the epidermis (pink arrows) where growth is inhibited by auxin. Auxin response is inferred using the *DR5::GFP* reporter.

1.3 Gravitropic Setpoint Angle (GSA)

In addition to primary root and shoot gravitropism, lateral branches in higher plants also respond to gravitropism while maintaining a nonvertical growth pattern that is referred to as an organ's GSA (Digby and Firn, 1995). The mechanism in which this nonvertical growth of lateral organs is maintained has been recently put forward (Roychoudhry et al., 2013). It has been shown that nonvertical growth of lateral root and shoots is maintained separately by an auxin-dependent antigravitropic offset. This antigravitropic offset is thought to operate in tension with the vertical gravitropic response, and this tension generates the nonvertical isotropic growth. This process has been shown to depend on TIR1/AFB-Aux/IAA-ARF dependent-signalling in the gravity-sensing cells (Roychoudhry et al., 2013). Mutants that are described as more sensitive to auxin, or having increased auxin response, have lateral organs that often have more vertical GSA, while mutants that are described as less sensitive to auxin, or having decreased auxin response, have lateral organs with a more horizontal GSA (Roychoudhry et al., 2013). While the underlying mechanism of GSA has begun to be uncovered, further research continues to better understand how the antigravitropic offset is regulated.

1.4 The Sine Law of Gravitropism

Just two years after Darwin's "*The power of movement in plants*" was published, Julius Sachs formulated the sine law of gravitropism: the component of gravity acting at a right angle to a plant's axis determines the magnitude of its response, i.e., the magnitude of its response is proportional to the sine of the angle between the organ axis and the vertical (Sachs, 1882). For example, when a seedling is rotated into a horizontal position its shoot and root initially show a large gravitropic response that slows as the shoot and root approach vertical. Since 1882, the sine law has been verified (with minor modifications) in maize, rice, and oat coleoptiles (Audus, 1964; Galland et al., 2002; Iino et al., 2005). The rate of gravity response in roots has also been found to depend on the sine of the stimulation angle in species such as *Lepidium savitium* (cress) (Larsen, 1969) and *Lens culinaris* (lentil) (Perbal, 1974). Most research cites approximately 130° as being the stimulation angle which leads to the greatest gravitropic response (Audus, 1964; Galland, 2002; Perbal, 1974; Larsen, 1969). Even beyond the plant kingdom, sine law has been described, for example, in the fungus *Phycomyces blakesleeanus* (Galland et al., 2002). While many researchers report that gravitropism in several species follows a sine law, a study found

no dependence between the rate of curvature and stimulation angle in maize roots (Barlow et al., 1993).

Recently, Arabidopsis has been used to investigate this so-called sine law of gravitropism. A new method has been introduced using a feedback system to measure the gravitropic response of an Arabidopsis root (Mullen et al., 2000). This feedback system comprises of a rotating stage platform and a video digitiser system which allows the experimenter to maintain a constant angle of gravistimulation over long time periods. In these experiments, the gravitropic output is measured every minute and recorded over several hours. Using this method, it was found that latency period before a gravitropic response is only 10 minutes, instead of the previously published 30 minutes (Mullen et al., 2000), suggesting that physical manipulation slows the onset of gravity response. Experiments using this method confirmed that the rate of root curvature depends on stimulation angle, although the stimulation angle which yielded the maximum response was found to be 90° using this system.

Although the sine law of gravitropism has been described in Arabidopsis and other species, its underlying mechanism has yet to be explained.

1.5 Auxin Transport

Since Cholodny-Went theory was proposed, there have been many advances in understanding how auxin is moved laterally during tropic responses, due to the discovery of the auxin efflux carriers, known as PINs, and AUX1, the auxin influx carrier (Marchant et al., 1999). IAA is the major form of active auxin and is present in its protonated form in the apoplast, where it is able to diffuse passively through the plasma membrane. However, the asymmetric auxin distribution necessary to regulate growth and development is generated by polar active transport (PAT), which distributes auxin in patterns often called gradients (Gälweiler et al., 1998; Benkova et al., 2003; Grieneisen et al., 2007). These gradients are actively maintained and dynamically regulated by active influx and efflux. This is achieved in Arabidopsis and in general higher plants by several specific auxin influx and efflux carriers.

AUX1

Auxin is transported into cells by the AUXIN1/LIKE AUX1 (AUX/LAX) family of transmembrane proteins (Marchant et al., 1999; Swarup et al., 2008). The *auxin resistant 1* mutant (*aux1)* was first identified in a screen for resistance to the application of the exogenous synthetic auxin 2,4-D (Pickett et al., 1990). These transmembrane proteins are similar to amino acid permeases, which are a group of proton gradient-driven transporters (Marchant et al., 1999). Currently, there is genetic and biochemical evidence of four influx carriers that have been identified in Arabidopsis, with AUX1 and LAX3 having been shown to mediate IAA uptake when expressed in Xenopus oocytes (Swarup et al., 2008). These auxin influx carriers are either polarly or apolarly localised in a cell-dependent manner and are assumed to act as H^+/IAA^- symporters (Yang and Murphy, 2009). The most studied member of the AUX1/LAX family, AUX1, has been found to antagonise the localisation of auxin efflux carriers (Swarup et al., 2001). Loss-of-function mutations in the *AUX1* gene lead to a reduced rate of carrier-mediated auxin transport that confers an agravitropic root phenotype (Marchant et al., 1999). *LAX3* is known to facilitate lateral root emergence, and roots with loss-of-function mutations in both *aux1* and *lax3* lack lateral roots (Swarup et al., 2008).

PIN-FORMED (PINs) Proteins

The investigation of several agravitropic Arabidopsis mutants such as *agravitropic 1* (*pin2*) and *pin-formed 1* (*pin1*) (Okada et al., 1991) have led to the identification of the auxin efflux carriers, named PIN-FORMED proteins (PINs). Molecular cloning of the *PIN1* gene revealed that *PIN1* encodes a transmembrane protein that is similar to bacterial and eukaryotic proteins (Gälweiler et al., 1998). The loss-of-function of mutants of *pin2* (Müller et al., 1998) and *pin3* (Friml et al., 2002) confer an agravitropic phenotype. Mutations in these genes also cause defects in organ initiation and phylotaxy which can be phenocopied by drug-induced inhibition of auxin efflux, such as the addition of 1-N-Naphthylphthalamaic acid (NPA).

Eight members of the PIN protein family have been identified in Arabidopsis and are commonly referred to as *PIN1* through *PIN8* (Vieten et al., 2007; Zazimalova et al., 2007). *PIN*s such as *PIN5*, *PIN6*, and *PIN8* have a reduced middle hydrophilic group and are thought to regulate the auxin exchange between the endoplasmic reticulum and the cytosol (Mravec et al.,

2009). The rest of the PINs, PIN1–PIN4 and PIN7 proteins are localised to the plasma membrane where they efflux auxin out of the cell. These canonical, plasma membrane-localised PINs, consist of two transmembrane regions separated by a long hydrophilic loop.

Since the direction and magnitude of auxin flow is crucial to so many developmental and directional growth processes, together with tropic growth, the control of auxin flow must be specific to both tissues and developmental stages. Through genetic and expression studies it has been found that the different members of the PIN family have tissue- and development-specific patterns (Vieten et al., 2005). Five of the eight PIN members have been shown to be expressed in the root cap and direct auxin flux throughout the primary root during gravity response, summarised in Figure 1.3A. Some of these *PIN*s are partially functionally redundant and are found to be upregulated in some *PIN* mutants such as the upregulation of *PIN1* in a *pin2* mutant (Vieten et al., 2005). Recently, PIN1 has been found to be ectopically expressed in the gravity-sensing cells in the *pin3* mutant and PIN1's expression domain is regulated by auxin (Omelyanchuk et al., 2016). This apparent redundancy might enable the stabilisation of auxin gradients and could contribute to the robustness of the auxin transport system.

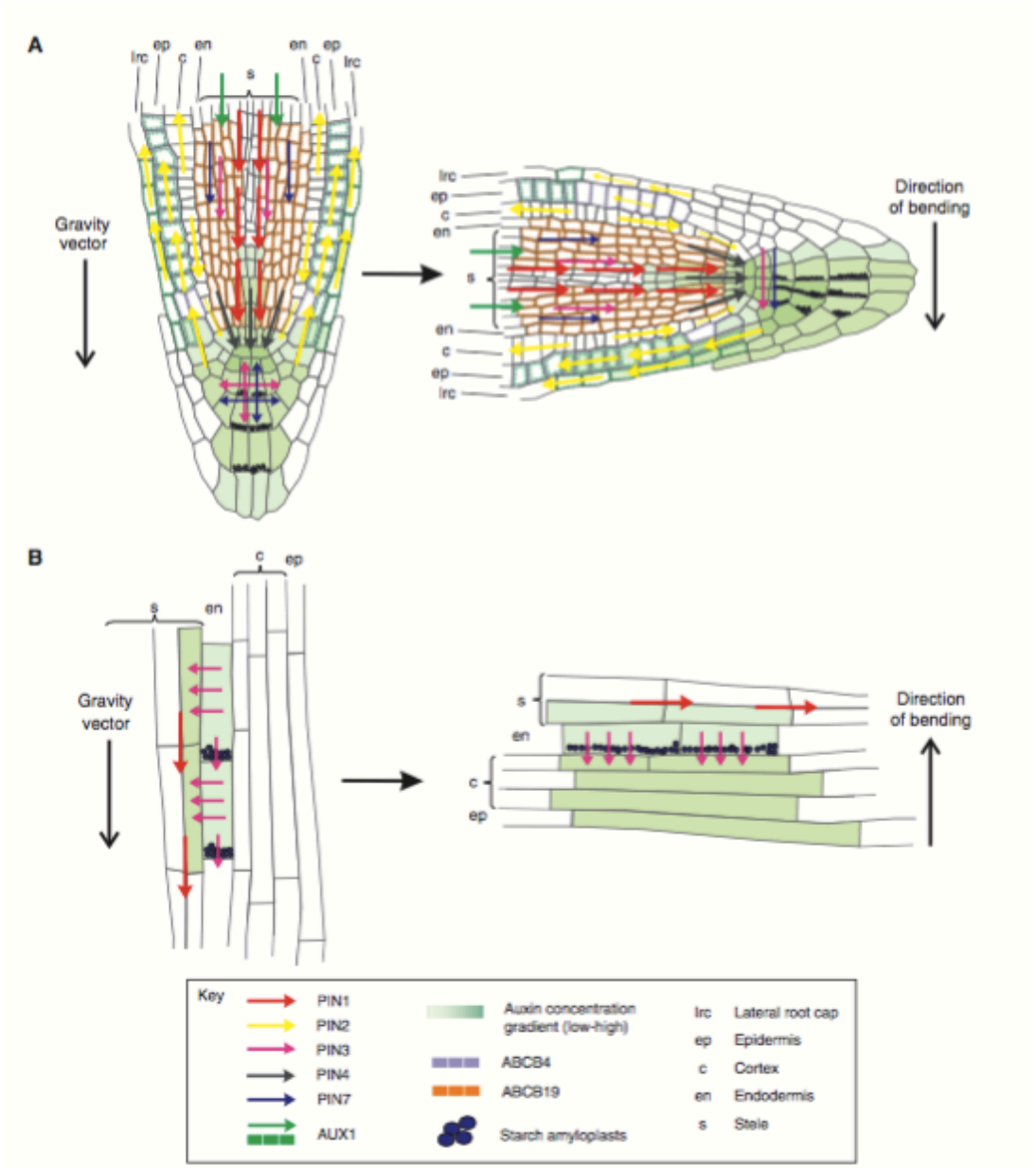

Figure 1.3 Auxin flow during gravity response in roots (A) and shoots (B) (taken from Petrasek and Friml 2009).
(A) Root gravitropism. In the columella, PIN3 is relocalised from a nonpolar distribution towards the new lower side after gravistimulation. Auxin is redirected to the lower side of the root tip and is then transported farther to the elongation zone by PIN2 and AUX1. There, it inhibits cell elongation and results in downward bending of the root. (B) Shoot gravitropism. In the endodermis, PIN3 relocalises to the new lower side of the gravity-sensing cells and redirects auxin to the outer cell layer, the epidermis, where auxin promotes shoot elongation. This results in the shoot bending upwards.

Regulation of auxin transport

Since the presence of auxin gradients have been shown to be vital to development and tropic responses, carrier-mediated transport of auxin is highly regulated at several levels (reviewed in (Grunewald and Friml, 2010)). The abundance of PINs is regulated at both the level of transcription and degradation (Sieberer et al., 2000). Furthermore their subcellular localisation is regulated by subcellular trafficking and targeting of the auxin carriers to a specific position in a cell (i.e., apical or basal); and by transport activity of the carriers, which is regulated through post-translational modification of the proteins, although less is known about this process (Willige et al., 2013).

Regulation of PIN abundance

The transcription of all known carrier proteins (PIN, ABCB and AUX1/LAX) is influenced by an auxin-triggered TIR1-signalling cascade (reviewed in (Petrasek and Friml, 2009)). *PIN* genes that are known to be upregulated by auxin treatment are upregulated in a tissue and *PIN* specific manner (Vieten et al., 2005). *PIN*s *1–7* are all upregulated the root in response to auxin treatment, with *PIN*s *1*,*3*, and *7* being highly upregulated (Vieten et al., 2005). These genes do not appear to be upregulated in the hypocotyl upon auxin treatment, further confirming that *PIN*s are regulated by auxin in a tissue specific manner (Vieten et al., 2005). *PIN* expression is dynamic during auxin transcriptional response, and during developmental stages (reviewed in (Vieten et al., 2007). Recently, *PIN3* and *PIN7* expression have been found to be regulated by a transcription factor FOUR LIPS (FLP) and its paralogue MYB88 (Wang et al., 2015). Finally, the abundance of PIN2 protein has been shown to be controlled by degradation via the vacuolar targeting pathway (Kleine-Vehn, Leitner, et al., 2008). In this control by degradation, the activity of an auxin cellular signalling pathway is required (Baster et al., 2012).

Subcellular trafficking and targeting of PINs

Current data suggests that the subcellular trafficking of PINs is the primary factor driving PIN polarity within the cell. It was first demonstrated that PINs are continuously internalised into vacuoles by visualizing PINs with the endocytic tracer FM4-64 (Geldner et al., 2003; Paciorek et al., 2005). It was

next shown that PIN proteins can be taken from the recycling endosome (RE) back to the plasma membrane (PM) in plants. When plant cells are treated with the fungal toxin, brefeldin A (BFA), PINs are internalised into compartments referred to as BFA bodies (Geldner et al., 2003). When cells are treated with BFA, trafficking from the RE to the PM is blocked, due to the inhibition of ADP-ribosylation factor guanine-nucleotide exchange factors (ARF-GEFS). These ARF-GEFS are necessary for the formation of coated vesicles important in various trafficking processes in the endomembrane system (Geldner et al., 2003). More recently, PIN cycling was demonstrated directly by tracking PINs using a photo-convertible EosFP fluorescent reporter (Dhonukshe et al., 2007).

The constitutive endocytosis of PIN proteins is dependent on the coat protein clathrin (Dhonukshe et al., 2007) and their recycling and targeting to different faces of the plasma membrane are pathways that occur in parallel, within the same cell, but are molecularly distinct. Basal targeting of PINs is carried out in a ARF-GEF mediated way that is dependent on the protein GNOM (Kleine-Vehn et al., 2009). When cells are treated with BFA, or GNOM is genetically inhibited, basal cargoes are recruited in the apical pathway. *gnom* mutants demonstrate severe developmental defects and GNOM has been found to co-localise to the basal plasma membrane. In the same set of experiments a putative GNOM-independent apical PIN recycling pathway was discovered that is less sensitive to BFA (Kleine-Vehn, Dhonukshe, et al., 2008).

Phosphorylation status and targeting

Not only endocytic cycling, but specific polarity signals within the protein sequence can determine the localisation of the protein at polar domains (Wisniewska et al., 2006). Furthermore, a mutation in the hydrophilic loops of PIN1 causes a basal-to-apical shift in its localisation (Wisniewska et al., 2006). Analysis of earlier investigated Arabidopsis mutants that have phenotypes typical of altered auxin transport such as *roots curl in NPA (rcn1)* and *pinoid (pid)* have led to the discovery of a regulatory subunit of PROTEIN PHOSPHATASE 2A (PP2A) (Deruère et al., 1999) and the serine/threonine protein kinase PINOID (Christensen et al., 2000) that are involved in the regulation of apical/basal polarity of PIN proteins.

The PID protein encodes a member of the AGCVIII family of protein kinases (Christensen et al., 2000). Its overexpression and/or disruption of PP2A activity (Michniewicz et al., 2007) leads to a basal-to-apical switch of PIN1, PIN2, and PIN4 (Friml et al., 2004). Conversely, the *pid* mutant exhibits a apical-to-basal polarity switch of PIN1 in the shoot apical meristem (Friml et al., 2004). This observation further confirms the role of PID in PIN polarity determination. Evidence suggests PID and its homologs directly phosphorylate PIN protein hydrophilic loops at three highly conserved motifs (Michniewicz et al., 2007; Zhang et al., 2010). PID's suggested functional antagonist, PP2A, was first isolated in a forward genetic screen for altered response to the PAT inhibitor NPA (Garbers et al., 1996). In a later study, severe auxin-related defects were found in multiple *pp2aa* mutants (Michniewicz et al., 2007). In addition, genetic interactions support that PP2A phosphatase function antagonises that of the PID kinases including a basal-to-apical polarity shift in PIN1 in PP2A-deficient plants (Michniewicz et al., 2007).

From these insights, a current model that PID phosphorylates PIN proteins promoting their apical targeting while PP2A antagonises this action, promoting basal PIN polarity (summarised in Figure 1.4) has been proposed. However, it is currently unclear where in the cell dephosphorylation and phosphorylation occurs. PID colocalises with PINs at the plasma membrane (Kleine-Vehn et al., 2009) while PP2A is distributed in the cell (Michniewicz et al., 2007). It is currently assumed that cargos are polarly sorted in the trans-golgi network/early endosome (TGN/EE) (Viotti et al., 2010). However, since PID is only found at the plasma membrane, it is likely that PID only affects previously targeted PIN proteins, not *de novo* synthesised PIN proteins. This idea is furthered by data suggesting that newly formed PIN proteins are distributed in an apolar manner and shortly undergo endocytic-dependent polarisation (Men et al., 2008). Although PP2A is distributed symmetrically in the cell, its place of action is still unclear (Michniewicz et al., 2007).

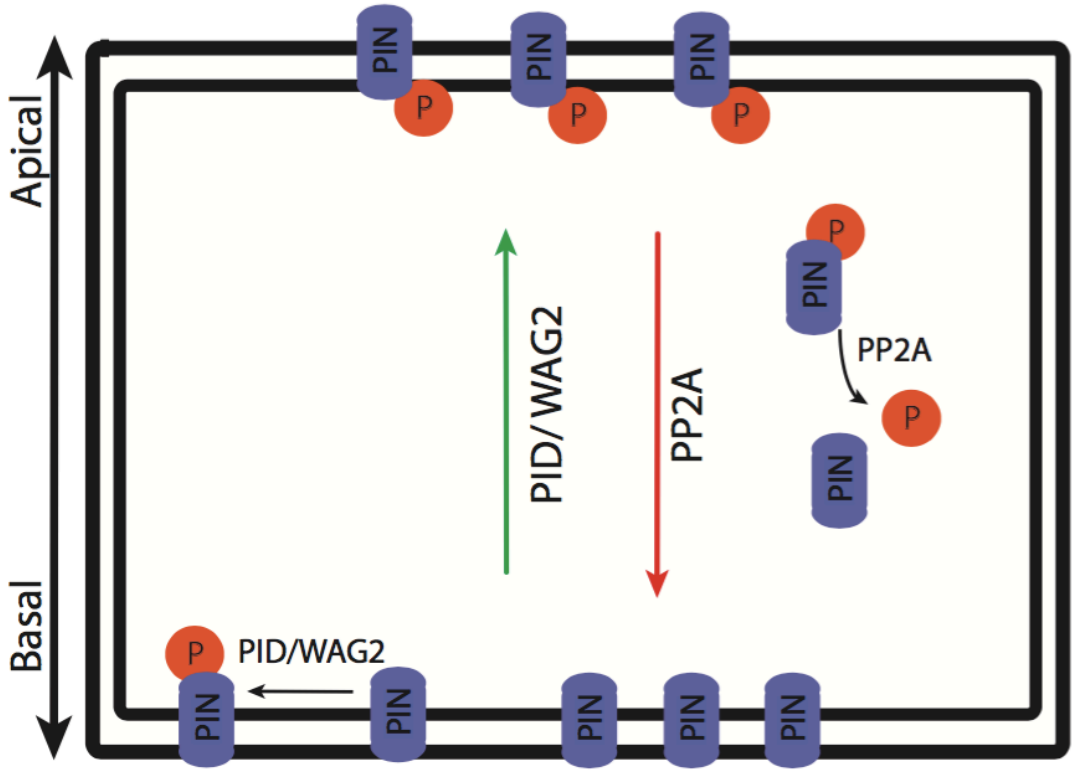

Figure 1.4 Phosphorylation status modulates PIN polarity.
PID/WAG2 and PP2A work antagonistically to modulate PIN polarity in the gravity-sensing cells. PID, which partially colocalises with PINs at the basal membrane, phosphorylates PIN proteins, targeting them to become apically localised. PP2A, which colocalises to the cytosol, dephosphorylates PINs, targeting them to the basal membrane.

Regulation of PIN activity

Another group of proteins have recently been found to modulate PIN activity from the same AGCVIII family of other protein kinases. These protein kinases, consisting of D6 protein kinase (D6PK) and D6 protein kinase-likes (D6PKL), have been implicated in the regulation of PAT (Willige et al., 2013; Zourelidou et al., 2014). The D6PKs have been found to phosphorylate plasma membrane localised PINs, but unlike PID, do not affect their polar localisations (Willige et al., 2013). Studies done in Xenopus ooyctes demonstrate that auxin is actively transported only when PINs are coexpressed with D6PK, suggesting that D6PKs act as activators of auxin efflux activity of the PIN proteins (Zourelidou et al., 2014). This is thought to occur at the basal polar domains where D6PK localises (Barbosa et al., 2014). The same auxin transport studies in Xenopus oocytes also showed that PID and its homolog WAG2 also activate PIN driven efflux (Zourelidou et al., 2014). It is currently thought that the AGCVIII family kinases have both different and potentially overlapping functions in regulating PIN activity (Willige and Chory, 2015).

It is also possible that protein-protein interactions can determine the effectiveness the auxin flow across the plasma membrane. The role of these interactions are not fully understood, but there is some evidence that the activity of enzymes STEROL METHYL TRANSFEREASE 1 (SMT1) and CYCLOPROPYL ISOMERASE 1 (CPI1), which affect the sterol composition of the plasma membrane, are necessary for the correct position of some PIN proteins (Men et al., 2008; Willemsen et al., 2003).

There are other putative factors in PIN regulation whose role has not yet been clearly defined. Importantly, the cytoskeleton may have a function in subcellular trafficking, as it is considered to provide guidance for vesicle trafficking in all eukaryotic cells. It has been shown that cytochalasin D and latrunculin B, which depolymerise actin filaments, inhibit BFA-induced intracellular PIN accumulation (Geldner et al., 2001). Further experiments show that the apical-localizing pathway, including AUX1 and apically targeted PIN proteins, is more sensitive to treatment of latrunculin B;

therefore the apical targeting pathway may be more actin-dependent than the basal targeting pathway (Kleine-Vehn et al., 2006).

Auxin based feedback regulation of PIN-mediated auxin transport

There is also evidence that auxin itself has the ability to influence the directionality and amount of auxin transport. First proposed in 1991, the canalisation hypothesis suggests self-organizing properties of PAT on the level of organs and tissues (Sachs, 1981). This feedback mechanism, in which the local flow of auxin affects the direction and the strength of auxin flux, results in a well-defined canal of cells that are able to transport auxin from the source of auxin to sink (Sachs, 1981). More recently, this hypothesis was confirmed through direct visualisation of PIN1 in wounded pea leaves (Sauer et al., 2006). When an auxin source is artificially provided, PIN1 is upregulated and polarised to create new canals to direct auxin from the new source to the sink (Sauer et al., 2006). In addition, auxin influences PIN polarities in the root apical meristem (Sauer et al., 2006). Specifically, exogenous application of auxin leads to a cell-type-specific lateral spread of PIN1 and PIN2 that is not caused by transcription, but is dependent on the Aux/IAA and ARF-dependent auxin signalling pathway (Sauer et al., 2006). Auxin is also found to inhibit endocytosis of PINs, leading to a stabilisation of PIN proteins at the plasma membrane and enhancement of auxin efflux capacity (Paciorek et al., 2005). Both endogenous and exogenous auxin also affect the abundance of PINs through PIN degradation in the vacuole (Abas et al., 2006; Baster et al., 2012) and transcriptional upregulation in a tissue- and *PIN*- specific manner (Vieten et al., 2005).

Integration of regulatory components

As previously discussed, the direction of auxin flux is crucial for plant development and tropic responses. The regulation of auxin transport is controlled at three main levels: transporter abundance, subcellular trafficking and targeting of transporters to specific positions on the membrane, and transporter activity (Petrasek and Friml, 2009). There is abundant evidence for the importance of these regulatory components. However, the location in the cell in which these processes occur and the integration of these regulatory components is still unclear. Both pharmacological and genetic studies point to the ARF-GEF GNOM pathway mediating basal polar targeting (Kleine-Vehn, Dhonukshe, et al., 2008; Steinmann et al., 1999).

Furthermore, *pp2a* loss-of-function mutant and *PID* overexpression lines demonstrate basal to apical shifts in polarity that is similar to those seen in *gnom* loss-of-function mutants (Kleine-Vehn et al., 2009). Taken together, these observations suggest that both GNOM and PID/PP2A act in an antagonistic manner and are part of the same mechanism that regulates polar PIN delivery (Kleine-Vehn et al., 2009). However, these pathways are molecularly distinct as PID does not appear to alter either GNOM localisation or activity. Furthermore, PID is still active in cells that have been treated with BFA (Kleine-Vehn et al., 2009). A plausible model to integrate phosphorylation mediated targeting and endocytic-mediated targeting is that phosphorylated PIN proteins have a decreased affinity for the GNOM-dependent basal recycling pathway and an increased affinity for the distinct apical targeting (GNOM-independent) pathway. This model, summarised in Figure 1.5, allows for different input signals to modulate the direction and magnitude of auxin flow via the regulation of PID activity and the resulting trafficking of PIN proteins.

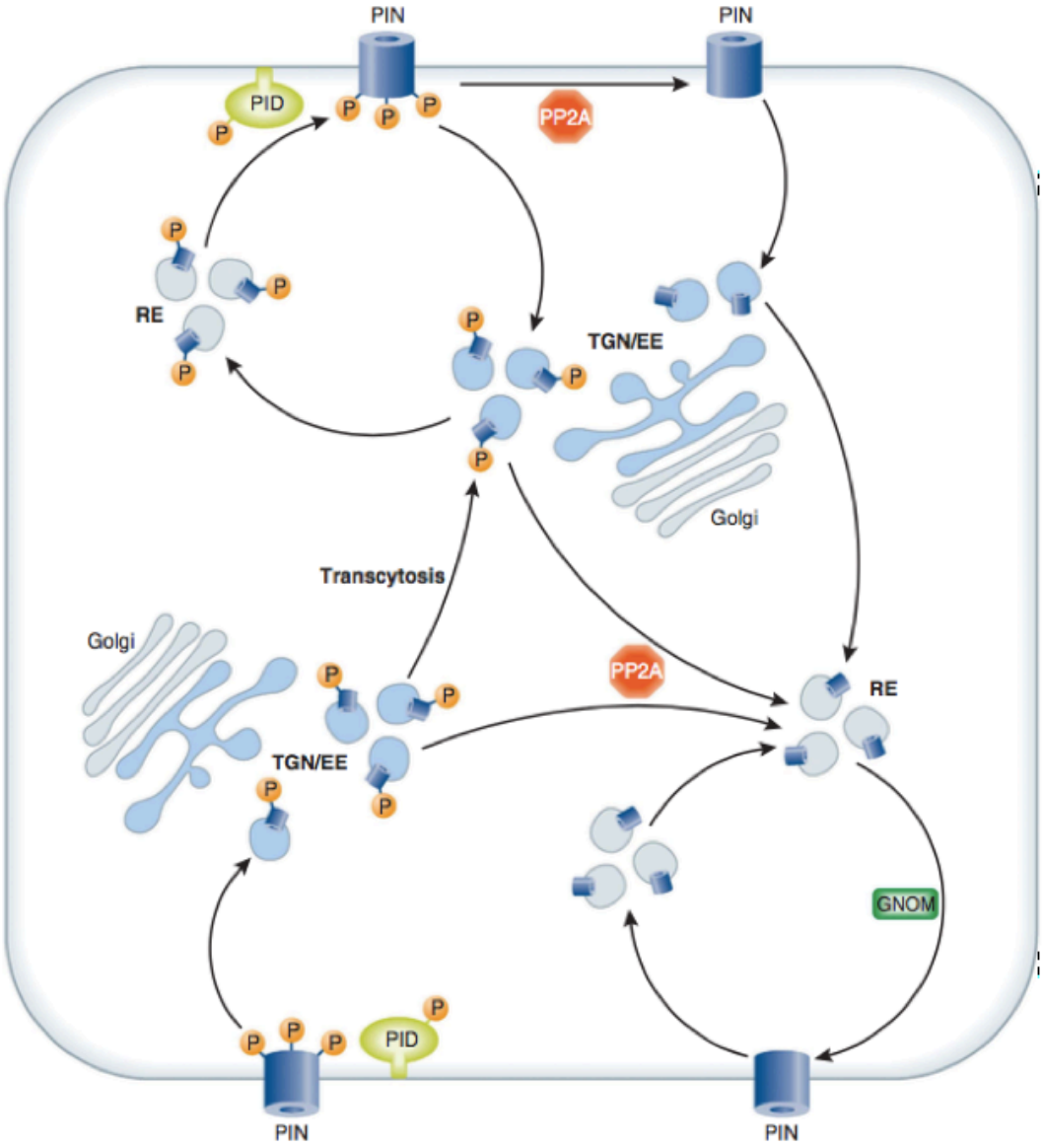

Figure 1.5 Integration of PIN regulatory components (taken from Grunewald, 2010).
Schematic representation of PIN regulatory components including transcytosis and phosphorylation-dependent polarity modulation. EE, Early endosomes; RE, recycling endosomes; TGN, trans-golgi network.

1.6 Auxin and Transcriptional Control of Auxin Response

Auxin response is cell and tissue specific

Auxins are a group of simple plant hormones that play a pivotal role in almost all aspects of plant growth and development, reviewed in (Del Bianco and Kepinski, 2010; Teale et al., 2006). As previously discussed, auxin is unique in the fact that it is transported in a very controlled and polar manner (Petrasek and Friml, 2009). Auxin maxima in both shoot and root tissues lead to developmental changes. For example, auxin maxima in the shoot apical meristem (SAM) give rise to leaf primordia, while auxin maxima in the root give rise to lateral root primordia (Scarpella et al., 2010; Dubrovsky et al., 2008). Importantly, auxin also modulates gravitropic and phototropic response in a tissue-type specific manner. A striking example of how auxin can be tissue specific is that auxin is cell growth promoting in shoots, while cell growth inhibiting in roots (Thimann, 1956). Since auxin is involved in so many developmental and tropic responses, the auxin response must be very context-specific, producing different responses depending on dose and tissue type. While the discovery of auxin and its importance dates back to the 1880s, the molecular mechanism of context-specificity still remains unclear (Del Bianco and Kepinski, 2010). The complexity of the Aux/IAA-ARF signalling system gives some clues to how context-specificity could be conferred.

*Aux/IAA*s and *ARF*s

There are two families of transcription factors known to specifically affect auxin-induced transcriptional responses, the AUXIN RESPONSE FACTORS (ARFs) and the AUXIN/INDOLE-3- ACETIC ACID (Aux/IAA) co-repressor proteins. Many of the *Aux/IAA* genes are auxin inducible and encode nuclear proteins that are very unstable (Abel et al., 1994). Their binding partners, the ARFs, are relatively more stable proteins that are also nuclear localised (Ulmasov et al., 1997; Okushima, 2005).

ARFs are known to bind DNA directly at the so-called auxin response elements (AuxREs), located in the promoters of auxin regulated genes (Ulmasov et al., 1997). AuxREs are *cis*-regulatory elements that contain a

TGTC motif that recruits ARF proteins to the DNA sequence (Ulmasov et al., 1997; Tiwari et al., 2003; Boer et al., 2014). Most of these proteins are also composed of a middle region and two other domains (Tiwari et al., 2003). The middle region (MR) is important as its sequences specify whether an ARF transcriptionally activates or represses the target gene. MRs that are glutamine-rich are known to promote transcription, while proline/serine/threonine-rich MRs repress transcription (Ulmasov et al., 1999; Tiwari et al., 2003). Of the 23 *ARF*s in Arabidopsis, only five (*ARF*s *5, 6*, *7*, *8*, and *19*) are known to be transcriptional activators (Ulmasov et al., 1999; Tiwari et al., 2003). Finally, the carboxyl terminal (c-terminal) of the ARF protein contains the so called domains III and IV that act as a pair of protein-protein interaction domains (Korasick et al., 2014). Via these domains, the ARFs form homo and heterodimers with other ARFs and with the Aux/IAAs. Under low-auxin conditions, Aux/IAAs bind ARFs via a c-terminal interaction and inhibit the transcriptional activity (Tiwari et al., 2001).

The Aux/IAAs are a family of co-repressor proteins with 29 members that have a four domain structure. They are not found to directly bind DNA but instead affect transcription of ARF-regulated genes by forming heterodimers with ARFs via domains III and IV (Tiwari et al., 2001). These co-repressor proteins bring about inhibition of activating ARFs bound to their target loci by recruiting corepressor complexes. The EAR (ERF-associated Amphiphillic Repression) repressor motif located in domain 1 interacts with proteins of the TOPLESS (TPL)/TOPLESS RELATED (TPR) family (Causier et al., 2012; Szemenyei et al., 2008). This complex also requires the recruitment of histone deactylases to induce the transcriptionally repressed state of the target genes (Szemenyei et al., 2008). Domain II of the Aux/IAA proteins contains the degron region, which is crucial to the auxin response system as it is recognised by the E3 ubiquitin-ligase complex $SCR^{TIR1/AFB}$ (Calderon-Villalobos et al., 2012; Ouellet et al., 2001). Mutations in this region lead to hyper stable Aux/IAA proteins which cause an auxin insensitive phenotype (Ouellet et al., 2001).

Auxin-mediated Aux/IAA degradation

Aux/IAA proteins are very unstable, with measured half-lives as short as 6 minutes (Abel et al., 1994), and their instability is auxin-enhanced (Gray et al., 2001). Aux/IAAs are degraded by the ubiquitin-proteasome system in

which the Aux/IAAs are targeted for degradation at the 26S proteasome by the addition of ubiquitin peptides (Gray et al., 2001; Moon, 2004). This proteasome is referred to as 26S, which is the sedimentation coefficient of the active proteasome as determined by density-gradient centrifugation analysis (Ferrell et al., 2000). The conjugation of ubiquitin to the Aux/IAA proteins is catalysed by an E3 ubiquitin-ligase complex referred to as the $SCF^{TIR1/AFB}$ (Gray et al., 2001; Gray et al., 1999). This complex contains four protein subunits: ARABIDOPSIS SKP1 HOMOLOGUE (ASK1), CULLIN-1 (CUL1), RING-BOX (RBX) and A TRANSPORT INHIBITOR RESISTANT 1/AUXIN SIGNALLING F-BOX (TIR1/AFB). The CULLIN subunit interacts with the RBX subunit to catalyse the ubiquitination reaction. The SKP1 subunit acts as a scaffold link to the CULLIN-RBX dimer (Moon et al., 2004). Specificity for both auxin and the Aux/IAAs is conferred by a TIR1 or AFB F-box protein (Dharmasiri, et al., 2005; Kepinski and Leyser, 2005). Crystallography studies show that TIR1 binds IAA via a binding pocket (Tan et al., 2007). The TIR1 subunit contains 18 leucine-rich repeats (LRRs) that form this pocket and bind auxin via hydrophobic reactions, van der Waals interactions, and hydrogen bonds (Kepinski, 2007; Tan et al., 2007).

When IAA is bound to TIR1, it enhances the interaction between $SCF^{TIR1/AFB}$ and the Aux/IAA protein, enabling the polyubiquitination of the Aux/IAA by the SCF complex (Dharmasiri et al., 2005; Kepinski and Leyser, 2005; Tan et al., 2007). This polyubiquitination of Aux/IAA proteins leads to degradation in the 26S proteasome (Santos Maraschin et al., 2009). Degradation of Aux/IAA proteins leads to the rapid release of the previously Aux/IAA bound ARFs' activity, allowing for regulation of the auxin response (Kepinski and Leyser, 2005; Dharmasiri et al., 2005). The TIR1/AFB-Aux/IAA-ARF-dependent signalling system is summarised in Figure 1.6.

Auxin signalling research has advanced, but many mechanistic links between the Aux/IAA and ARF transcription factors and their downstream effects on development and tropic responses are still unclear. One impediment to understanding how the Aux/IAA and ARF topologies confer context- and tissue-specificity is the complexity and size of the auxin signalling framework. With 29 known Aux/IAAs and 23 ARFs, there are many possibilities for specific binding pairs and interactions. Furthermore, other cofactors such as PHYTOCHROME INTERACTING 4 (PIF4) and BRASSINOLE RESISTENT 1 (BZR1) have been found to interact with ARF6

and ARF6 function may be dependent on these proteins (Oh et al., 2014). While the complexity and size of the system makes understanding the pathway difficult, it allows for many possibilities for the auxin transcriptional framework to confer specificity and regulate auxin response.

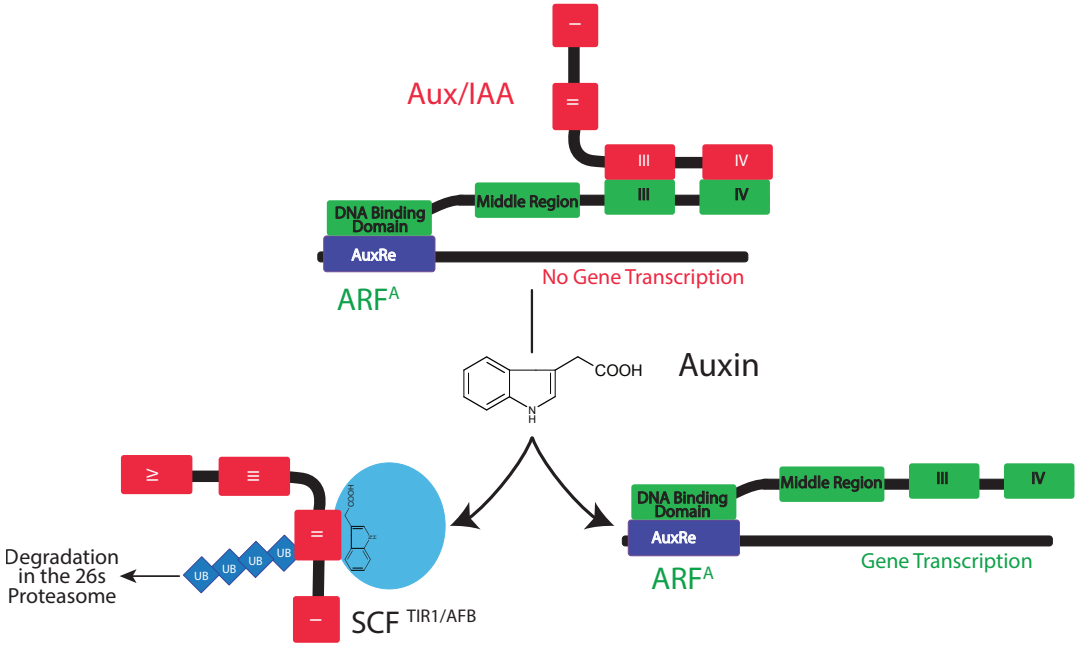

Figure 1.6 The transcriptional control of auxin response via the Aux/IAA and ARF transcription factors.
In low auxin conditions, Aux/IAAs dimerise with the ARFs via a domain III and IV interaction. These corepressor proteins cause the repression of the activating ARF (ARF^A) by recruiting other corepressors that inhibit transcription of the ARF-bound loci. As auxin levels rise, the recruitment of Aux/IAAs by the $SCF^{TIR1/AFB}$ complex leads to the polyubiquitination and subsequent degradation of the Aux/IAAs by the 26S (sedimentation coefficient) proteasome. The degradation of the Aux/IAAs leads to a derepression of the ARF-bound loci and transcription of the targeted genes can begin.

1.7 Project Aims

The sine law has been described in maize, rice, and oat coleoptiles (Audus, 1964; Galland et al., 2002; Iino et al., 2005). While this so-called sine law was first described in 1882, it has only been described in cress (Iversen and Rommelhoff, 1978) and lentil roots (Perbal, 1974). More recent work has been published using the plant model species, *Arabidopsis thaliana,* using a constant feedback response system (Mullen et al., 2000). Using this system, it has been recently found that Arabidopsis primary root gravitropism approximates the so-called sine law between the angles of 20° and 120° (Mullen et al., 2000). However, this recent work described that the greatest gravitropic response in Arabidopsis roots occurred at a stimulation angle of 90°, which is in contrast to most of other the previously published work. Root gravitropism is believed to be governed by Cholodny-Went theory, stating that a lateral redistribution of the plant growth hormone auxin in response to a gravity stimulus induces a growth curvature (Thimann, 1956). If this theory is assumed correct, the magnitude of the angle-dependent response would be dictated by an auxin dependent mechanism either in the growth zone or the gravity-sensing cells.

During root gravity response, auxin is rapidly redistributed to the lower side of the growth zone epidermis from the columella, creating an auxin gradient (Friml et al., 2002; Band et al., 2012). It has been published that auxin gradient is maintained until an apparent loss at 42° to the horizontal (Band et al., 2012). Thus, a “tipping point” mechanism has been proposed that reverses the asymmetrical auxin flow at the midpoint of root bending. The root then continues to grow towards the vertical without a visible asymmetrical gradient at the growth zone epidermis. A “tipping point” mechanism, however, is incompatible with the complete physiology of plant gravitropism kinetics and the Cholodny-Went theory. Plants respond to smaller changes in angle than 42°. In particular, it has been both observed and demonstrated that at displacement angles greater than 20°, roots respond to stimulation and grow towards the vertical (Mullen et al., 2000). While the sine law of gravitropism was put forward over 200 years ago, there are still many open questions left to be understood. Fortunately, new, more sensitive tools have become available during the course of this work that enable the measurement of small differences in auxin response in the Arabidopsis root tip (Liao et al., 2015).

The aims of this project were:

1) To determine the relationship between stimulation angle and gravitropic response in the Arabidopsis root.
2) To establish the role of auxin gradients gravitropic response in the Arabidopsis root.
3) To identify possible mechanism(s) which might determine the magnitude of these auxin gradients.

Chapter 2
Materials and Methods

2 Materials and Methods

2.1 Plant Lines and Growth Conditions

2.1.1 Plant lines

Table 2.1 Plant lines used during the course of this project.

Plant line	Background	Source
Columbia (Col-0)		Martin Kieffer, Leeds
Landsberg erecta (Ler-0)		Martin Kieffer, Leeds
Wasilewskija (Ws-0)		Martin Kieffer, Leeds
Cape Verde Island (Cvi-0)		NASC
Col-0 x Col-24		Suruchi Roychoudry
arf7 arf19	Col-0	Martin Kieffer, Leeds
ARL2::2xGFP	Col-0	This project
ARL2::ARF7△	Col-0	This project
ARL2::ARF7−SRDX	Col-0	This project
ARL2::axr3-1	Col-0	This project
ARL2::axr3-3	Col-0	This project
ARL2::RCN1	Col-0	Suruchi Roychoudry, Leeds
ARL2::WAG2	Col-0	Suruchi Roychoudry, Leeds
ATML1::ARF7	Col-0	This project
ATML1::ARF7△	Col-0	This project
ATML1::mir3/4a	Col-0	This project
axr2-5	Ws-0	NASC
axr3-1	Col-0	Leyser Lab, Cambridge
axr3-10	Ler-0	Leyser Lab, Cambridge
axr3-3	Col-0	Leyser Lab, Cambridge

DII28:VENUS	Col-0	Martin Kieffer, Leeds
DR5::GFP	Col-0	Martin Kieffer, Leeds
DR5V2	Utrecht	Dolf Weijers, Wageningen
J0951	Col-24	NASC
mDII:VENUS	Col-0	Martin Kieffer, Leeds
pPIN3::PIN3–GFP	Col-0	Jiri Friml, IST Austria
pPIN4::PIN4–GFP	Col-0	Jiri Friml, IST Austria
pPIN7::PIN7–GFP	Col-0	Jiri Friml, IST Austria
R2D2	Utrecht	Dolf Weijers, Wageningen
tir1-1	Col-0	Mark Estelle UCSD
UAS::ARF7△ x J1095	Col-0 x Col-24	This project
UAS::axr3-1	Col-0 x Col-24	Leyser Lab, Cambridge
UAS::axr3-1 x J1095	Col-0 x Col-24	This project
UAS::axr3-3 x J1095	Col-0 x Col-24	This project
UAS::mir393a	Col-0	This project

2.1.2 Seed sterilisation and stratification

Arabidopsis thaliana seeds were sterilised using a chlorine gas sterilisation method. Seeds were exposed to chlorine gas in open 1.5 mL tubes for 3 hours and then ventilated for 1 hour. The chlorine gas used was created with 3 mL of hydrochloric acid and 100 mL of liquid bleach. Following sterilisation, seeds were stratified at 4°C for 48 hours on autoclaved media, or soil if the seeds were to be grown in a greenhouse, for growth.

2.1.3 Plant growth media preparation

Arabidopsis plants were germinated on circular petri dishes (92 mm x 16 mm) or square petri dishes (120 mm x 120 mm x 17 mm) with sterile ATS growth media (5 mM KNO_3, 2.5 mM KPO_4 (pH 5.5), 2 mM $MgSO_4$, 2 mM $Ca(NO_3)_2$, 50 µM Fe-EDTA), 1 mL of micronutrients (70 nM H_2BO_3, 14 mM $MnCl_2$, .5 mM $CuSO_4$, 1 mM $ZnSO_4$, .02 mM Na_2MoO_4, 10 mM NaCl, .01 mM $CaCl_2$), 1% sucrose, 0.8% plant agar (Lincoln et al., 1990). All hormones were added after autoclaving and cooling. Petri dishes were sealed with micropore tape.

Beans (*Phaseolus vulgaris*) were grown in individual 'cyg' brown paper pouches standing in Hoagland's No. 2 Basal Salt Mixture (Sigma), 1.6 g/L.

2.1.4 Plant growth conditions

Petri dishes were placed in controlled growth rooms under long day conditions (16 hours light/8 hours dark) at a temperature of 20–22°C. Seeds that were grown in the greenhouses were sown on a 3:1 soil to sand ratio in trays with individual cells and grown with long day conditions at 20–25°C.

2.1.5 Arabidopsis transformation via the floral dip method

Prior to transformation, wild type plants were grown in square 6-cm pots with five seedlings each for 4–6 weeks. A minimum of four pots were used for each transformation. The day prior to transformation, a 500 mL culture of *Agrobacterium tumefaciens* was inoculated with a 2 mL culture from a single colony. The culture was grown overnight at 28°C shaking at 200 RPM with LB (Luria-Bertani media) containing rifampicin (100 mg/L), gentamycin (25 mg/L), and with either kanamycin (40 mg/L) or spectinomycin (50 mg/L). The morning of transformation the bacterial culture was centrifuged at 12,000 RPM for 12 minutes at 28°C. The supernatant was then discarded and the bacterial pellet was re-suspended in 250 mL of floral dipping solution (5% w/v sucrose, 10 mM $MgCl_2 \bullet 6H_20$, 25 µL Silwett Vac in Stuff®). The young flowers of each pot were dipped into the transformation solution for 2–3 minutes. The transformed plants were then covered with an autoclave bag for 24 hours to retain humidity. Plants were grown for 4–5 weeks and then bagged. When seeds were dry, T0 seeds were collected.

2.1.6 Selection of transgenic plants by BASTA® resistance

Transgenic seeds transformed with constructs made in the pGreen 0229 binary vector were selected with BASTA® resistance (D-phosphinothricin). Seeds collected from transformed plants were sown evenly on soil in trays and allowed to germinate. After seeds had reached the two-cotyledon stage they were sprayed with a solution containing 75 mg/L BASTA® and 1% Silwett Vac in Stuff®. Seedlings that survived the initial spray were transferred to individual pots and sprayed again in the same manner. Survivors of the second spray were marked as T1 plants and were grown for seed. T2 seeds were collected from the T1 plants and sown on plates with 10 mg/L BASTA® to check for a 3:1 segregating population, indicative of a single insertion of the transgene. The T2 plants were then grown for seeds to be selected for the T3 population for homozygous lines.

2.1.7 Selection of transgenic plants by seed coat fluorescence

Transgenic seeds transformed with constructs made in the pAlligator III binary vector were selected by seed coat fluorescence. Matured seeds collected from transformed plants were selected for analysis by seed-coat-specific GFP expression using an OLYMPUS® SZX12 stereo microscope. Highly fluorescent seeds were selected as T1 plants and were grown for seed. Seeds collected from these plants were selected in the same manner looking for a 3:1 ratio of fluorescent to non-fluorescent seeds, indicating that a single insertion of the transgene was present. These seeds were grown to T3 homozygous lines.

2.2 Bacterial Growth Conditions and Transformation

2.2.1 *Escherichia coli* (*E. coli*) growth conditions and media

After transformation, *E. coli* that were used for propagation of plasmid DNA were grown at 37°C on solid LB (Luria-Bertani: tryptone 10 g/L, NaCl 10 g/L, yeast extract 5 g/L, 2% agar) supplemented with the appropriate antibiotics overnight. Overnight liquid cultures from single colonies were grown at 37°C shaking at 200 RPM.

2.2.2 *Agrobacterium tumefaciens* (*A. tumefaciens*) growth conditions

Following transformation, the *A. tumefaciens* strain GV3101 was grown for 2–3 days at 28°C on solid LB plates supplemented with gentamycin (50

mg/L), rifampicin (100 mg/L) and an antibiotic specific to the plasmid. Liquid cultures were grown at 28°C shaking at 200 RPM.

2.2.3 Transformation of α-select® chemically competent *E. coli* (Bioline)

Aliquots of competent cells were thawed on wet ice. A maximum of 5 µL of plasmid DNA was placed in 50 µL aliquots of cells and incubated on ice for 30 minutes. Then the aliquots were heat shocked at 42°C for 30 seconds and returned to ice for 2 minutes. The liquid suspension was then diluted with 1 mL of pre-warmed liquid LB and incubated at 37°C shaking at 200 RPM for 1 hour. The liquid suspension was then spread on LB-agar plates containing the appropriate antibiotic for each vector and incubated inverted at 37°C overnight.

2.2.4 One Shot® TOP10 chemically competent *E. coli* (Invitrogen)

Aliquots of competent cells were thawed on wet ice. A maximum of 5 µL of DNA was placed in 50 µL aliquots of cells and incubated on ice for 30 minutes. Then the aliquots were heat shocked at 42°C for 30 seconds and returned to ice for 2 minutes. The liquid suspension was then diluted with 1 mL of pre-warmed S.O.C. medium (2% tryptone, 0.5% yeast extract, 10 mM NaCl, 2.5 mM KCl, 10 mM $MgCl_2$, 10 mM $MgSO_4$, and 20 mM glucose) supplied by Invitrogen. The cells were incubated at 37°C for 1 hour shaking at 200 RPM. After incubation, less than 300 µL of cells were spread on LB-agar plates containing the appropriate antibiotic for each vector and incubated inverted at 37°C overnight.

2.2.5 Preparation of *A. tumefaciens* competent cells

Cells from a GV3101 glycerol stock (with or without the helper plasmid pSOUP) were streaked onto a LB-agar plate containing rifampicin (100 mg/L) and gentamycin (50 mg/L) and incubated at 28°C for 2–3 days. Single colonies were selected and used to inoculate a 50 mL culture containing antibiotics. The liquid culture was grown at 28°C shaking at 200 RPM until the bacteria had reached a period of steady-state growth (OD_{600} at 0.6–1 measured with a spectrophotometer), generally between 4–6 hours. The culture was then transferred to pre-chilled 50 mL falcon tubes and centrifuged at 4000 RPM for 20 minutes at 4°C. The supernatant was discarded and the cell pellets were gently re-suspended in 1 mL of 20 mM

$CaCl_2$ solution. Aliquots of 100 µL were then made and frozen in liquid nitrogen before being stored at -80°C.

2.2.6 Transformation of *A. tumefaciens* competent cells

A maximum of 1 µg of plasmid DNA was added to a 100 µL aliquot of frozen competent *A. tumefaciens* cells. The cells were heat-shocked in a 37°C water bath for 5 minutes. 750 µL of warm LB was added to the cell suspension. The cells were then incubated at 28°C shaking at 200 RPM for 4 hours. Two aliquots of 200 µL and 500 µL each were spread on LB-agar plates containing the appropriate antibiotics. The plates were allowed to dry before being incubated at 28°C for 2–3 days.

2.3 Molecular Biology

2.3.1 Plasmid miniprep with QIAGEN Plasmid Mini Kit®

Pelleted bacteria were re-suspended in 250 µL of P1 Buffer and transferred to a microcentrifuge tube. 250 µL of P2 Buffer was then added to each tube, and the tubes were inverted four to six times. The lysis reaction was neutralised after 1 minute by adding 350 µL of Buffer N3 to each reaction. Reactions were then centrifuged at 13,000 RPM for 10 minutes. The supernatants were applied to QIA spin columns, centrifuged for 30–60 seconds, and the flow-through discarded. The column was washed twice by adding 750 µL of Buffer PE. A final spin was done with a clean collection tube to each reaction to ensure residual ethanol was removed from the column. DNA was eluted by adding 30–50 µL of elution butter (10 mM Tris-CL, pH 8.5) to the spin column. After an incubation time of 1 minute the column was spun at 13,000 RPM to recover DNA. All DNA samples were assessed using a NanoDrop.

2.3.2 Isolation of RNA with QIAGEN RNAeasy Plant Mini Kit®

Young plants were frozen in liquid nitrogen and finely ground in a mortar and pestle. The approximately 100 mg of plant tissue was ground thoroughly while adding liquid-nitrogen repeatedly until tissue was powder-like. Buffer RLT was added and the tissue was vortexed vigorously. The resulting lysate was transferred to a QIAshredder spin column and vortexed at full speed for two minutes. The resulting supernatant was transferred to a microcentrifuge and 0.5 mL of 100% ethanol was added. The sample was then transferred to

RNAeasy Mini spin columns to bind RNA. The column was washed 3 times with wash buffers (RNeasy, RPE, and RWI). The sample was eluted in 50 µL RNAse-free water after a 1-minute incubation time.

2.3.3 Conditions of amplification of plant gene coding sequences

Both Phusion® (NEB) and Velocity® (Bioline) proofreading enzymes were used to amplify cDNA and genomic DNA for the creation of constructs. Wild type (WT) Col-0 cDNA, mutant cDNA, or plasmid vectors containing desired sequence were used to amplify the gene sequences for constructs. For promoter regions, WT Col-0 genomic DNA was used. DMSO was only added with Phusion® polymerase due to the high GC content of the UAS promoter sequence. All reactions were carried out as in tables below and were done on ice until being added to a preheated PCR block.

Table 2.2 Typical PCR reaction set-up for PCR.

	Phusion® polymerase	Velocity® polymerase
Reaction component	Final concentrations	
Buffer	5X GC buffer (1X)	5X Hi-FI Reaction Buffer (1X)
dNTP	200 µM each	250 µM each
Forward and reverse primers	0.5 µM each	0.4 µM each
DNA template	variable (< 250 ng)	variable
DMSO	3%	none used
DNA polymerase	1.0 units/50 µL PCR	1.0 units/50 µL PCR
Sterile water	up to volume	up to volume

Table 2.3 PCR cycling conditions used for reactions with Phusion® polymerase.

Step	Temperature (°C)	Time
Initial denaturation	98	30 s
30–34 cycles	98 primer dependent	10 s 15–20 s

	(52–72) 72	 15–30 s/kb
Final extension	72	5–10 min

Table 2.4 PCR cycling conditions used for reactions with Velocity® polymerase.

Step	Temperature (°C)	Time
Initial denaturation	98	2 min
30-34 cycles	98 primer dependent (52–68) 72	30 s 30 s 15–30 s/kb
Final extension	72	4–10 min

2.3.4 PCR purification with QIAspin® columns

PCR products were purified using a QIAGEN PCR Purification Kit®. 5 volumes of Buffer PB were added to each 1 volume of PCR reaction and mixed. The mix was added to a QIAquick column with a 2 mL collection tube. The DNA was bound during a centrifugation of 30 seconds at 13,000 RPM. After the flow-through was discarded, 0.75 mL of Buffer PE (wash buffer) was added and centrifuged for an additional 30 seconds. The wash step was repeated twice with a clean collection tube. DNA was eluted after adding 50 µL of EB to the column and incubating for 1 minute. The DNA was recovered after centrifugation for 30 seconds at 13,000 RPM.

2.3.5 RNA clean-up using RNAeasy Plant Mini Kit®

The sample was adjusted to a volume of 100 µL of RNase-free water. 350 µL of Buffer RLT was added and mixed well. 250 µL of ethanol was added and transferred to an RNeasy Mini spin column and centrifuged for 10 seconds at 10,000 RPM with the flow-through being discarded. Buffer RPE was added to wash the column and was centrifuged for 15 seconds and the flow-through discarded. A second wash of 500 µL Buffer RPE was added and centrifuged again for 2 minutes and discarded. 30 µL of EB Buffer was added to the spin column and incubated for 1 minute. The RNA was eluted

in the final centrifugation step at 10,000 rpm for 1 minute. RNA was assessed with the NanoDrop.

2.3.6 DNase treatment of RNA

RNA was treated with DNase prior to first-strand synthesis. The components in Table 2.5 were added to a PCR tube and allowed to incubate at room temperature for 15 minutes. The RNA was cleaned up using a QIAGEN RNAeasy Kit ® and eluted in EB buffer.

Table 2.5 Reaction components for DNase treatment of RNA.

Reaction component	Volume (µL)
RNA at 355 ng/µL	8.45
10x DNase Buffer	2
Sterile water (up to 20 µL)	8.55
DNase	1

2.3.7 cDNA synthesis

SuperScript II RT® (Invitrogen) was used for the first-strand synthesis from the cleaned-up RNA.

Table 2.6 Reaction components used in first-strand synthesis reactions.

Component and concentration added	Volume (µL)
Oligo(dT) (500 µg/mL)	1
RNA (55 ng/µL)	10
dNTP mix (10 mM each)	1

The components from Table 2.6 were added to a nuclease-free microcentrifuge tube and the mixture was heated to 65°C for 5 minutes and then chilled on ice. The contents were then collected by brief centrifugation. Prior to synthesis, 4 µL of 5X First-Strand Buffer, 2 µL 0.1 M DTT, and 1 µL of RNasin were added. The mixture was heated at 42°C for 2 minutes with 1 µL of SuperScript II RT added after. The tube was incubated for 50 minutes at 42°C and then heat inactivated at 70°C for 15 minutes.

Prior to use as a template for PCR, the RNA was removed from the cDNA by adding 1 µL (2 units) of *E. coli* RNase H and incubated at 37°C for 20 minutes.

2.3.8 Agarose gel electrophoresis

DNA size was analysed using agarose gels at 1.1%, 1.6% or 2% concentration. Agarose was dissolved in 1X Tris-acetate-EDTA (TAE) buffer (40 mM Tris, 20 mM acetic acid, pH 8.0, 1 mM EDTA) with 5 µL of ethidium bromide (final concentration of 0.1 ng/mL) per 200 mL of TAE buffer. DNA samples were diluted with 6X Orange DNA Loading Dye. A voltage between 60 V and 90 V was applied in 1X TAE running buffer using Bio-Rad gel tanks. A UV trans-illuminator was used to visualize the bands.

2.3.9 Extraction of PCR products from an agarose gel using Qiaquick Gel Extraction Kit®

DNA that was extracted from agarose gels was purified with a QIAquick Gel Extraction Kit®. The gel slice was initially solubilised with 3 volumes of QG buffer to 100 mg of gel. The gel slice was incubated in the buffer at 50°C for 10 minutes with brief vortexing every 2 minutes. After solubilisation, 1 volume of isopropanol was added to the mixture. This mixture was added to a Qiaquick spin column in a 2 mL collection tube. DNA was bound to the column during a 1-minute centrifugation at 13,000 RPM. After the discard of the flow-through, 0.5 mL of Buffer QG was added to remove all traces of agarose. Two wash steps with 0.75 mL buffer PE were added to the column and centrifuged for 1 minute at 13,000 RPM each. A final centrifugation was done to remove all traces of ethanol from the column. DNA was eluted in 50 µL of EB Buffer and assessed after a 1-minute incubation time and 30 seconds centrifugation at 13,000 RPM. DNA was eluted in 20 µL of water and placed in the -20°C immediately.

2.3.10 DNA digestion with restriction enzymes

Restriction digests were used to check for the correct insertion of cloned sequences into entry and destination vectors. A typical reaction was done in 20 µL and incubated at 37°C (except for digests with SmaI) for 1 hour, as stated in Table 2.7 and then run on an agarose gel to check resulting band

pattern and sizes. Buffers and enzymes were purchased from New England Biolabs (NEB).

Table 2.7 Components and volumes for a typical restriction enzyme digests.

Reaction component	Volume (µL)
DNA substrate	3
NEB Buffer (varies based on enzyme)	2
Sterile water	14–14.5
Restriction enzyme (s)	0.5–1

In addition to diagnostic digests, pGreen 0229 was linearised with SmaI previous to a ligation reaction. The components from Table 2.8 were added to a PCR tube and incubated for 3 hours at 25°C and then heat inactivated at 65°C for 20 minutes.

Table 2.8 Components and volumes used for plasmid linearizing digests.

Reaction component	Volume (µL)
DNA substrate	25 (2.5 ng)
NEB4 buffer	15
Sterile water	107
Restriction enzyme	3

2.3.11 Dephosphorylating DNA with Calf Intestinal Phosphatase (CIP)

Phosphate groups on the 5' end of linearised pGreen 0229 were removed to prevent self-ligation. To dephosphorylate with CIP, 0.5 µL of enzyme was added directly to the SmaI digest. The mixture was incubated at 37°C for 15 minutes and then incubated at 56°C for 15 minutes. This was repeated after the addition of another 0.5 µL of enzyme. The mixture was purified by PCR spin column purification and eluted in 30 µL elution buffer.

2.3.12 Ligations using T4 ligase

Ligations were carried out to create a destination vector with a termination sequence for the UAS constructs. A previously made Gateway cassette containing a NOS terminator sequence was inserted into a pGreen 0229 backbone. The components in Table 2.9 were added to a PCR tube on ice, with the T4 ligase added last. The mixture was vortexed and centrifuged briefly and incubated at 4°C overnight and allowed to sit at room temperature for an additional hour. Prior to transformation the ligation product was cleaned up with a PCR purification column and precipitated with yeast tRNA.

Table 2.9 Reaction components for T4 Ligase mediated ligations.

Reaction component	Volume (µL)
pGreen 0229 SmaI CIP treated at 32 ng/µL	1.6
Insert GWB:NosTer at 6 ng/µL	3
T4 Ligase Buffer (10X)	1
T4 Ligase	1
Sterile water	3.4

2.3.13 DNA precipitation with yeast tRNA

To increase transformation efficiency of ligations, DNA precipitation with yeast tRNA was done. 5 µL of the ligation produce was mixed with 1 µL of 1 µg/µL yeast tRNA and 14 µL of distilled water was added. To precipitate the DNA, 50 µL of chilled 100% ethanol was added. The sample was incubated at -20°C for 15 minutes. And then centrifuged at 14,000 RPM at 4°C. The supernatant was removed and the pellet was washed with 100 µL of 70% ethanol and air-dried. The DNA pellet was then dissolved in 20 µL of distilled water and assessed for concentration and purity via a Nanodrop.

2.3.14 Construction of microRNA constructs

Artificial microRNAs were constructed to knock down the expression of *ARF1* and *ARF2*, and *ARF3* and *ARF4*. Two microRNAs were constructed for each set of genes to increase the likelihood of creating knock down lines.

Gateway extensions were also designed into the microRNA precursor to allow for multiple promoters. The oligonucleotides designed to create the constructs are displayed in Table 2.10.

Table 2.10 Sequences of oligonucleotides for microRNA design of *amirRNA-ARF1/2* and *amirRNA-ARF3/4*.

amirRNA-ARF1/2			
Oligos for amiRNA 1/2a CAGGCGATGCGTTTATATTTA	Sequence	Oligos for aMir1/2b ATGGCATTTTAGGCACATTTA	Sequence
I miR-s	gaCAGGCGATGCGTTTATATTTAtctctcttttgtattcc	I miR-s	gaATGGCATTTTAGGCACATTTAtctctcttttgtattcc
II miR-a	gaTAAATATAAACGCATCGCCTGtcaaagagaatcaatga	II miR-a	gaTAAATGTGCCTAAAATGCCATtcaaagagaatcaatga
III miR*s	gaTACATATAAACGCTTCGCCTGtcacaggtcgtgatatg	III miR*s	gaTACATGTGCCTAATATGCCATtcacaggtcgtgatatg
IV miR*a	gaCAGGCGAAGCGTTTATATGTAtctacatatatattcct	IV miR*a	gaATGGCATATTAGGCACATGTAtctacatatatattcct
amirRNA-ARF3/4			
Oligos for amiRNA3/4a TCGGCTCAATATAATCAGAAA	Sequence	Oligos for amirRNA3/4b AAGTGCTTAAGAGGTCTAATA	Sequence
I miR-s	gaTCGGCTCAATATAATCAGAAAtctctcttttgt	I miR-s	gaAAGTGCTTAAGAGGTCTAA

	attcc		TAtctctttttgtattcc
II miR-a	gaTTTCTGATTATATTGAGCCGAtcaaagagaatcaatga	II miR-a	gaTATTAGACCTCTTAAGCACTTtcaaagagaatcaatga
III miR*s	gaTTCCTGATTATATAGAGCCGTtcacaggtcgtgatatg	III miR*s	gaTACTAGACCTCTTTAGCACTTtcacaggtcgtgatatg
IV miR*a	gaACGGCTCTATATAATCAGGAAtctacatatatattcct	IV miR*a	gaAAGTGCTAAAGAGGTCTAGTAtctacatatatattcct

Table 2.11 Sequences of Gateway® extension primers.

Sequences of oligos A and B with Gateway® extensions	
Primer	Sequence
BamH1RS300b2 (B)	ggggaccactttgtacaagaaagctgggtggatccccccatggcgagcct
B5RS300EcoR1 (A)	ggggacaactttgtatacaaaagttgaattcctgcagccccaaacacac

Table 2.12 PCR strategy for construction *of amirRNA 1/2a*, *amirRNA 1/2b*, *amir3/4a*, and *amir3/4b*.

PCR reaction	Forward oligo	Reverse oligo	Template
a	A	IV	pRS300
b	III	II	pRS300
c	I	B	pRS300
d	A	B	(a), (b), (c)

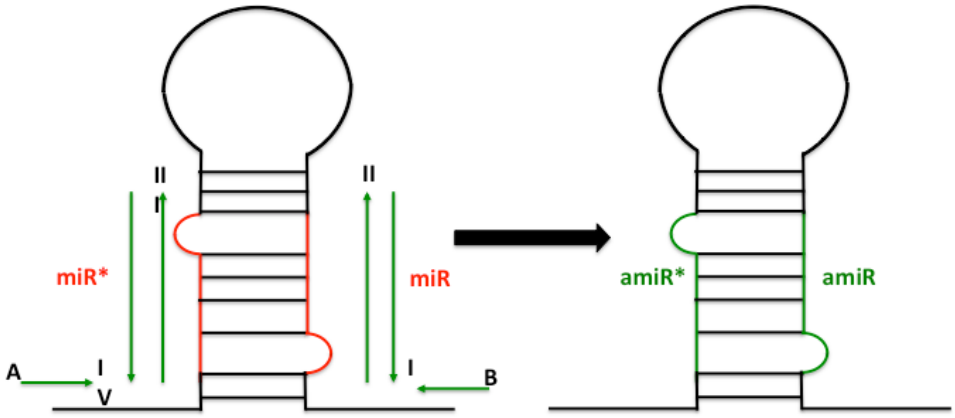

Figure 2.1 Construction strategy for microRNAs for the *ARF* genes *1*, *2*, *3*, and 4.

Table 2.13 Components of PCR reactions a, b, and c.

Reaction component	Volume (µL)
Hi-Fi Velocity Buffer (5X)	10
dNTPS at 2 mM each	5
oligos at 10 µM each	2
pRS300	1
Water (up to 50 µL)	31.5
Velocity polymerase	0.5

Table 2.14 PCR cycling conditions for PCR reactions a, b, and c.

Step	Temperature (°C)	Time
Initial denaturation	95	2 min
24 cycles	95 55 72	30 s 30 s 40 s
Final extension	72	7 min

The PCR was done with the conditions as in Table 2.14. PCR products were run on a 2% gel and the bands were cut using a UV trans-illuminator with sterile surgical blades. The resulting gel slices were cleaned up with a QIAquick Gel Extraction Kit®.

The final reaction to fuse the components of the amiRNA together was done in a PCR reaction, D. The reaction was done as in Table 2.15. The products of these reactions were run on a 1% agarose gel and cleaned up with the QIAquick Extraction Kit® and eluted in 20 µL of water. After clean up, the products of these reactions were placed in an entry clone for Gateway cloning via a BP reaction.

Table 2.15 Reaction components for PCR reaction D.

Reaction Component	Volume (µL)
Hi-Fi Velocity Buffer (5X)	10
dNTPS at 2 mM	5
oligo A at 10 µM	2
oligo B at 10 µM	2

PCR product (a)	1
PCR product (b)	1
PCR product (c)	1
Water (up to 50 µL)	27
Velocity polymerase	1

Table 2.16 PCR cycling conditions for reaction D.

Step	Temperature (°C)	Time
Initial denaturation	95	2 min
30 cycles	95 53 72	30 s 30 s 90 s
Final extension	72	7 min

2.3.15 Real time quantitative PCR (RT-qPCR) analysis of PIN expression in ARL2 constructs

RT-qPCR was carried out using CFX Connect Real-Time PCR Detection System® (Biorad UK) with Universal SYBR® Green Supermix. This supermix contains all components necessary for the qPCR reaction. 96-well propylene plates were used and sealed with optical quality sealing film. A two-step amplification profile was used including an initial denaturation step of 95 for 10 minutes and cycled 36 times for 30 seconds and 60 for 10 seconds, with the fluorescence data being measured at this phase. In addition, a melt curve was completed for each primer set. *Glyceraldehyde-3-phosphate dehydrogenase (GAPDH)* was used as a housekeeping gene to normalise target genes for all experiments, with 4 biological replicates and 2 technical replicates for each gene in each genotype. A crossing point (Cp) value was obtained for each gene per sample and at each point of the corresponding standard curve. The relative expression of each gene was calculated according to the 2-ΔΔCt method (Livak and Schmittgen, 2001) with some modifications. An arbitrary unit was attributed to each Cp of the standard curve and then converted into base 10 logarithm value. After determining the equation of the standard curve, the logarithm value and thus the arbitrary unit was deduced for each sample. The final results were

expressed as the ratio between the gene of interest and the housekeeping gene arbitrary units.

2.4 Cloning Using Gateway® Invitrogen Modular Cloning System

2.4.1 Introduction and cloning strategy

For completion of most of the constructs Invitrogen's Multisite Gateway® technology was used. This modular system uses site-specific recombination cloning which allowed the building of individual cassettes. These cassettes containing promoter sequences (PS) and gene sequences (GS) could be recombined in different combinations with relative ease. This technology is a universal cloning method based on bacteriophage lambda site-specific recombination which facilitates the integration of lambda into the *E. coli* chromosome and the switch between the lytic and lysogenic pathways (Landy, 1989). Recombination occurs between phage and *E. coli* DNA via specific, conservative recombination at sites referred to as *att* sites. These recombinations are catalysed by the Clonase enzyme mixes. A schematic of the cloning strategy for these constructs is outlined in Figure 2.2.

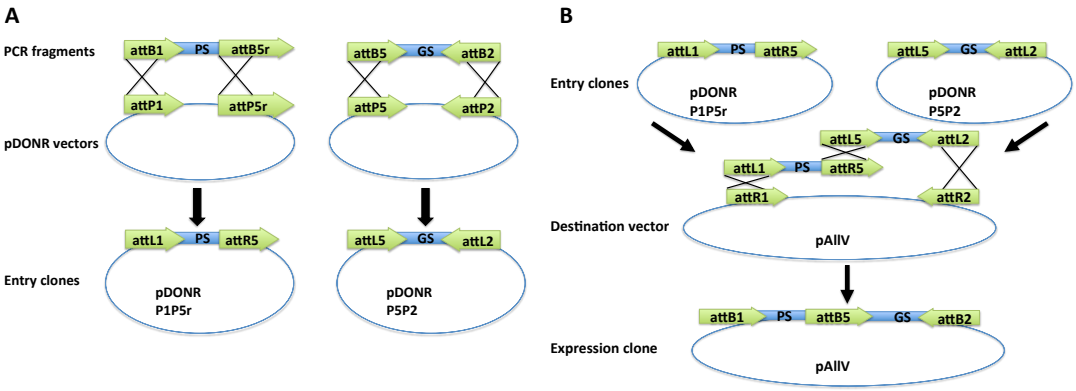

Figure 2.2: Gateway cloning strategy.
Schematic of the strategy for creating entry clones via a BP Reaction (A) and creating expression clones via a LR reaction (B).

2.4.2 Vector maps of Gateway® vectors pDONR 221, pAlligator III, and pGreen 0229

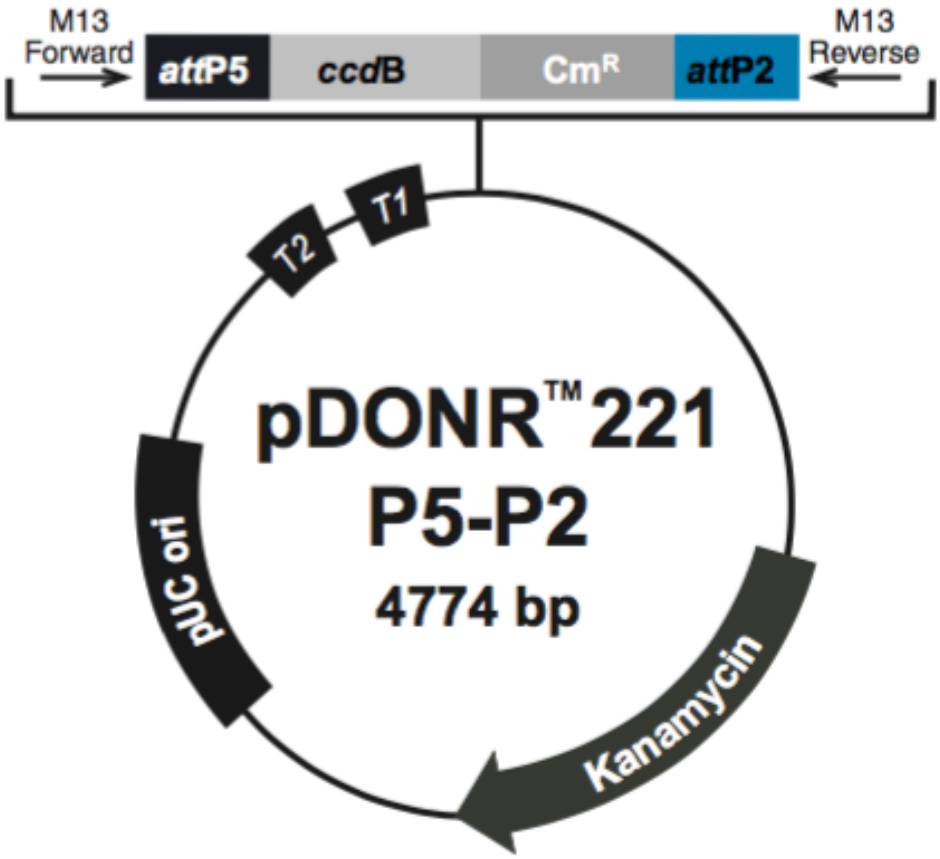

Figure 2.3 Invitrogen Gateway® vector map of pDONR 221.
Entry vectors contain *att* recombination sites for incorporation of DNA sequences. Entry clones also contain kanamycin resistance genes for selection of positive transformations as well as the toxic *ccdB* gene to α-select competent cells. The *ccdB* gene is excised upon recombination with amplified gene products. All pDONR 221 vectors contain these elements.

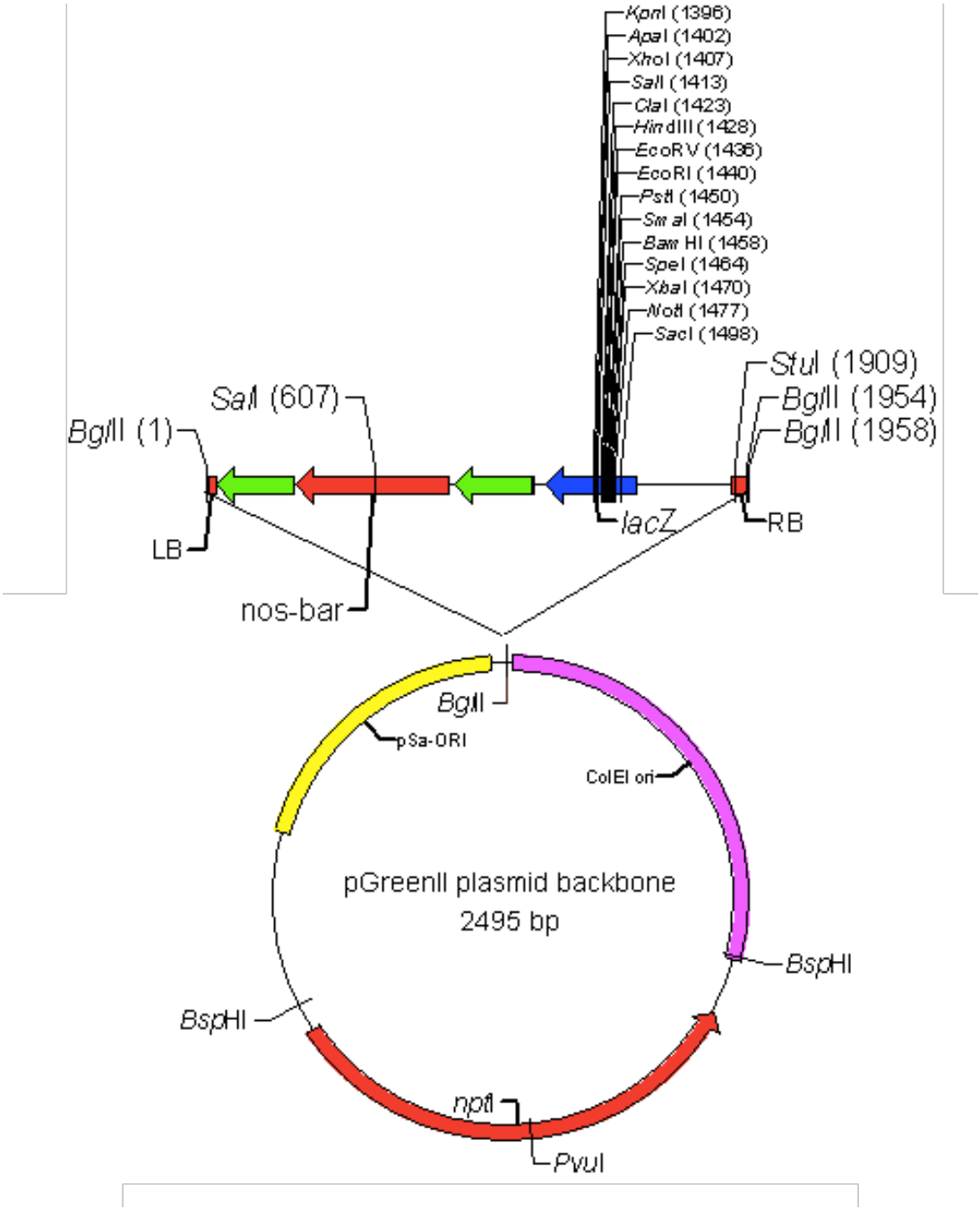

Figure 2.4 Vector map of pGreen 0229 that was used as a destination vector for UAS constructs.

2.4.3 Generation of GATEWAY® Entry clones

Amplified PCR products containing the appropriate *att* sites (see Figure 2.2 and Table 2.17) were cleaned up as previously described. All *pAtML1*, *pARL2*, and *pUAS* constructs were made using 2-way gateway technology. *pUBI10* constructs were created using 3-way technology using vector pDONR P1-P4 (promoter PCR products), P4r-P3r (gene sequence PCR products), and P3-P2 (gene sequence PCR products). For 2- way technology, for promoter PCR products pDONR 221 P1-P5R was used. For non-promoter PCR products, pDONR 221 P5-P2 was used.

BP recombination reactions were done to create entry clones. All of the reaction components in Table 2.18 were added to a PCR tube and vortexed briefly. BP Clonase II was thawed on ice and added last. The reaction was centrifuged briefly and incubated at 25°C for 1–4 hours. BP Clonase II was then inactivated with 1 µL of 2 µg/µL Proteinase K solution (supplied by Invitrogen) and incubated at 37°C for 10 minutes. BP reactions were then transformed with chemically competent *E. coli* cells and selected with 50 mg/mL kanamycin. Single colonies were used to inoculate an overnight liquid culture. The resulting liquid culture was prepped using a Qiagen Plasmid Mini Kit® and a restriction digest was done to confirm insertion and orientation.

Table 2.17 Sequences of *att* sites for Gateway® cloning.

*att*B Site	Sequence (5'–3')	Cassette type	Vector
B1	GGGG ACA AGT TTG TAC AAA AAA GCA GGC TTA	promoter sequence	P1-P5r, P1-P4
B5r	GGGG AC AAC TTT TGT ATA CAA AGT TGT	promoter sequence (reverse)	P1-P5r
B5	GGGG ACA ACT TTG TAT ACA AAA GTT GTA	gene sequence	P5-P2

B2	GGGG AC CAC TTT GTA CAA GAA AGC TGG GTT	gene sequence (reverse)	P5-P2, P3-P2
B4	GGGG AC AAC TTT GTA TAG AAA AGT TGG GTG	promoter sequence (reverse)	P1-P4
B4r	GGGG ACA ACT TTT CTA TAC AAA GTT GTA	gene sequence	P4r-P3r
B3r	GGGG AC AAC TTT ATT ATA CAA AGT TGT	gene sequence (reverse)	P4r-P3r
B3	GGGG ACA ACT TTG TAT AAT AAA GTT GTA	gene sequence	P3-P2

Table 2.18 Components of BP reactions.

Reaction component	Volume (µL)
attB-PCR product	2–3
pDONR vector (70 ng/µL	3
1X TE buffer, pH 8.0	2–3 (up to 10 µL)
BP Clonase II	2

2.4.4 Generation of Gateway® expression clones

To transfer entry clones into the destination vectors, LR recombination reactions were done. For the *pAtML1*, *pARL2*, and *pUBI10* constructs, the pAlligator II destination vector was used (described in (Bensmihen et al.,

2004)). For *UAS* constructs, pGreen 0229 that had been modified was used. The modification of this vector is briefly explained in 2.3. The components of the LR reactions (Table 2.19) were set up in a PCR tube and incubated overnight (up to 16 hours) at 25°C. After 16 hours, 2 µL of Proteinase K was added to the LR reaction and incubated at 37 for 10 minutes. Chemically competent *E. coli* cells were transformed with 3 µL of the LR reaction mixture and selected with the appropriate antibiotic. Single colonies were used to inoculate an overnight liquid culture. The resulting liquid culture was prepped using a Qiagen Plasmid Mini Kit® and a restriction digest was done to confirm insertion and orientation.

Table 2.19 Components of LR reactions.

Reaction component	Volume (µL)
pDONR entry vector(s) (75 ng/µL)	2–6
Destination vector (150 ng/µL)	2–6
1X TE Buffer, pH 8.0	to 8
LR Clonase/ LR Clonase Plus®	2

2.4.5 Construction of *ARL2::2xGFP*

To specifically express genes in the gravity-sensing cells of Arabidopsis roots, the promoter sequence of *ARL2* was used. The upstream sequence of ARL2 was amplified with B1 and B2 Gateway™ primers and inserted into pJGT01 to check for specific expression in the columella cells.

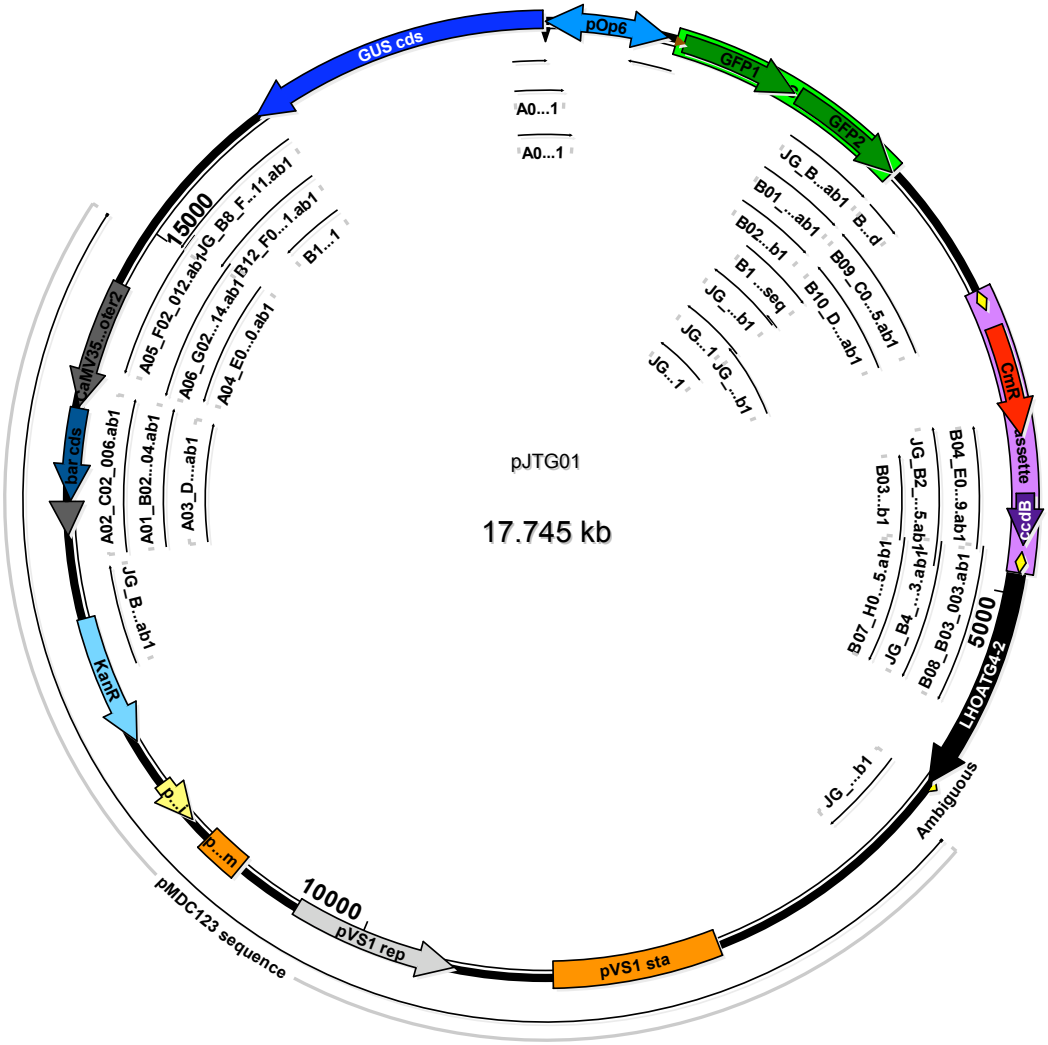

Figure 2.5 2xGFP vector used for *ARL2::2xGFP*.

2.4.6 Primers used in cloning and genotyping

See appendix Table 7.1

2.5 Kinetics Experiments

2.5.1 Gravitropism experiments of roots using time-lapse photography

In order to analyse the gravitropic response of Arabidopsis and Bean roots without affecting the phototropic response, all experiments were conducted in the dark using an Infrared converted Canon camera with an 830 nm filter (http://www.protechrepairs.co.uk/infrared_conversion.html). Infrared LEDS with an approximate 940 nm-emitted wavelength was used. All images were captured using Apple Image Capture software and processed with NIH ImageJ software.

For primary experiments, 5-day-old seedlings grown on circular plates were allowed to rest vertically in the dark imaging box for 1 hour prior to reorientation. Plates were manually rotated to a specific angle and imaged at 1-minute intervals (Arabidopsis) or 10-minute intervals (Beans and Wheat) for 6–12 hours. The root tip angle was measured manually using ImageJ software. For lateral experiments, 10–12 day-old seedlings were reoriented 45° and imaged at 1-minute intervals for 12 hours.

2.5.2 Gravitropism experiments of shoots and hypocotyls using time-lapse photography

Primary shoots of 10–15 cm in length (approximately 4.5 weeks old) were allowed to rest growing upright in the dark for 1 hour. The shoots were then turned on their side and imaged at 10-minute intervals for 3 hours. Shoot angle was manually measured using NIH ImageJ software. For hypocotyl experiments, hypocotyls were etiolated for 24 hours before gravitropism experiments.

2.5.3 Gravitropism experiments using ROTATO

For some gravitropism assays, a method using a constant gravitropism feedback system was used as previously described (Mullen et al., 2000). Briefly, an image is taken of a single root tip, a software program determines the angle, the difference between the desired and actual angle is calculated, and the vertical stage rotates the seedling back to the desired angle of constraint. During the experiment, the total adjustment angle is calculated at each reorientation. This allowed constant stimulation at a desired angle of constraint as the software determined the current angle every 60 seconds. For these experiments 5-day-old seedlings grown on 60 mm petri dishes were placed on the vertical stage for 1 hour prior to gravistimulation. The seedling was then constrained to a specific angle for 2.5–6 hours and their response outputs recorded. The ROTATO software output files consisted of a time, determined angle, and total adjustments. The time and total adjustments were plotted as seen in Figure 3.4. From this data, a bending rate was calculated at both 1 hour and 2 hours by averaging the total adjustments divided by the time at both of these time points and averaged as described in (Mullen et al., 2000). Experiments were carried out on seedlings to test whether or not manually manipulating the seedlings 1 hour to gravistimulation significantly affected response and it was found to be insignificant (Figure 7.2).

2.5.4 Clinorotation experiments

For clinorotation experiments of Arabidopsis primary roots, 5-day-old seedlings growing on 9 cm petri dishes were placed on a 1-D clinostat in an orientation parallel to the axis of rotation at 1 RPM for 6 hours. After clinorotation, petri dishes were scanned using an HP Scanjet G4050 photo scanner. The resulting images were measured using ImageJ software.

2.5.5 Drug and hormone treatments used during gravitropism experiments

For drug treatments on primary roots used to investigate the role of cytoskeleton in gravitropic response, 5-day-old seedlings were transferred to inoculated plates 1 hour prior to gravistimulation and allowed to rest vertically in the dark. Experiments were first done with a 24-hour incubation time. However, this resulted in a highly effected growth response in vertically

growing roots. Since basal elongation is necessary for a gravitropic response, 1-hour incubations were used.

2.5.6 Dexamethasone treatment of GR inducible plant lines

Transgenic GR inducible plants (*SCR::arf7delete::GR*) and control plants were grown in individual cells as previously described. After primary shoots bolted (approximately 3–4 weeks after germination), plants were sprayed with a solution of 30 µM Dexamethasone solution for 7 days prior to experimentation. Treated plants were then used for gravitropism experiments.

2.5.7 Stripflow to measure elongation rates

To measure elongation rates precisely, a program called Stripflow was used which creates a spatial profile of an elongating root. The program is an updated version of RootflowRT (van der Weele et al., 2003). 5-day-old seedlings were imaged using an Olympus BH-2. Growth profiles were calculated for output files using MATLAB software and plotted in Excel.

2.6 Microscopy

2.6.1 Confocal microscopy

Fluorescent plant lines for *DR5* and *DR5v2* analysis were imaged using a Zeiss LSM 700 inverted confocal microscope with Argon (488 nm) lasers and transmitted bright field with a 20X objective. For experiments involving drug treatments of the *DR5v2* reporter, the LSM 880 confocal microscope was used.

For experiments using *DR5::GFP* using ROTATO, an Olympus FV300 confocal microscope was used with an Argon (488 nm) and transmitted bright field using a 10X objective.

2.6.2 Vertical Imaging

For *R2D2* analysis, the LSM700 was used as previously described. However a periscope attachment, the Inverterscope® allowing for vertical imaging was used (http://lsmtech.com). Plants were imaged in chamber slides by Lab-tek® and mounted on a rotatable XYZ stage® also made by LSM Tech. Plants were mounted on chamber slides, allowed to rest for 1 hour on the

rotatable stage growing vertically. After this rest period, control images were taken prior to reorientation. Images were processed using NIH ImageJ software.

For vertical PIN experiments done at IST Austria, experiments were done as described above using a vertically positioned LSM700 at 20X with an Argon laser line (488 nm). For each root, multiple images through the width of the root were imaged and then a z-projection was made using the max setting in ImageJ.

Chapter 3
Gravity Response in Arabidopsis Roots is Angle-Dependent and Governed by Auxin Asymmetries

3 Gravitropism in Arabidopsis Roots is Angle-Dependent and is Governed by Auxin Asymmetry

3.1 Introduction

In 1882, Julius Sachs formulated the sine law of gravitropism that states that the component of gravity acting at a right angle to an organ's axis determines the magnitude of its tropic response, i.e., the magnitude of gravity response is proportional to the sine of the angle between the organ axis and the vertical. For example, when a seedling is rotated into a horizontal position its shoot and root initially show a large gravitropic response that slows as the shoot and root approach the vertical. Since 1882, this so-called sine law has been verified (with minor modifications) in maize, rice, and oat coleoptiles (Audus, 1964; Galland et al., 2002; Iino et al., 2005). While good progress has been made in describing shoot gravitropism (Bastien et al., 2013) and describing angle-dependent response in Arabidopsis roots (Mullen et al., 2000), the mechanism governing these angle-dependent differences in magnitude of gravitropic response is still not fully understood. The basic mechanisms underlying shoot and root gravitropism are similar, but there are important differences. In shoots, gravity perception and response occur in separated but still adjacent tissues with bending occurring along the whole organ (Chen et al., 1999). In roots, gravity perception and response occur in more spatially separate tissues: gravity perception occurs in the gravity-sensing cells of the root tip columella, while response occurs farther back in the growth zone (Baldwin et al., 2013). Therefore, roots and shoots require two different models of gravitropism to fully describe gravity response kinetics.

All available evidence indicates that gravitropism can be accounted for by the Cholodny-Went theory of tropic growth. This theory states that changes in the orientation of growth of an organ in response to directional stimuli such as gravity and light are governed by the lateral redistribution of auxin, producing a gradient of auxin across the organ (Thimann, 1956). This asymmetry in auxin distribution is what drives the formation of tropic curvature. Auxin generally inhibits cell elongation in roots (Thimann, 1939), so when auxin is moved to the lower side of a root, it causes the root to grow downwards. If Cholodny-Went theory is assumed correct, the magnitude of

the angle-dependent response would be dictated by an auxin dependent mechanism either in the growth zone or the gravity-sensing cells.

During root gravity response, it has been shown that there is an increase in the amount of auxin being redistributed from the columella to the epidermis of the elongation zone on the lower side of the root, creating an auxin gradient across the organ (Friml et al., 2002; Band et al., 2012). A recent model of root gravitropism states that as the root responds to gravity, this auxin gradient is maintained until an apparent loss at ~42° from the horizontal (Band et al., 2012). Thus, a “tipping point” mechanism has been proposed that reverses the asymmetrical auxin flow at the midpoint of root bending. According to this model, the root then continues to grow towards the vertical without a visible asymmetrical gradient. However, this mechanism is incompatible with some basic features of root gravitropism. For example, it has been demonstrated with experiments using a feedback response system that at displacement angles greater than 20°, primary Arabidopsis roots respond to stimulation and grow towards the vertical (Mullen et al., 2000). This feedback system, comprising of a rotating stage platform and a video digitizer system, allows the experimenter to maintain a constant angle of gravistimulation of Arabidopsis roots over long time periods. Using this system, it was also found that for Arabidopsis the rate of curvature approximates a sine law for angles between 20° and 120° (Mullen et al., 2000).

Previous work on understanding the role of auxin asymmetries in gravitropism has been based on two auxin response reporters, *DR5::GFP* (Ottenschläger et al., 2003) and *DII-VENUS* (Brunoud et al., 2012). *DR5::GFP* is a reporter of transcriptional responses to auxin, consisting of the synthetic *DR5* promoter (9 inverted repeats of TGTGTCTC) that drives GFP expression (Ottenschläger et al., 2003). This promoter, based on an auxin response element that was first identified in soybean (Ulmasov et al., 1997), has been recently found to have limited sensitivity due to the use of a medium-affinity ARF-binding element (Liao et al., 2015). Another IAA-based auxin signalling reporter, *DII-VENUS* (Brunoud et al., 2012), has been used to study auxin gradients in gravity responding roots (Band et al., 2012). This reporter is a fusion of a degron motif from domain II of the Aux/IAA IAA28 to a VENUS fluorescent protein (Brunoud et al., 2012). *DII-VENUS* reports on auxin-dependent signalling events at an earlier stage in the signal

transduction pathway and is more sensitive than *DR5::GFP*. Nevertheless, *DII-VENUS* is only a semi-quantitative measurement of auxin input into the auxin signalling pathway.

During the course of the present work, new tools became available to better quantify auxin gradients in Arabidopsis. First, a new version of *DR5::GFP* called *DR5v2* has been developed with a newly improved auxin response element (TGTCGG) that detects a tenfold-lower auxin concentration (Liao et al., 2015). Second, a ratiometric version of *DII-VENUS* called *R2D2* has been developed. *R2D2* contains in a single transgene a *RPS5A*-driven degron (DII) fused to a nuclear localised GFP and a *RPS5A*-driven mutated degron fused to a nuclear localised tdTomato fluorescent protein (Liao et al., 2015). Together with vertical confocal imaging, these tools allow for highly sensitive, more quantitative read-outs of auxin gradients in gravity responding roots.

In this chapter, the angle-dependence of gravitropism is explored to investigate the mechanism governing the so-called sine law of gravitropism. Using these data, an angle-dependent model is explored. Data supporting this model is collected using infrared time-lapse imaging of large populations of *Arabidopsis thaliana* (Col-0 and Cvi-0 ecotypes) primary roots. Gravitropic response experiments are also conducted on bean (*Phaseolus vulgaris*) and wheat (*Triticum aestivum*). Furthermore, experiments using more sensitive auxin reporters are used to investigate the governing mechanism.

3.2 Results

3.2.1 Gravitropic response of *Arabidopsis* is angle-dependent

Extensive reorientation experiments were done to characterise the gravitropic response of Arabidopsis (Col-0) from different stimulation angles (30°, 60°, 90°, 120°, 150°, and 170°)(Figure 3.1). In this experiment, roots were imaged in the dark for 6 hours and the root tip angles were measured using NIH ImageJ software at 30-minute intervals. This large scale experiment suggests that there is an angle-dependent response in Arabidopsis in both ecotypes (Figure 3.1). There are differences in the first hour bending rates of both ecotypes, with the greatest response at approximately 130° ($p < 0.05$, 1-way ANOVA).

To confirm angle-dependence, experiments with a fixed stimulation time and varying angles were performed, a method adapted from (Larsen, 1969). In these experiments, roots were gravistimulated at different angles (30°, 60°, and 90°) for 30 minutes and then rotated on a 1 RPM clinostat for 6 hours to deprive the roots of a stable gravity reference. After 6 hours, the root tip angle was measured using NIH ImageJ software. This experiment shows that, after 6 hours, roots reoriented at higher angles displayed more gravitropic bending in a dose-dependent manner (Figure 3.1A–B). Another ecotype of Arabidopsis, Cape Verde Islands (Cvi-0) was also tested (Figure 3.2A–B). This ecotype exhibits a natural right handed skew, so it was tested for gravity response by reorienting the plates in both directions (Figure 3.2C, right). Experiments carried out with each Arabidopsis ecotype shows an angle-dependent mechanism of gravity response. However, while both ecotypes of Arabidopsis displayed angle-dependence within the first hour, the bean and wheat roots (Figure 3.3) did not. The average bending rate of the bean roots when reoriented at angles 60°–120° was the same across all angles. After a fast initial bend rate, there is a very slow gravity response. More work has to be done to investigate why bean and wheat roots do not respond in an angle-dependent manner, although many other species such as *Lepidium savitium* (Larsen, 1969)*, Lens culinaris* (Perbal, 1974) and Arabidopsis (Mullen et al., 2000) do exhibit angle-dependent gravitropism.

To further explore gravitropic response at higher angles, experiments using a using a constant feedback system to constrain roots at angles greater than 90° were performed (Figure 3.4). In this method a root is kept at a chosen angle using a constant feedback system known as ROTATO (Mullen et al., 2000). A root is imaged every minute and a software program calculates how many degrees it has responded from the chosen stimulation angle. The software then uses this change in angle to rotate a gear holding the growth plate, so that the root is once again aligned with the chosen stimulation angle. For this experiment, roots were constrained at different angles (120°, 135°,150°, and 165°) for at least 3 hours and the bending rate was calculated (°/hour). The bending rate is calculated from fitting a line of best fit during the linear portion of the gravity response curve that is created by the original output file from ROTATO (Figure 3.4B). At these higher angles no significant difference in bending rate is found (Figure 3.4). This suggests that angle-dependence is either lost at angles greater than 120° (which at first

sight is inconsistent with data gathered from freely responding roots) or the ROTATO method has a unique effect on gravitropism at angles greater than 120°.

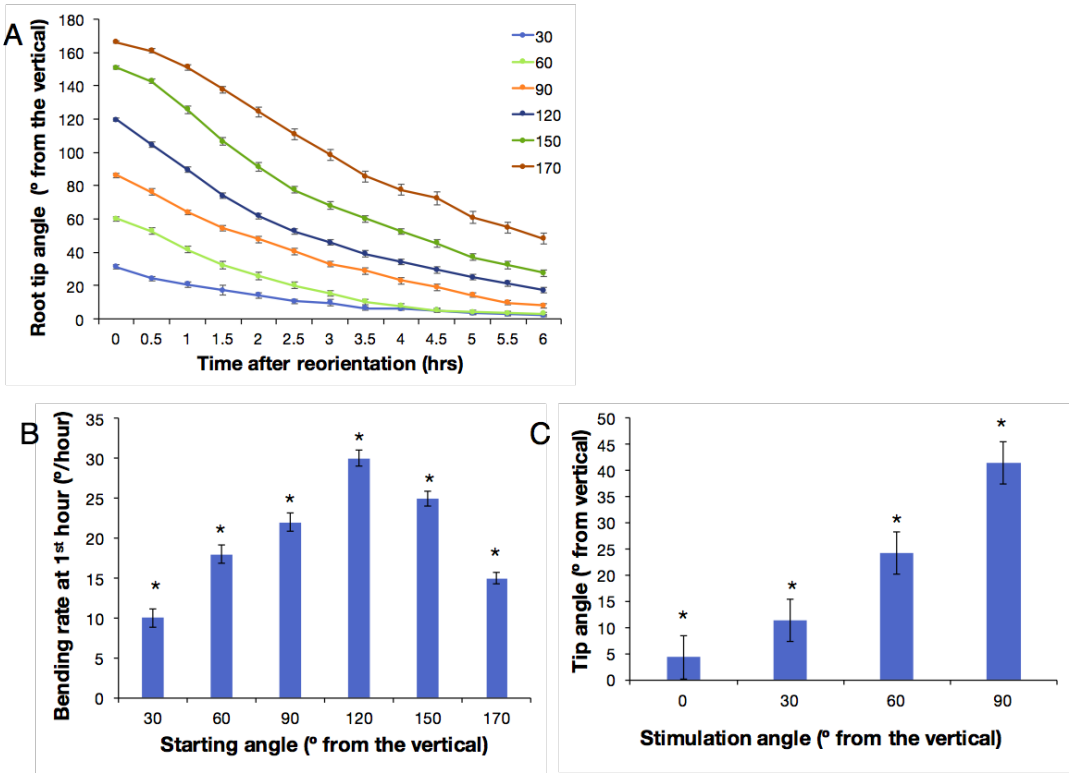

Figure 3.1 Gravitropic responses of Arabidopsis are angle-dependent.
(A) Gravitropic response kinetics assays of Arabidopsis at different stimulation angles (30°–170°). (B) The first hour bending rate for each angle, $n \geq 76$ at each angle, bars represent s.e.m., stars represent a p value of < 0.05, 1-way ANOVA, Tukey's HSD test between all angle pairs. (C) Measurement of root tip angle after 6 hours of clinostat rotation after a 30-minute gravity stimulation at different angles, $n \geq 39$ at each angle, bars represent s.e.m., stars represent a p value of < 0.05, 1-way ANOVA, Tukey's HSD test between all angle pairs.

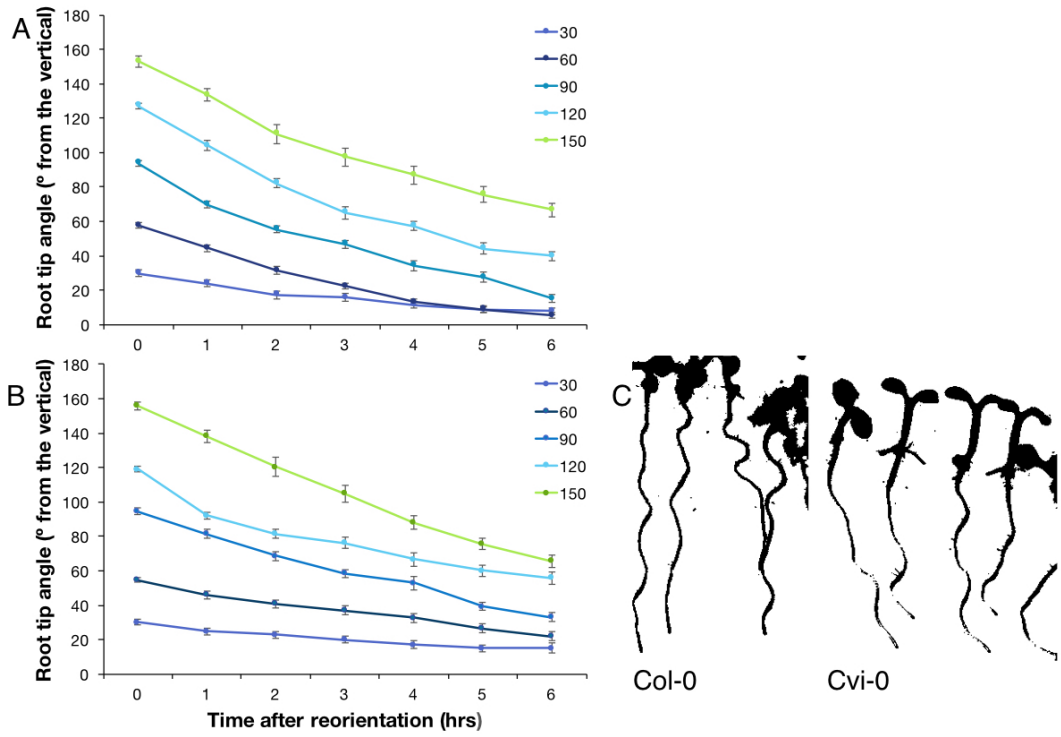

Figure 3.2 Gravitropic response of the Arabidopsis ecotype Cvi-0.
(A) Gravitropic response assays reoriented between 30°–170° and with their natural skew and (B) against their natural skew, n ≥ 30 at each angle, bars represent s.e.m. (C) Example images of Col-0 (left) and Cvi-0 (right) 5-day-old seedlings.

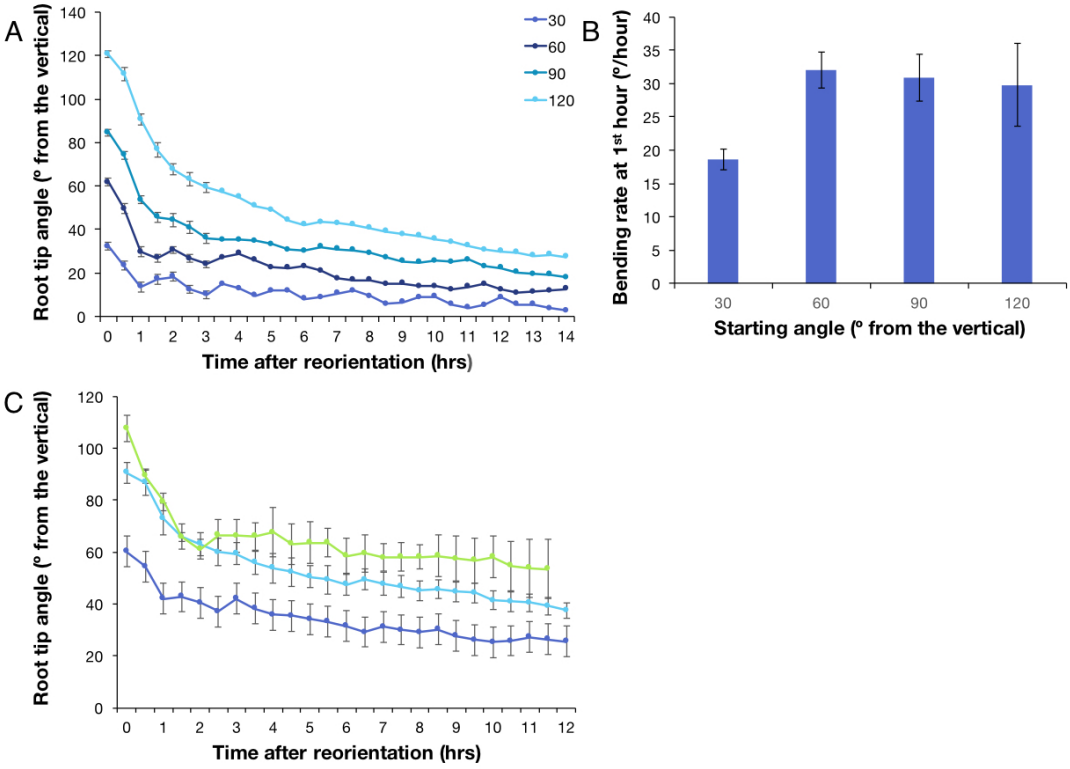

Figure 3.3 Gravitropic response of bean and wheat.
(A) Gravitropic response assays of bean plants reoriented at angles 30°–120°, n ≥ 9 at each angle, bars represent s.e.m. (B) The first hour bending rate was calculated for each angle for bean, n ≥ 9 at each angle, bars represent s.e.m. (C) Gravity response kinetics of wheat roots n ≥ 7 at each angle, bars represent s.e.m.

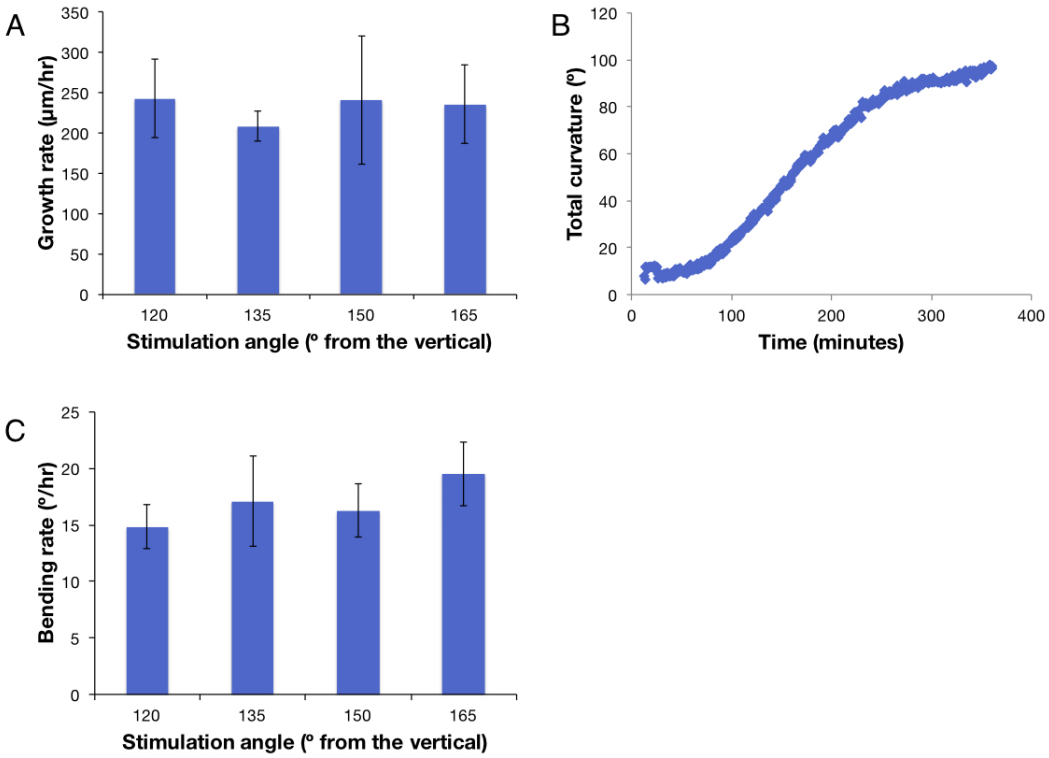

Figure 3.4 Gravitropic response of Arabidopsis at higher angles.
(A) Growth measurements of plants used in gravitropism assays using root tracker software (Mullen et al., 2000) prior to reorientation. (B) Example response curve created from output data from the ROTATO program. (C) Gravitropic bending rates at different stimulation angles measured using a constant feedback analysis system (ROTATO) (Mullen et al., 2000), $n \geq 8$ at each angle, bars represent s.e.m.

3.2.2 Using the auxin reporter *DR5v2* to measure auxin response asymmetries in the Arabidopsis root tip during gravistimulation

The apparent applicability of Cholodny-Went theory, and the existence of angle-dependence in root gravity response, led us to examine the possibility of angle-dependent differences in auxin asymmetry in gravistimulated roots. Previous studies using the reporter *DII-VENUS* failed to detect any auxin asymmetry below ~48° to the vertical (Band et al., 2012). To investigate this question we used the modified DR5–based auxin response reporter *DR5v2* (Liao et al., 2015). Five-day-old roots were maintained at specific angles of stimulation for 1.5 hours by manually rotating the root tips as they responded (Figure 3.5D) or maintained via ROTATO (Figure 3.5A–C), and then imaged through the center of the root. The GFP fluorescence of each nucleus was imaged on the upper and lower side of the root epidermis extending away from the stem-cell niche under the lateral root cap (LRC) (Figure 3.4A). The GFP fluorescence ratio between lower and upper sides of the root was used as a proxy for the auxin asymmetry at a given angle (Figure 3.5A–D). This experiment confirms that there are angle-dependent differences in auxin response asymmetries, however, only when comparing angle differences of 30° or more, $p < 0.05$, 1-way ANOVA, Tukey's HSD test. Auxin asymmetries were also plotted against stimulation angle (°) (Figure 3.5C). A linear regression was fitted to the plot and a R^2 calculated to validate a correlation between stimulation angle and auxin asymmetry. With a R^2 value of 0.35 it is possible to say there is a moderate positive correlation between the stimulation angle and the auxin response asymmetry. The data show a trend between auxin asymmetry and stimulation angle for roots constantly stimulated by ROTATO (Mullen et al., 2000) (Figure 3.5C), manually constrained, and allowed to freely respond (Figure 3.5D). However, the roots that were stimulated on ROTATO (Mullen et al., 2000) showed stronger auxin asymmetries at all angles, although still do not show significant differences at the resolution of 15°. Moreover, a quantifiable statistically significant auxin asymmetry was not found at 30°. If Cholodny-Went theory is correct, then an auxin asymmetry is expected at angles greater than 15°, which is the stimulation angle at which more than 50% of roots respond (Mullen et al., 2000). Therefore, this lack of a significant auxin asymmetry at 30° and significant differences in roots reoriented within 15° of one another is most likely due to the limited dynamic range of the reporter.

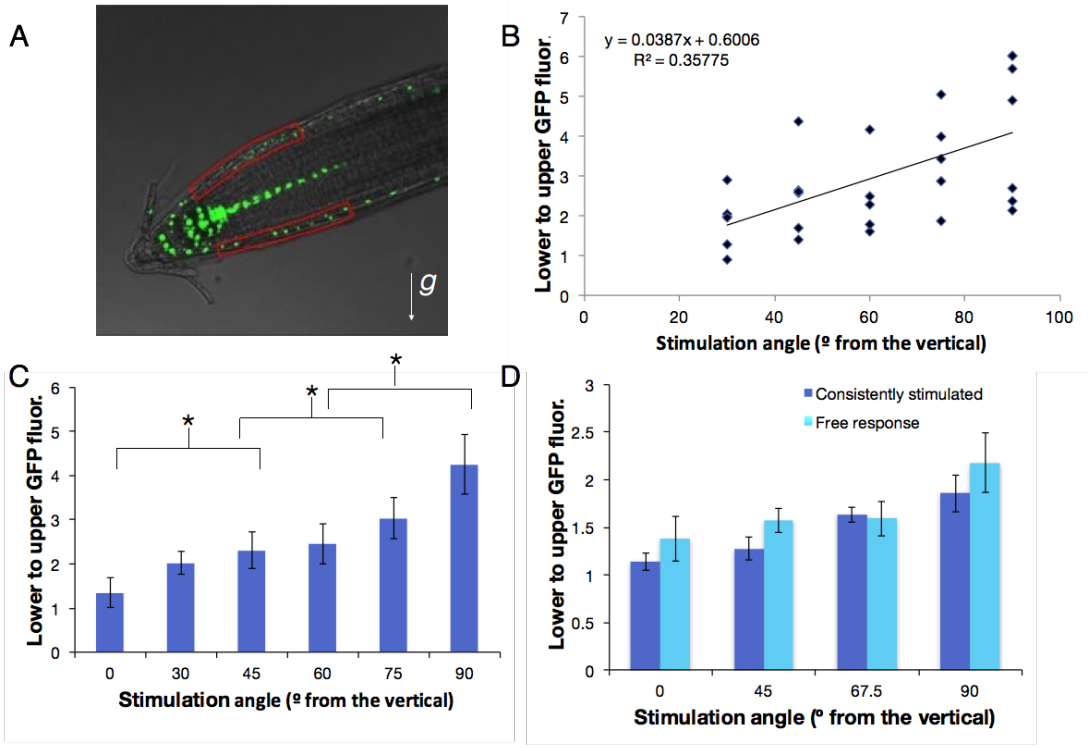

Figure 3.5. Angle-dependent auxin asymmetries can be visualised using *DR5v2*.
(A) An example image used for analysis of inferred auxin asymmetries using the *DR5v2* reporter. (B-C) Inferred auxin asymmetries stimulated at different angles using ROTATO (Mullen et al., 2000), $n \geq 7$ each angle, stars represent $p < 0.05$, 1-way ANOVA with Tukey's HSD results showing significance between pairs. (D) Inferred auxin asymmetries from roots either gravistimulated by hand or allowed to freely respond for 1.5 hrs, $n \geq 9$ each angle and type of stimulation. All bars represent s.e.m.

3.2.3 Using the ratiometric auxin reporter *R2D2* to measure auxin asymmetries in the Arabidopsis root tip during gravistimulation

The experiments described using the *DR5v2* reporter showed that there is a positive trend between auxin response asymmetries and stimulation angle. To relate these observations to auxin levels in graviresponding root tips, the auxin signalling input reporter *R2D2* was used (Liao et al., 2015). *R2D2* is a degradation-based auxin reporter that shows exogenous auxin-induced degradation of GFP within 5 minutes (Liao et al., 2015). Therefore, analysis was performed using a vertical-stage confocal imaging setup (see Methods 2.6.2). For this experiment, 5-day-old *R2D2* seedlings were allowed to rest vertically for an hour on a rotatable stage and were then imaged through the centre of the root before reorientation (Figure 3.6A–D). An example image of an imaged root can be found in Figure 3.6A. The roots were then gravistimulated at different angles (30°–120°) for 40 minutes and imaged again. Ratios of the non-degradable ntdTomato fluorescent protein to degradable VENUS fluorescent protein were obtained for each nucleus of the upper and lower root epidermis extending away from the stem-cell niche under the LRC (Figure 3.6A–D).

This ratio was used to infer relative auxin levels in the upper and lower epidermis of the roots. The important observation was made that there are inherent differences in R2D2 signals between hair and non-hair cell types (Figure 3.6B, Student's t-test, $p < 0.01$). From these measurements in vertically growing roots, it is clear that non-hair cells contain more auxin than hair cells. These innate differences in cell types affect the measured ratios (Figure 3.6C), obscuring auxin asymmetries at low angles. To overcome these inherent differences between hairs and non-hair cell types, only ratios taken of the same cell type were used to compare auxin asymmetries between angles (Figure 3.6D). When only the same cell types are compared, there is an angle-dependent increase in auxin gradients as the stimulation angle increases. These data support the idea that Arabidopsis root gravitropism is controlled by angle-dependent differences in auxin asymmetry across the root. It is possible that these auxin asymmetries were previously unreported for two reasons. Firstly, the new version of *R2D2* allows for more sensitive measurements in auxin changes of auxin 'input'

due to its ratiometric ability. Secondly, in this approach, the innate differences between hair and non-hair cells were taken into account. It is possible that at lower stimulation angles, the presence of an auxin asymmetry could be obscured by the noise generated by the differences between these two cell types, as the asymmetry is already expectedly low.

To investigate the possibility that time affects the magnitude of the angle-dependent auxin asymmetry, experiments were first done comparing roots gravistimulated for 1 and 3 hours (Figure 3.7A). In these experiments roots were kept close to 90° through frequent monitoring and carefully rotated back to 90° after a gravity response. Roots gravistimulated in this manner for 3 hours showed a larger auxin asymmetry than roots reoriented for 1 hour ($p < 0.05$, Student's t-test). This experiment demonstrated that the auxin asymmetry increases with continued gravistimulation. Following this idea, to ensure that roots gravistimulated at higher angles do not have a larger asymmetry than roots gravistimulated at lower angles merely due to time spent responding, a longer experiment was performed (Figure 3.7B). In this experiment, roots were stimulated at 120°, and 90°, respectively, and then allowed to respond freely for 2 hours, during which the roots responded approximately 30°. These roots were also imaged to quantify auxin asymmetries. The roots stimulated at 120° still had a larger auxin asymmetry than roots stimulated at 90°, $p < 0.05$, Student's t-test. This experiment confirmed that even with longer time points, there still exists an angle-dependent affect. Together, these data demonstrate that angle-dependent differences in auxin asymmetry exist independent of the period of gravistimulation and response.

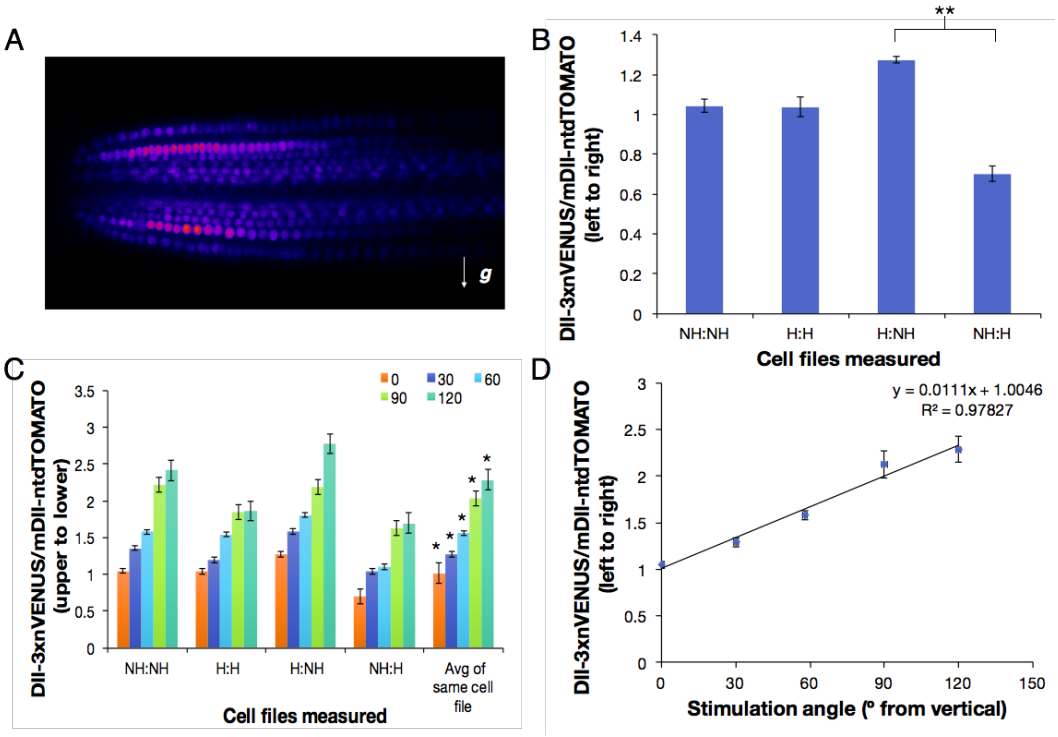

Figure 3.6 Angle-dependent auxin asymmetries in the Arabidopsis primary root tip can be quantified using R2D2.
(A) An example image used for analysis of inferred auxin asymmetries using the R2D2 reporter. (B-D) Inferred auxin asymmetries of primary roots gravistimulated at angles (30°, 60°, 90°, and 120°) and imaged vertically. (B) GFP and ntdTomato fluorescence of *R2D2* comparing auxin asymmetries between NH and H cell files in vertically growing roots, $n \geq 5$, stars represent $p < 0.01$, Student's t-test. (C-D) Inferred auxin asymmetries of roots gravistimulated for 40 minutes at different angles. (D) Inferred auxin asymmetries of gravistimulated roots based on auxin measurements in only the same type of cells, $n \geq 12$ for each cell file plants each angle, stars represent $p < 0.05$, 1-way ANOVA, Tukey's HSD between each pair when compared within the same cell file. All bars represent s.e.m.

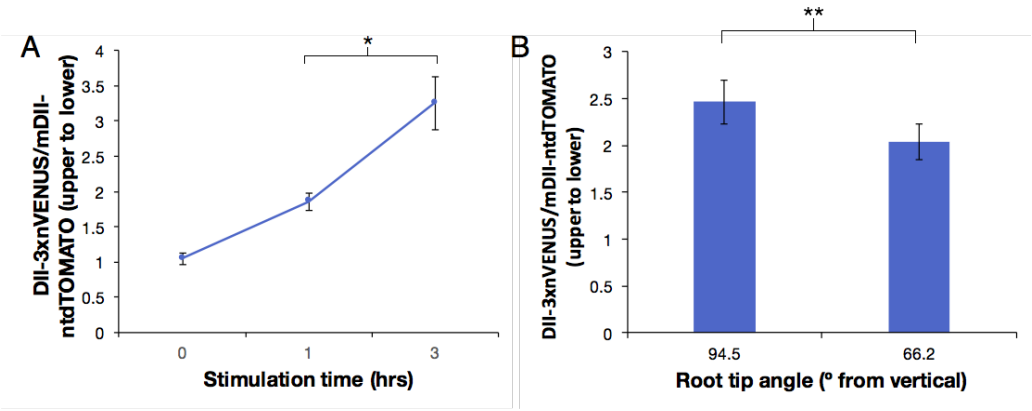

Figure 3.7 The relationship between auxin asymmetry and stimulation time in the Arabidopsis primary root tip.
(A) Inferred auxin asymmetries of *R2D2* seedlings continuously gravistimulated for 3 hours by manual rotation at 90°. Plants were imaged at 1 hour and 3 hours after gravistimulation and the magnitude of the auxin asymmetry was quantified within the same type of cell file (H-H, NH-NH), $n \geq 6$, bars represent s.e.m., stars represent $p < 0.05$, Student's t-test. (B) Inferred auxin asymmetries of *R2D2* seedlings that were reoriented 120°, and 90° and allowed to freely respond for 2 hours, imaged, and the magnitude of the auxin asymmetry was quantified, $n \geq 16$ each angle, stars represent $p < 0.01$, Student's t-test.

3.2.4 Auxin asymmetries in gravity responding lateral roots

Angle-dependent variation in gravity response is a key component of a recently proposed model for the maintenance of nonvertical gravitropic setpoint angles (GSAs) in lateral roots and shoots (Roychoudhry et al., 2013). Crucially, lateral roots can robustly maintain a given GSA against displacement above or below that angle, meaning that lateral roots must be able to undergo negative, as well as positive, gravitropism. To test if these gravity responses were associated with the generation of auxin asymmetries that are consistent with Cholodny-Went theory, the *R2D2* reporter and vertical-stage confocal imaging were used. Significant differences were observed in both up-bending and down-bending lateral roots (Figure 3.8B). This result confirms that the maintenance of GSA in Arabidopsis lateral roots involves the regulation of auxin distribution, entirely consistent with Cholodny-Went theory. Furthermore, the data provide mechanistic insight into the kinetic differences between up-graviresponding and down-graviresponding lateral roots. Lateral roots reoriented above their GSA respond more quickly than those reoriented below their GSA (S. Roychoudhry, pers. comm.). In Figure 3.8 we see larger auxin gradients in roots that are reoriented above their GSA, which, assuming Cholodny-Went theory is correct, is consistent with a faster response rate.

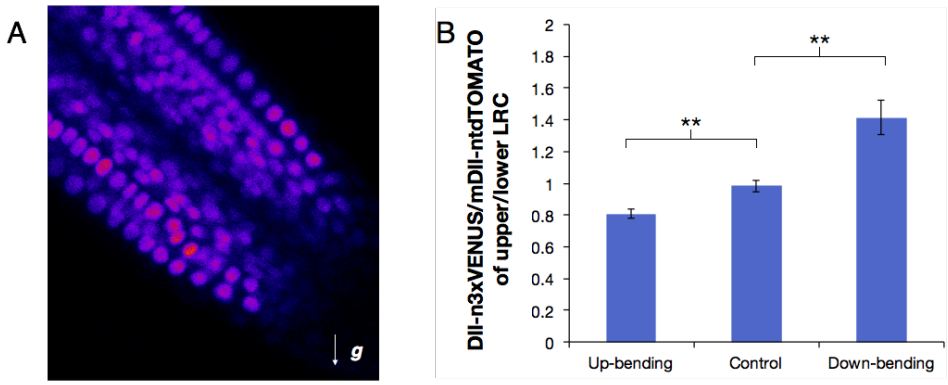

Figure 3.8 Lateral roots exhibit quantifiable auxin asymmetries when reoriented above and below their GSA.
(A) Example image of an *R2D2* lateral root. (B) Auxin asymmetries of lateral roots of 10-day-old seedlings were imaged growing at their GSA and then reoriented 45° and imaged 40 minutes later. Ratio of upper to lower auxin asymmetries were calculated in the same way as Figure 3.6 comparing only roots of the same cell type, $n \geq 12$ for each reorientation direction, bars represent s.e.m., stars represent $p < 0.01$, Student's t-test.

3.3 Discussion

A unified model of root gravitropism taking into account both angle-dependent differences in the magnitude of gravity response and the full physiology of the kinetics of gravitropism has yet to be put forward. A time-dependent model based on a “tipping point” mechanism with auxin asymmetries being lost at ~48° from the vertical has been previously proposed (Band et al., 2012). However, as previously stated, this model is inconsistent with the complete physiological kinetics of primary root gravitropism. Since 2012, when this model was proposed, there have been improvements in the tools to quantify auxin asymmetries in a gravity responding root. The new *R2D2* reporter, together with the use of vertical imaging, allows a more sensitive read-out of auxin asymmetries in the root. From these experiments, it became clear that the inherent variation in auxin levels in hair and non-hair cell types can obscure auxin asymmetries at low stimulation angles (Figure 3.6). This is not surprising, as differences of auxin levels in hair and non-hair cell types have been previously reported (Jones et al., 2008; Löfke et al., 2015). Further work can be done to investigate the role of hair and non-hair cell types in gravitropism.

In addition, previous models that are based on time-dependence could possibly conflate the timing of the degradation of the DII-VENUS fluorescent protein and the timing of gravity response (Band et al., 2012). Using both a time-dependent model and a degradation–based reporter, it is difficult to tease apart whether or not the observed time-dependent events reflect the time required for an auxin asymmetry to occur during early gravity response, rather than the time it takes for the fluorescent protein to degrade. In this thesis we use both new techniques and an angle-dependent approach to attempt to create a model that describes the entirety of primary root gravitropism kinetics.

To characterise and understand the mechanism governing gravitropic response, experiments were focused on an angle-dependent approach. First, large scale experiments of Arabidopsis in both Col-0 and Cvi-0 ecotypes were done to characterise and confirm that gravity response is indeed angle-dependent in Arabidopsis. In addition, clinostat experiments, in which roots are gravistimulated at different angles for the same length of time, confirm that gravitropic response is mainly angle-, not time-, dependent

(Figure 3.1). Both of these experiments support the idea that primary roots show a stronger gravitropic response at higher stimulation angles (less than 135°) than at lower stimulation angles. This result is consistent with observations from Julius Sachs to more recent research (Iino et al., 2005; Galland, 2002; Mullen et al., 2000). Since Julius Sachs, the rate of gravity response has been found to be dependent on the sine of the stimulation angle for roots in species such as *Lepidium savitium* (Larsen, 1969), *Lens culinaris* (Perbal, 1974), and most recently Arabidopsis (Mullen et al., 2000). As well as roots, angle-dependent gravity response has been found in the coleoptiles of *Avena* (oat) (Galland, 2002), maize (Iino et al., 2005) and rice (Iino et al., 2005). Even beyond the plant kingdom, sine law has been observed in the fungus *Phycomyces blakesleeanus* (Galland et al., 2002). Given the plethora of data demonstrating angle-dependent gravitropism across many species, it is surprising that primary root gravitropism in beans and wheat is not angle-dependent (Figure 3.3). However, these data appear to be similar to a lack of angle-dependence found in previous studies with maize roots (Barlow et al., 1993). Further work could be done to investigate the differences in gravitropic response across species, as this information could give further mechanistic insight into how this varying magnitude of response is specified.

While most of the data presented corroborates previous work, some other inconsistencies were found. Data shown in (Figure 3.1) suggest that at higher stimulation angles there is a maximum speed of response at approximately 130°. While our results are incongruous with the most current work on Arabidopsis roots (Mullen et al., 2000), it is in agreement with other previously published works. Works such as (Larsen, 1969) and older data plotted by Audus (Audus, 1964) cite approximately 130° as the “optimum” angle for gravistimulation. Furthermore, another work suggested adding a cosine term to this so-called sine law to explain an observed maximum gravitropic bending angle between 120°–130° (Galland, 2002). In contrast, the previously published work on Arabidopsis (Mullen et al., 2000) used a constant feedback response system, called ROTATO, and states that the stimulation angle leading to the greatest gravitropic response is 90°. To further investigate this, in this thesis, experiments were done on ROTATO at higher stimulation angles (120°–165°). The data from these (Figure 3.4) suggest that there is a loss of angle-dependence at higher angles, as the rate of response does not increase or change between these higher angles.

These ROTATO data are also inconsistent with the data gathered from roots allowed to respond freely (Figure 3.1). This suggests that it is unlikely that angle-dependence is broken at these higher angles. These differences may be due to the method of using ROTATO as a way to constantly gravistimulate the roots. It is possible that when roots are stimulated on ROTATO, the statoliths have time to settle on the lower cell wall during the early stages of the experiment and the rates are only sampled after this process has happened. If this is true, it is possible that the latency period would be shorter at higher angles, even if the maximum response speed at 90° and 120° appears the same when measured on ROTATO. A future possible experiment that could be done is to measure the latency period of roots gravistimulated on ROTATO between 90°–120°. This experiment would also provide mechanistic insights into gravity perception.

Another possible explanation for the differences in optimum angle for gravistimulation between roots allowed to freely respond and roots stimulated on ROTATO is that the columella creates auxin asymmetries based on information gathered on a population level. It is possible that each statolith-containing cell provides information about the gravity vector, and the sum of this information determines gravity response. It is perhaps necessary to create a working model in which statoliths are analysed at a population level as there is already evidence that different tiers of the columella contribute at different angles of reorientation (Blancaflor et al., 1998). To address how statolith sedimentation affects gravity perception and response, live-cell imaging of statoliths within a gravity responding root is necessary. As part of this thesis, a published amyloplast fluorescent marker (Nelson et al., 2007) was used to attempt to analyse the movement of statoliths during gravity response (Figure 7.5). However, this marker was not expressed in the columella adequately enough to quantify statolith movements. Future work to image statoliths could include the generation of a better amyloplast marker expressed via a more columella-specific promoter such as *ARG1-LIKE2* (*ARL2)* (Harrison and Masson, 2007) in the root and/or visualisation via cryogenic electron microscopy and differential interference contrast microscopy (Leitz et al., 2009).

The work presented in this thesis is consistent with Cholodny-Went theory, and the results point towards auxin being the governing mechanism behind the so-called sine law. However, experiments with the *DR5v2* reporter did

not yield significant results between 0° and 30° (Figure 3.1). If auxin asymmetries are the governing mechanism for gravity response in the root, there must be quantifiable auxin response asymmetries at a stimulation angle of 30°, since all primary roots respond at this stimulation angle (Mullen et al., 2000). While the experiments with *DR5v2* did not find a significant, measurable asymmetry in the *DR5v2* signal in roots stimulated at 30° (Figure 3.5), it is likely that this small asymmetry is out of the dynamic range or sensitivity of the reporter. *DR5v2* is an improvement upon *DR5::GFP*, but it is likely not sensitive enough to detect these small changes. However, these results do confirm that there are angle-dependent differences in auxin asymmetries, albeit only significant when comparing differences of 30° or more apart.

While *DR5v2* (and *DII-VENUS* from previous studies (Band et al., 2012)) appear not sensitive enough to detect small auxin asymmetries that are most likely present at lower angles, the data using the *R2D2* reporter suggest that *R2D2* is sensitive enough. The results of the experiments with *R2D2* (Figure 3.6) show a significant auxin asymmetry between the upper and lower LRC at 30°. This confirms Cholodny-Went theory, but is inconsistent with a previous report (Band et al., 2012). However, the result in this thesis is most consistent with the kinetics of root gravitropism. The previous “tipping point” model suggested that there is a loss of auxin asymmetry after ~100 minutes of gravity response. In that model, either Cholodny-Went theory is incorrect and there is another mechanism driving differential growth in roots at angles below ~48°, or the tools used at that time were not sensitive enough to detect these asymmetries. Indeed, in this chapter, the use of *R2D2,* together with both vertical imaging and comparing only the same type of cells against each other, demonstrates both a measurable and significant auxin asymmetry at 30° and an angle-dependent root gravitropism.

In Figure 3.7, the effect of time on auxin asymmetries was also explored. The data show that an increase in time does lead to a greater auxin asymmetry (Figure 3.7), but when allowed to freely respond for a longer period of time, there is still an angle-dependent effect. In previously published work, these time-dependent changes in the fluorescence of graviresponding *DII-VENUS* plants were used to create a model of root gravitropism (Band et al., 2012). It is difficult to tease apart time parameters

arising from the degradation of the fluorescent protein and the kinetics of the establishment of an auxin asymmetry that occurs in early gravity response. In the approach of this thesis, we try to isolate changes in the gravitropic response that are dependent on auxin asymmetry by keeping the time in which the auxin asymmetry was measured constant.

Despite giving insight into the mechanisms of angle-dependent gravitropism, there is much further work to be done. This should include more vertical imaging at angles greater than 120°. If the maximum response occurs at ~130°, it is very likely that the magnitude of auxin asymmetry will decrease at angles greater than 135°. This would further confirm that auxin asymmetries govern the magnitude of gravitropic response in primary roots. Furthermore, with live-cell imaging of statoliths, the mechanism of gravity perception and the basis of this angle-dependent specificity could be further understood.

During this thesis, the auxin asymmetries in lateral roots of Arabidopsis were also investigated. Lateral roots are constantly responding to gravity as they maintain their gravitropic set point angle (GSA). The mechanism in which lateral roots maintain their GSA is likely similar to the mechanism which governs primary root angle-dependent gravitropism. The results presented in Figure 3.8 with *R2D2*, show that auxin asymmetries likely drive gravity response in lateral roots as well as primary roots. It is interesting to note that lateral roots that are responding downwards show twice the magnitude of auxin asymmetry in comparison to lateral roots that are responding upwards. This is currently unexplained but is somewhat consistent with the kinetics of lateral root reorientation, as roots reoriented above their GSA respond more quickly than lateral roots reoriented below their GSA (S. Roychoudry, pers. comm.). There also seems to be a weaker auxin asymmetry in lateral roots than primary roots. This may be explained by kinetics of gravity response as lateral roots respond more slowly than primary roots. This result gives further mechanistic insight into how lateral roots maintain their GSA and the kinetics of downward and upward reorienting lateral roots. Another possible explanation could involve the sensitivity of young lateral roots to auxin. It is possible that a drop in auxin concentration on the lower side of a lateral root that has been moved below its GSA is sufficient enough to promote elongation of the cells on its lower side. This possibility could also account

for differences in the magnitude of asymmetries in up- and down-responding roots.

In summary, the results presented in this chapter support an angle-dependent model of gravitropism. Since the 1880s it has been observed that the farther a plant organ is displaced from its GSA, the greater the magnitude of response. This has been confirmed across many species using classical techniques and with new methods of constant stimulation such as ROTATO in Arabidopsis (Mullen et al., 2000). While unlike previously published work in Arabidopsis (Mullen et al., 2000), work presented here suggests that the angle of highest gravitropic response may be higher than 90°. Previously, a time-dependent "tipping-point" mechanism has also been proposed for root gravitropism. However, it is demonstrated in this chapter that a different mechanism may in fact control root gravity response. Experimental evidence suggests that auxin asymmetry arising from angle-dependence dictates the magnitude of the growth response. The present work furthers the understanding of root gravitropism by demonstrating an angle-dependence in the magnitude of the response and elucidating its underlying auxin asymmetries. Furthermore, inherent differences in auxin amount in hair and non-hair cells types was shown (Figure 3.6). However, more work is needed to better understand the governing mechanism. In the coming chapters, the role of *PIN*s and their localisation and activity are investigated further to delve deeper into this mechanism.

Chapter 4
Mechanisms Generating and Maintaining Auxin Asymmetry During Gravity Response

4 Mechanisms Generating and Maintaining Auxin Asymmetry During Gravity Response

4.1 Introduction

Cholodny-Went theory dictates that auxin gradients are the driving force behind tropic responses. In both roots and shoots, when a plant is reoriented on its side, auxin is transported laterally to the new lower side of the organ. In roots, PIN3 is known to direct auxin in the statocytes of the columella towards the new lower side (Friml et al., 2002). Auxin that is redirected to the lower side of the root is then transported to the epidermis in the elongation zone by PIN2/AUX1-mediated flow, where auxin inhibits cell elongation, and causes downward bending of the root (Luschnig et al., 1998; Swarup et al., 2005; Marchant et al., 1999). In shoots, PIN3 is also presumed to move auxin laterally from the statocytes in the endodermis to the epidermis, where auxin promotes cell elongation, causing shoots to bend upwards. This model of auxin flow during tropic responses has been further corroborated by genetic studies. Mutations in *PIN3* lead to defects in both gravitropic and phototropic responses (Friml et al., 2002). Moreover, *PIN3* has been visualised rapidly relocalizing to the new lower side of the Arabidopsis root columella during gravistimulation by confocal fluorescence microscopy and immunolocalisation techniques (Friml et al., 2002; Harrison and Masson, 2007).

In addition to *PIN3*, *PIN4* and *PIN7* are also expressed strongly in the statocytes and the vasculature of the primary root (summarised in Figure 4.1) and likely contribute to auxin flux during gravity response (Rosquete et al., 2013).

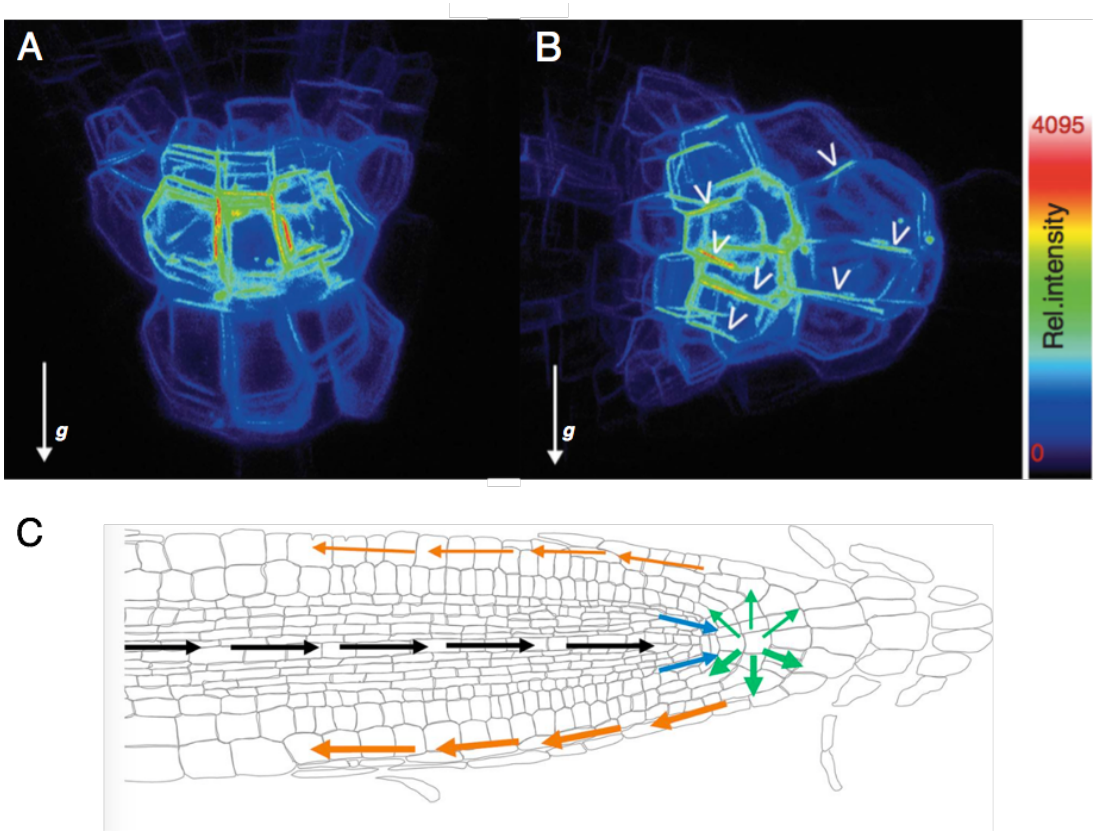

Figure 4.1 PINs direct auxin in the Arabidopsis root.
(A–B) PIN3 polarisation in the root statocytes in response to gravity. Arrowheads indicate polar localisation of PIN3 (adapted from Grundewald, 2010). (C) Gravity signal transmission in the Arabidopsis root. After statolith sedimentation, PIN3 and PIN7 (green arrows) redirect auxin in the statocytes (columella), and PIN2 and AUX1 transport auxin through the lateral root cap to the elongation zone (orange arrows), where the gravity response occurs (from Sato, 2014).

The abundance, subcellular localisation, and activity of PINs are regulated at the level of transcription, protein degradation, and subcellular trafficking (Vieten et al., 2007; Tanaka et al., 2009; Petrasek and Friml, 2009). Subcellular trafficking has been found to be one of the primary processes driving PIN subcellular localisation (Kleine-Vehn, Dhonukshe, et al., 2008). This process of constant endocytosis and recycling of the plasma membrane localised PINs is mediated by the ARF-GEF-dependent pathway and is clathrin-dependent (Dhonukshe et al., 2007). A current model gathered from data in cortex cells suggests that PINs destined to be basally localised are shuttled via a GNOM-dependent ARF-GEF pathway, while PINs that are destined to be apically localised are shuttled via a GNOM-independent ARF-GEF pathway (Kleine-Vehn, Dhonukshe, et al., 2008). Furthermore, the shuttling of PINs between these two trafficking pathways, which ultimately determine their subcellular localisation within the cell, is at least partially dependent on the phosphorylation status of serine and threonine residues within the central hydrophilic region of the long PINs (Dhonukshe et al., 2010).

The PID/WAG family of the serine/threonine protein kinases (consisting of PINOID (PID), WAG1, and WAG2), and the protein phosphatase 2A (PP2A/RCN1) are thought to modulate the phosphorylation status of PINs antagonistically (Christensen et al., 2000; Michniewicz et al., 2007; Sukumar et al., 2009). Transgenic plants overexpressing *PID* and *rcn1* loss-of-function mutants have more apically localised PIN1, PIN2, and PIN4 (Michniewicz et al., 2007), while loss-of-function *pid* mutants have more basally localised PINs (Friml et al., 2004). These observations led to the current model, which suggests that dephosphorylated PIN proteins are preferentially recruited into the basal targeting pathway, while phosphorylated PIN proteins are recruited into a putative apical targeting pathway.

In the previous chapter, data were presented to support a model of gravitropism in Arabidopsis that is dictated by angle-dependent auxin asymmetries. In this chapter, the mechanism in which the auxin asymmetries are generated and maintained at different angles is investigated, focusing on the role of *PIN3* and *PIN7* and their regulation.

4.2 Results

4.2.1 PIN3 and gravity response

To assess how *PIN3*, *PIN4*, and *PIN7* might affect auxin gradients in Arabidopsis roots, the gravity response kinetics of two different *PIN3*, *PIN4*, and *PIN7* triple loss-of-function mutants were investigated in the primary and lateral roots. Five-day-old loss-of-function *pin3 pin4 pin7* mutants were gravistimulated at 90° for 6 hours for primary root experiments. Ten-day-old loss-of-function *pin3 pin4 pin7* mutants were gravistimulated 45° above their GSA for lateral root experiments. The triple loss-of-function mutant *pin3-3 pin4-2 pin7EN* only displayed significant gravitropic defects during the 1st and 2nd hours of gravitropic response ($p < 0.05$, Student's t-test). Another triple loss-of-function mutant *pin3-3 pin4-101 pin7-102* only showed gravitropic defects after 3 hours of gravity response ($p < 0.05$, Student's t-test). There were not any significant differences in the kinetics of lateral roots reoriented above their GSA, only a significant difference ($p < 0.05$, Student's t-test) between the wild type and both triple mutants at 5 and 6 hours following reorientation (see Figure 4.2). This is a surprising result, since a previous report states that the single *pin3* mutant is gravitropically deficient (Friml et al., 2002), although another report shows only mild effects in the loss-of-function *pin3-3* mutant (Harrison and Masson, 2007). However, the homozygosity of the loss-of-function mutation of *PIN7* could not be confirmed by a genotyping PCR. Further work must be done to better characterise the role of these *PIN*s at different angles of gravity response, when true triple mutants are created.

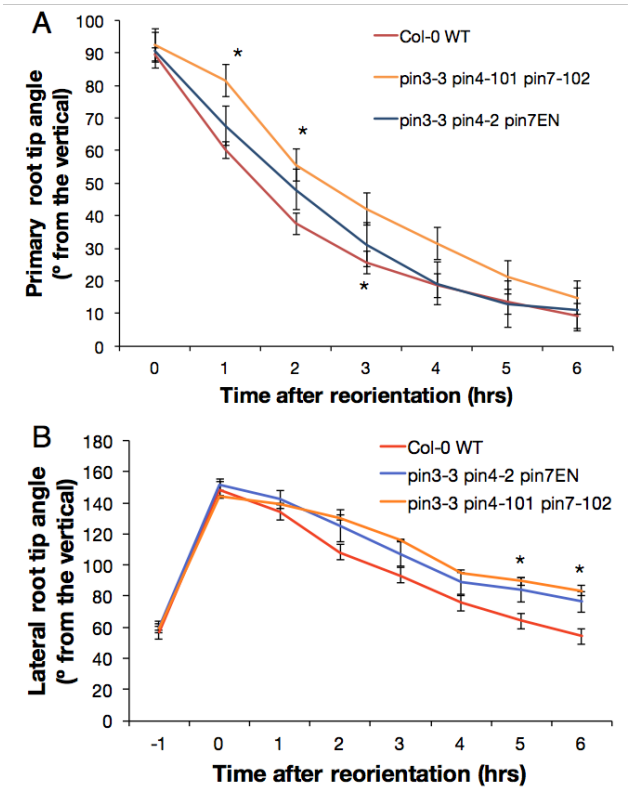

Figure 4.2 Gravity response of loss-of-function *pin3 pin4 pin7* triple mutants. (A) Gravity response kinetics of *pin3-3 pin4-101 pin7-102* and *pin3-3pin4-101 pin7EN* primary roots, n ≥ 28 each genotype. (B) Gravity response kinetics of *pin3-3 pin4-101 pin7-102* and *pin3-3 pin4-101 pin7EN* lateral roots, n ≥17 each genotype. All bars represent s.e.m., stars represent $p < 0.05$, Student's t-test.

4.2.2 PIN abundance and gravity response

One of the many ways auxin transport might be regulated during gravity response is the regulation of PIN abundance in the statocytes. Figure 4.3A assesses the abundance of *PIN3::PIN3–GFP* following a gravity stimulus. In this assay, primary roots were gravistimulated at 90° and the expression in the central columella was measured before and after gravistimulation. From these results, *PIN3* does not appear to be significantly upregulated following gravistimulation, $p = 0.128$, paired Student's t-test. It is currently thought that *PIN3* and *PIN7* are functionally redundant in the primary root columella (Zazimalova et al., 2010) as they share functional domains. Through laser ablation studies, it has been shown that the flanking cells of the columella may contribute more to gravitropic response at higher stimulation angles than at lower stimulation angles (Blancaflor et al., 1998), and there is some evidence that *PIN7* may have a more vital role at higher stimulation angles (C. Wolverton, pers. comm.). Taken together, this could mean that *PIN3* and *PIN7* are expressed preferentially in different cells of the columella, and contribute to auxin transport at different stimulation angles. To further investigate the possible role of *PIN3* and *PIN7* abundance in gravity response, *PIN3::PIN3–GFP* and *PIN7::PIN7–GFP* were analysed growing vertically and after 3 hours of gravistimulation (Figure 4.3B–C). From these images, the mean GFP fluorescence was measured separately in the central columella and in the flanking cells, and a ratio was taken to quantify the centrality of the expression of *PIN3* and *PIN7*. In comparison to PIN7, *PIN3* is more abundant in the central columella than in the flanking cells, both during vertical growth and following gravistimulation (Figure 4.3) ($p < 0.05$, Student's t-test). *PIN7–GFP* abundance did not increase overall during gravistimulation. This is similar to our previous result with *PIN3–GFP* whose abundance did not increase during similar experiments. It is clear from these experiments that the abundance of *PIN3* and *PIN7* does not regulate angle-dependent auxin gradients, therefore more regulatory components must be investigated. However, these results do confirm the possibility that *PIN3* and *PIN7* may have overlapping, but slightly different, roles during root gravitropism.

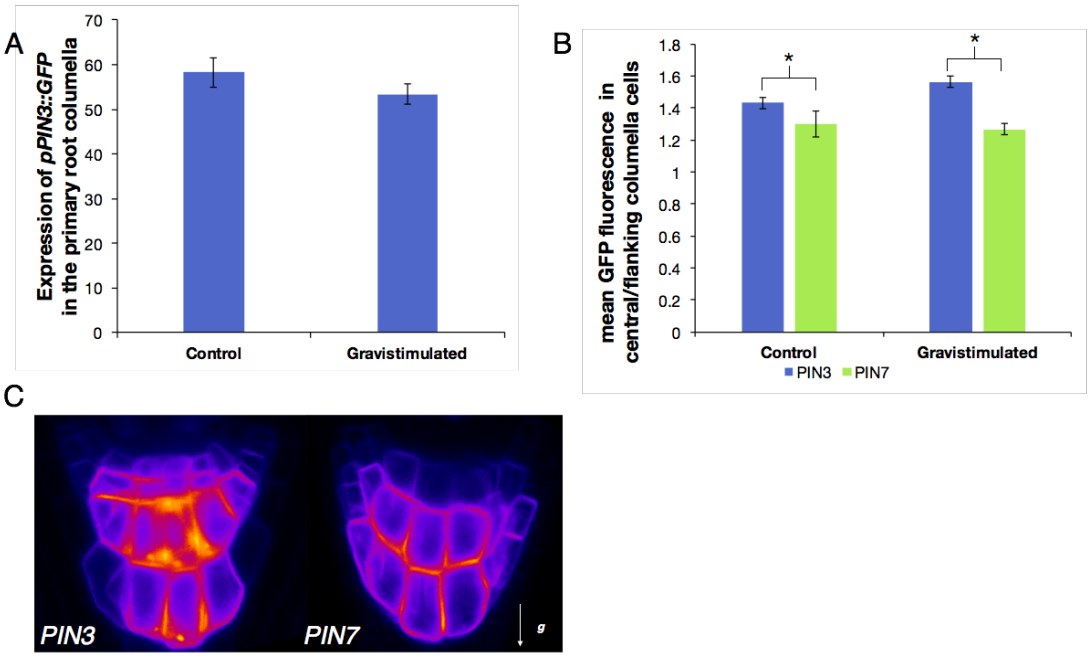

Figure 4.3 Expression patterns and abundance of *PIN3–GFP* and *PIN7–GFP* during vertical growth and gravistimulation.
(A) Mean GFP fluorescence of *PIN3::PIN3–GFP* in the columella of gravistimulated and control roots, n = 14, bars represent s.e.m., two biological replicates, p = 0.128, paired Student's t-test. (B) Expression pattern of 5-day-old *PIN3::PIN3–GFP* and *PIN7::PIN7–GFP* control roots and roots that were gravistimulated for 3 hours. Expression of GFP in the central and flanking cells of the columella was imaged and measured, n = 7, bars represent s.e.m, $p < 0.05$, Student's t-test. (C) Example expression patterns of *PIN3::PIN3–GFP* and *PIN7::PIN7–GFP* growing vertically.

4.2.3 PIN subcellular localisation correlates with stimulation angle

The previous results indicate that PIN abundance does not increase following gravity stimulation. Therefore, PIN abundance is unlikely to be driving angle-dependent auxin gradients. Since PIN3 has been shown to relocalise to the new lower side of the plasma membrane (PM) of the statocytes of the primary root of Arabidopsis during gravistimulation (Friml et al., 2002), the lower to upper subcellular localisation of *PIN3::PIN3–GFP* and *PIN7::PIN7–GFP* was investigated at different stimulation angles (Figure 4.4). In particular, to investigate whether PIN3 and PIN7 were targeted more to the lower side of the PM during gravistimulation at higher angles, *PIN3::PIN3–GFP* and *PIN7::PIN7–GFP* were imaged after a 40-minute gravistimulation at 0°, 45°, 90°, and 135°. Since it is not possible to discern PINs localised to the upper PM of one cell from PINs localised to the lower PM of a neighbouring cell, only the cells at the edge of the PIN3 and PIN7 expression domain were used (see outlined regions in example image, Figure 4.4A). To quantify the upper vs lower subcellular localisation of *PIN3–GFP* and *PIN7–GFP* at different stimulation angles, the ratio of the mean PIN3/PIN7–GFP fluorescence of the lower PM edge was divided by the mean PIN3/PIN7 GFP fluorescence of the upper PM edge of each root.

First, the percentage of roots that have a lower PM polarised columella (lower to upper PM GFP ratio greater than 1.2) was quantified for each stimulation angle (Figure 4.4B). For both PIN3–GFP and PIN7–GFP, the primary roots stimulated at 45° were more likely to show a lower PM polarisation when compared to unstimulated roots. The percentage of roots showing a PIN7–GFP lower PM polarised columella further increased above 45°, reaching almost the totality of plants at 90° and 135°. In contrast, for PIN3–GFP, the percentage of root that were polarised to the lower PM were similar after 45°.

Second, the overall ratio of lower to upper PM subcellular localisation of PIN3–GFP and PIN7–GFP was quantified for each stimulation angle (Figure 4.4B–C). These data suggest that PIN3 and PIN7 become targeted to a greater extent to the lower side PM of the columella cells with increasing stimulation angle (Figure 4.4B). PIN3–GFP is targeted more to the lower side PM following a 45° reorientation and all higher stimulation angles.

However, PIN7–GFP first shows a preferential targeting to the lower side PM following 90° reorientation ($p < 0.01$, 1-way ANOVA with Tukey HSD test).

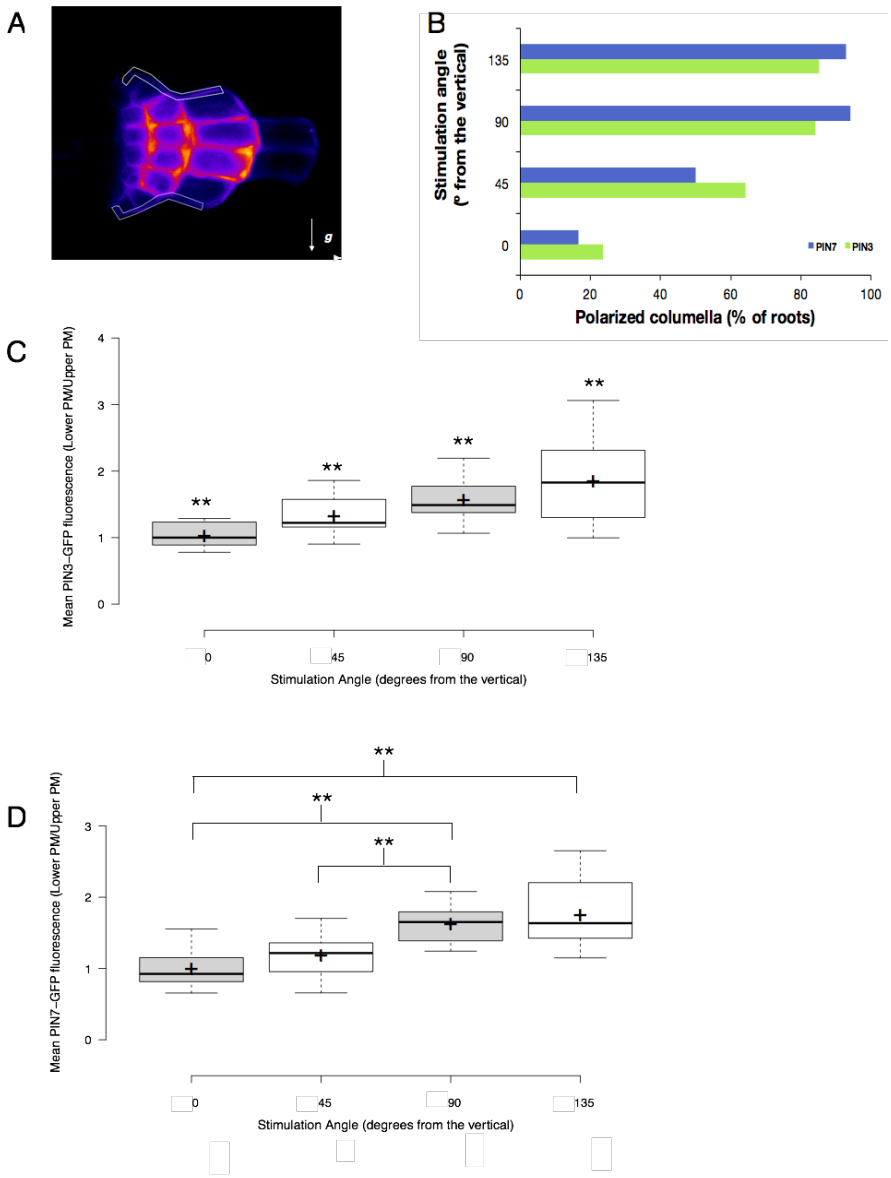

Figure 4.4 Lower to upper subcellular localisation of PIN3-GFP and PIN7-GFP at different angles of gravistimulation.
(A) Example image of a *PIN3::PIN3–GFP* root showing the expression of PIN3–GFP in the plasma membrane and the outlined lower and upper edges of the domain (B) Percentage of roots with a preferentially lower polarised columella in *PIN3::PIN3–GFP* and *PIN7::PIN7–GFP* roots while gravistimulated at different angles, $n \geq 17$ each genotype and each angle (C) Ratio of lower to upper localisation of *PIN3::PIN3–GFP,* $n \geq 17$ at 0°, 45°, 90°, and 135°, $p < 0.01$, 1-way ANOVA with Tukey HSD test. (D) Ratio of lower to upper localisation of *PIN7::PIN7–GFP*, $n \geq 17$ at 0°, 45°, 90°, and 135°, $p < 0.01$, 1-way ANOVA with Tukey HSD test. The box signifies the upper and lower quartiles, the mean is represented by a cross within the box, and the median is represented by a short black line within the box. The whiskers represent the highest and lowest values within a set.

4.2.4 Possible mechanisms involving phosphorylation regulating PIN activity during gravity response

Phosphorylation is an important component of the regulation of the apical to basal polarity of PIN proteins at the plasma membrane. A current model states that dephosphorylated PIN proteins are more likely to be trafficked into the basally localised GNOM-dependent pathway (Kleine-Vehn et al., 2009). Furthermore, previous work using the auxin response reporter *DR5rev::GFP* has shown that kinase and phosphatase inhibitors block auxin response asymmetries (Sukumar et al., 2009). To investigate the role of phosphorylation status of PINs on auxin asymmetries in gravity responding roots, gravistimulation experiments using the new *DR5v2* reporter and kinase (staurosporine) and phosphatase (cantharidin) inhibitors were carried out. Five-day-old primary *DR5v2* roots were treated with either staurosporine or cantharidin, and then gravistimulated. In this assay, after 4 hours, only 40% of staurosporine-treated roots had an auxin response asymmetry (defined by a ratio of lower to upper GFP fluorescence of greater than 1.15), while 83% of mock treated gravistimulated roots and 100% of cantharidin-treated roots had visible auxin response asymmetries (Figure 4.5). Even though a higher proportion of cantharidin-treated roots had a visible *DR5v2* asymmetry, the magnitude of the auxin response asymmetry was not greater than the staurosporine- or mock-treated roots . These data support a role for phosphorylation in PIN polarity regulation in gravity response. This result is mostly in agreement with previous studies using the *DR5rev::GFP* reporter (Sukumar et al., 2009), however the results from Figure 4.5A suggest that blocking phosphatase activity does not completely block auxin response asymmetry in the primary root tip.

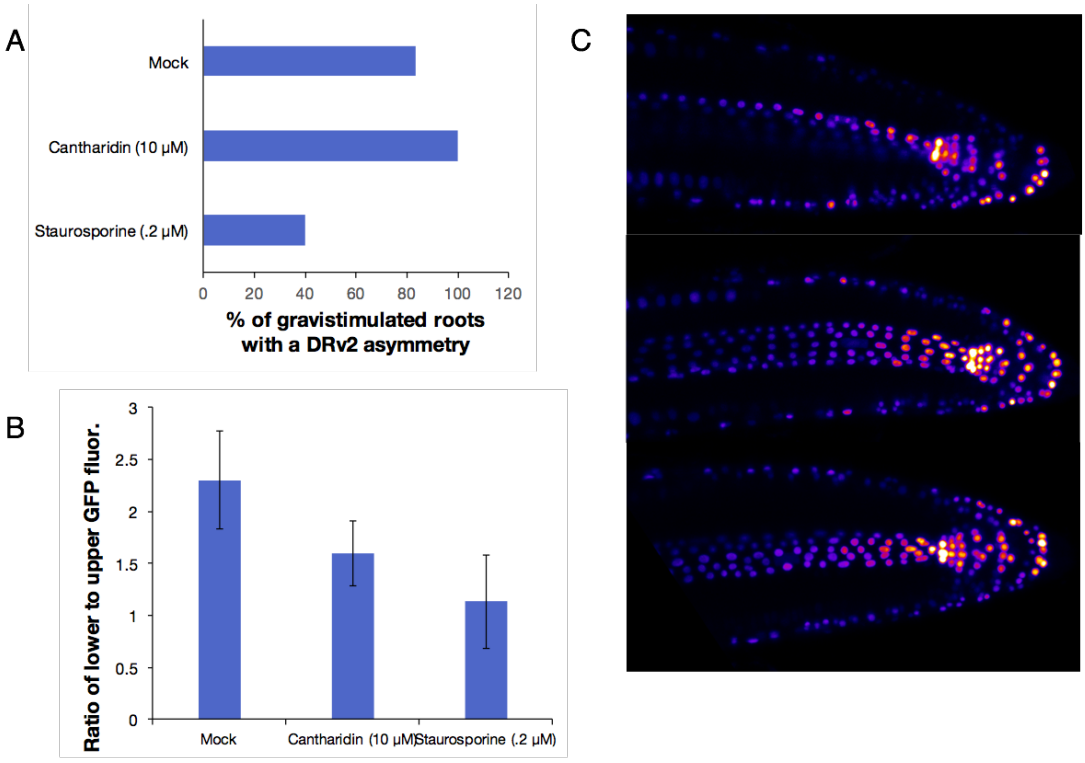

Figure 4.5 Effect of kinase and phosphatase inhibitors on auxin response gradients in gravity stimulated roots.
(A) Percentage of primary roots showing an auxin response asymmetry after 4 hours of gravistimulation, indicated by the *DRv2* reporter, n = 6 each treatment. (B) Magnitude of the *DR5v2* asymmetry in primary roots treated with cantharidin (10 µM) and staurosporine (0.2 µM) and gravistimulated for 4 hours, n = 6 each treatment, bars represent s.e.m. (C) Example images of gravistimulated mock-treated roots (top), cantharadin-treated roots (middle), and staurosporine-treated roots (bottom).

From the kinase/phosphatase inhibitor assay (Figure 4.5) it is clear that altering the possible phosphorylation status of PINs during gravity response does alter the percentage of auxin asymmetries formed. To further investigate the role of phosphorylation status in regulating the subcellular localisation of PIN3 and PIN7 during gravity response, the abundance of PIN phosphorylation regulators and their role in the statocytes were investigated. The PID/WAG family of serine/threonine protein kinases and the protein phosphatase (PP2A/RCN1) have been shown to antagonistically modulate the phosphorylation status of PINs (Christensen et al., 2000; Benjamins et al., 2001; Michniewicz et al., 2007; Sukumar et al., 2009) and therefore their subcellular localisation. Since *PID* is not expressed in the statocytes of primary or lateral root tips (Benjamins et al., 2001), *PID* was excluded from the analysis and only the role of *RCN1* during gravitropism was investigated. *RCN1* is expressed in almost all plant tissues (Blakeslee et al., 2007), including the primary root columella. To investigate whether *RCN1* is upregulated in the columella during gravity response, 5-day-old *RCN1::RCN1–GFP* seedlings were imaged before and following 3 hours of gravity stimulation at 90° (Figure 4.6). These results indicate that RCN1 does not become more abundant during gravity response and therefore, the abundance of RCN1 likely does not have a role during gravity response. Alternatively, the amount of RCN1 in the gravity-sensing cells is adequate to dephosphorylate PIN3 and PIN7 in the primary root columella. It is possible that RCN1 activity, not protein level, is regulated post-transcriptionally following gravistimulation.

Previous published data suggest *RCN1* and *PID* contribute to regulating the subcellular localisation of PINs. Furthermore, the previous experiment showed that phosphatase/kinase inhibitors affect auxin asymmetries (Figure 4.5). However, the phosphatase/kinase inhibitors could act on either the statocytes or the elongation zone. To test whether or not affecting phosphorylation status in the statocytes affects gravity response, *RCN1* and *WAG2* were expressed in the root statocyte using the *ARL2* promoter. *ARL2 (ARG1-LIKE2*) is a J-domain protein that is required for normal root gravitropism and in the root is expressed specifically in the statocytes (Harrison and Masson, 2007). Expressing *RCN1* in the statocyte of the root increases gravitropic response of primary roots (Figure 4.6). This result is in

accordance the proposed model, since an overexpression of *RCN1* would likely cause more dephosphorylation of PINs in the statocyte, potentially recruiting more PIN3 and PIN7 into the basally localised pathway, allowing either a greater magnitude of auxin asymmetry or an auxin asymmetry to occur more quickly. It does not appear that expressing the protein kinase *WAG2* in the statocyte affects gravity response in primary roots.

The D6 protein kinase (D6PK) and the D6 protein kinase-like proteins (D6PKL3) are a group of protein kinases that have been found to modulate PINs (Willige et al., 2013; Zourelidou et al., 2014). These kinases, which are expressed everywhere, including the root statocyte, are localised to the basal plasma membrane and have been found to phosphorylate PM localised PINs. Unlike PID, these proteins are not known to affect PIN polar localisations, but are thought to act as regulators of PIN activity (Zourelidou et al., 2014). To investigate this new family of kinases, gravity response experiments were done with the triple and quadruple loss-of-function mutants *d6pk012, d6pk013, and d6pk0123* (Figure 4.7). Surprisingly, none of these mutants had any gravitropic defects in the primary root. While none of these mutants displayed primary root gravitropism defects, a hypocotyl gravitropic response experiment confirmed their published phenotype (Figure 4.7B).

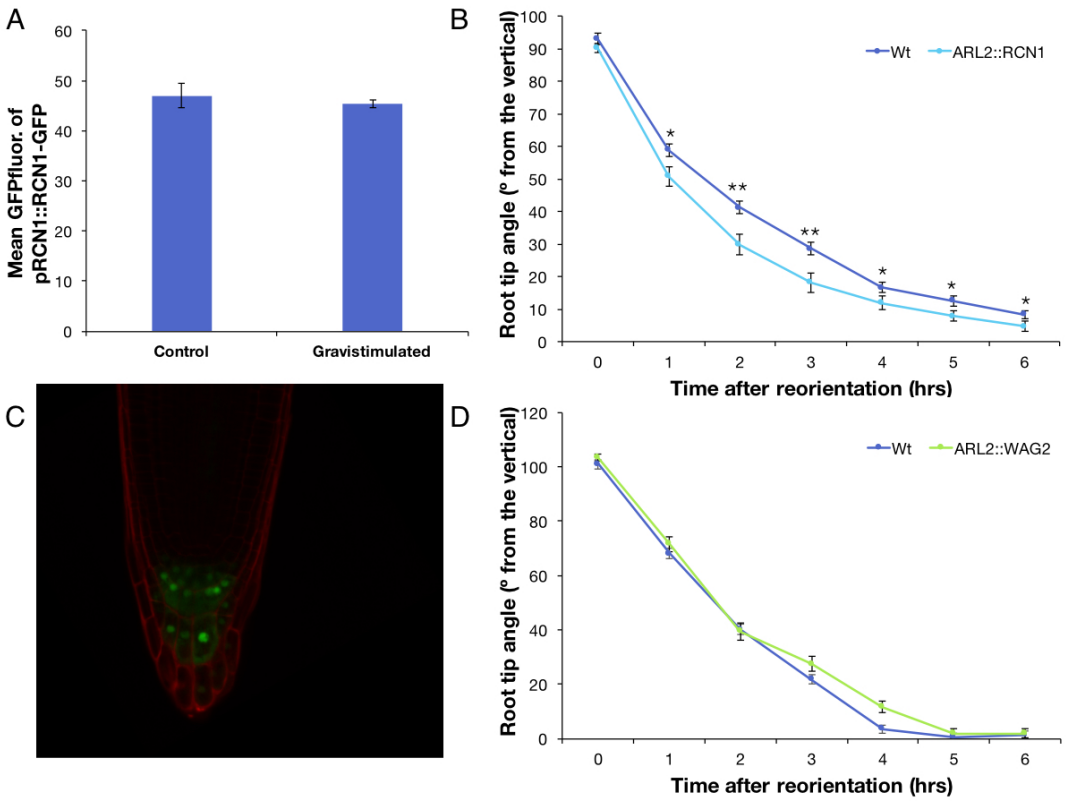

Figure 4.6 The effect of protein kinase and phosphatases on the gravity response of primary roots.
(A) Expression of *RCN1* during gravistimulation, n ≥ 10, bars represent s.e.m, $p < 0.05$, Student's t-test. (C) Example expression of *pARL2::2xGFP*. (B) Gravity response kinetics of *ARL2::RCN1* primary roots, n ≥ 27 each genotype, bars represent s.e.m., $p < 0.05$, all angles after 1st hour, Student's t-test. (D) Gravity response kinetics of *ARL2::RCN1* primary roots, n ≥ 27 each genotype, bars represent s.e.m.

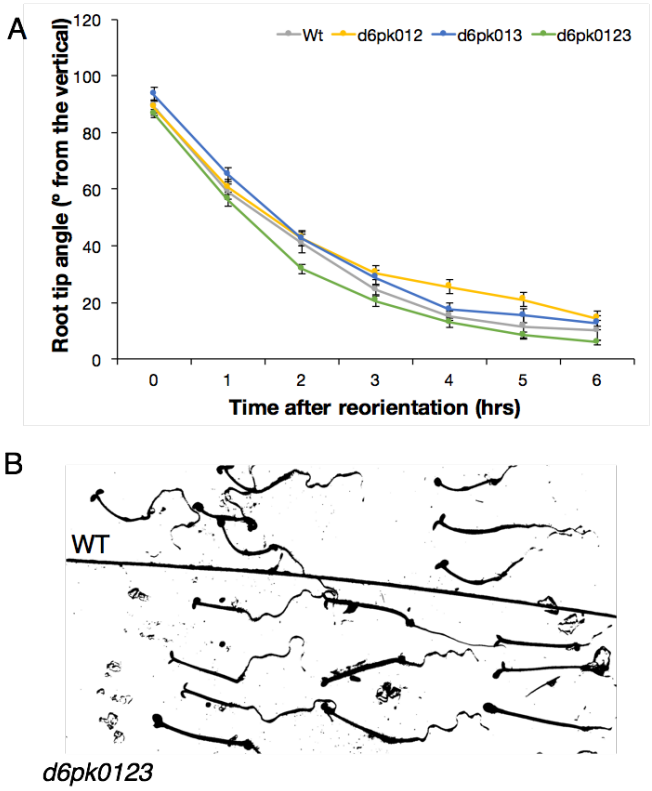

Figure 4.7 Primary root gravity response kinetics of *d6pk* mutants.
(A) Primary root gravity response kinetics of *d6pk012*, *d6pk013*, *d6pk0123* mutants, n ≥ 26 each genotype, bars represent s.e.m. (B) Gravity response of dark grown hypocotyls of Col-0 WT (top) and *d6pk0123* (bottom) 24 hours following after a reorientation by 90°.

4.2.5 The role of the cytoskeleton in regulating PIN activity and localisation during gravity response

The cytoskeleton has been implicated in several aspects of gravitropic response (see review (Blancaflor and Masson, 2003)). The role of the cytoskeleton has been probed with the use of cytoskeleton inhibiting drugs (Blancaflor and Masson, 2003). Latrunculin B is an actin depolymerising chemical and cytochalasin D inhibits new actin polymerisation. Oryzalin targets microtubules and is a known inhibitor of microtubule polymerisation. Treatment with latrunculin B has been found to inhibit the BFA-induced cycling of the auxin efflux carriers, therefore, potentially having a role in auxin efflux carrier cycling (Kleine-Vehn et al., 2006), specifically the apical targeting pathway (Kleine-Vehn et al., 2006). While these reports suggest that the actin cytoskeleton has a role in auxin efflux carrier cycling, treatment of latrunculin B does not seem to prevent an auxin asymmetry inferred from the *DR5::GFP* reporter, but actually prolonged the signal (Hou et al., 2004). In this chapter, the effects of short treatments of cytoskeleton inhibitors on the kinetics of gravity response were investigated (Figure 4.8). From these results, it is confirmed that treatment of latrunculin B does not inhibit gravity response, but actually increases the rate (Figure 4.8), while treating with the inhibitor cytochalasin D at a similar concentration does not appear to have an effect. Treating with 170 nM of oryzalin, instead, inhibits gravity response, but the effect of oryzalin on the gravity response could be due to oryzalin affecting microtubules, which are required for differential growth (Baskin et al., 1994).

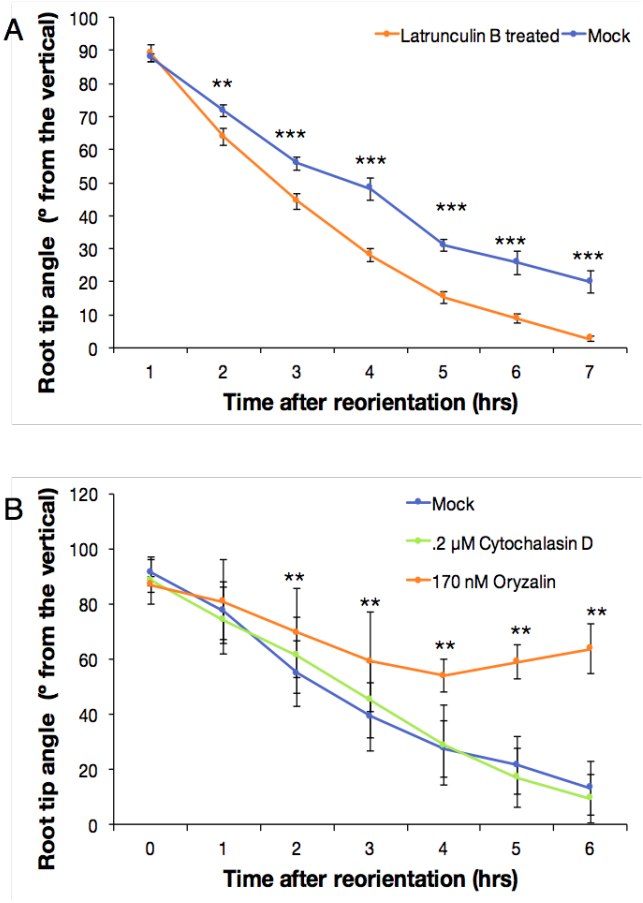

Figure 4.8 Effects of cytoskeleton inhibitors on primary root gravity response. (A) Primary root gravity response kinetics of Col-0 WT roots treated with 100 nM latrunculin B for 1 hour prior to reorientation, $n \geq 54$ each treatment, bars represent s.e.m., $p < 0.001$, Student's t-test. (B) Primary root gravity response kinetics of Col-0 WT roots treated with cytochalasin D and oryzalin for 1 hour prior to reorientation, $n \geq 21$ each treatment, bars represent s.d., $p < 0.001$, Student's t-test.

4.3 Discussion

In this chapter, the mechanism driving the angle-dependent auxin asymmetries described in Chapter 3 was sought. Since there is a lot of evidence supporting the role of PINs in transporting auxin during gravity response, the regulation of PIN abundance, subcellular localisation, and activity were investigated. *PIN3*, *PIN4*, and *PIN7* were analysed because of their expression in the statocytes of Arabidopsis primary roots.

To assess the role of *PIN3*, *PIN4*, and *PIN7* in gravity response, several triple mutants were studied. Surprisingly, two previously published triple mutants of PIN3, PIN4, and PIN7 showed very mild gravitropic defects in both the primary and lateral roots. This is contradictory to some previous reports that *pin3* loss-of-function mutants have gravitropic defects (Friml et al., 2002), but consistent with some previous reports of a mild phenotype (Harrison and Masson, 2007). To explain this mild gravitropic defect, a genotyping PCR was done on these triple mutants to try to confirm the loss-of-function mutations in all three *PIN*s. In both transgenic lines, the mutant *pin3-3* allele was confirmed. For *PIN4*, only the transgenic line containing *pin4-2* could be confirmed to be homozygous. Both transgenic lines appeared to be heterozygous for *PIN7*. While these plants were not found to be loss-of-function mutants in all three *PIN* genes, primary roots of these transgenic plants, despite having at least a single loss-of-function mutation of *pin3*, were very gravitropically capable (Figure 4.2). These results may suggest PIN functional redundancy. In addition to possible remaining wild type copies of *PIN7* being present, it is possible that other PINs may be ectopically expressed in these transgenic lines. Giving evidence for this, *PIN1* has recently been shown to be ectopically expressed in the columella in the *pin3* mutant (Omelyanchuk et al., 2016). Alternatively, it is possible that a loss-of-function triple is embryo lethal, leaving only heterozygote seeds. Further work is being done to create a true triple mutant for these *PIN*s. While a true triple loss-of-function mutant was sought, the role of PIN abundance, subcellular localisation, and activity in maintaining angle-dependent auxin gradients was further explored.

While the results of Figure 4.3 do not show that the abundance of PIN3 in the statocytes of gravity responding roots likely plays a role in gravity response, it is possible PIN3 and PIN7 have specific contributions in gravity response. An unpublished report by Chris Wolverton suggests that *PIN7* may have a more vital role during gravity response at higher stimulation angles (C. Wolverton, pers. comm.). Another set of research suggests that different cells of the columella may contribute at different angles of gravity stimulation (Blancaflor et al., 1998). Our results indicate that *PIN7* is preferentially expressed in the flanking cells in comparison to *PIN3* (Figure 4.3). Taken together, this suggests that *PIN3* and *PIN7*, while mostly functionally redundant, actually contribute to gravitropism at different angles of gravity stimulation, further explaining how the magnitude of the auxin asymmetry is specified. However, it is not only the expression pattern, but localisation and activity, that could affect the amount of auxin moved by a PIN protein.

Since the abundance of PIN proteins is an unlikely source for a mechanistic control of angle-dependent auxin gradients, the subcellular localisation of both *PIN3::PIN3–GFP* and *PIN7::PIN7–GFP* was investigated. These data show that PIN3 and PIN7 are targeted to the lower side of the plasma membrane in the statocytes as stimulation angle increases. It was further found that PIN7 was only differentially targeted to the lower side of the columella PM following a 90° and 135° stimulation, not at angles below 45°. This suggests that PIN7 is more important for moving auxin out of the gravity-sensing cells at higher angles.

While the results in Figure 4.4 do confirm published results that PIN3 is mostly localised to the lower side of the cell during gravity response, not all roots showed polarisation to the lower PM at 45° and 90°. If the subcellular localisation of PIN3 and PIN7 were solely responsible for driving the auxin gradient at these angles, it would be expected that PIN3 and PIN7 would be strongly polarised to the lower side of the PM in all gravistimulated roots. This is not the case in our results. Furthermore, the extent to which PIN3 and PIN7 are polarised to the lower side of the PM is low. Even in high angles of gravity stimulation, PIN3 and PIN7 are less than 2 times more localised to the lower side of the PM than the upper side of the PM.

To further this work, an immunolocalisation approach could be used for a more complete experiment, allowing the measurement of all membranes within the columella to be used (Harrison and Masson, 2007). An immunolocalisation approach would allow the membranes between two neighbouring cells to be resolved, allowing all of the cells of the columella to be accounted for. This approach would allow for the columella to be analysed as a population of cells. One attractive hypothesis is that different statocytes within the columella send different information via auxin transport, and it is the sum of these cells that could give a varying magnitude of auxin response.

While data on abundance and subcellular localisation of PIN3 and PIN7 have given insights into the mechanism governing angle-dependent auxin asymmetries, more efforts were given towards understanding the mechanism behind PIN asymmetric distribution. With evidence suggesting that the phosphorylation status of PIN3 and PIN7 could partially determine their subcellular localisation (Kleine-Vehn et al., 2009), it is possible that this process determines the magnitude of auxin flux during gravity response. Our results show that treatment with kinase (staurosporine) and phosphatase (cantharidin) inhibitors lowered and increased, respectively, the percentage of roots showing an auxin asymmetry. However, the magnitude of the auxin response asymmetry was not greater in the cantharidin-treated roots than in those treated with staurosporine. The role of known phosphatases involved in PIN localisation was also taken into account. PID was excluded from the analysis, since *PID* is not expressed at all in these cells (Benjamins et al., 2001). Moreover, it did not appear that expressing *WAG2* in the statocyte had any effect. This however, does not rule out the role of WAG2 in gravity response, as it is possible that the amount of WAG2 in the statocytes is adequate to phosphorylate PINs. The expression of *RCN1* in the statocyte of the primary root increases the rate of gravity response, likely due to an increased amount of dephosphorylated PINs. However, the amount of RCN1 does not change in response to gravistimulation, pointing towards another mechanism. Other kinases involved in the regulation of PIN activity, such as members of the D6PK family were also investigated. While it is published that *d6pk* mutants have gravitropic defects in the hypocotyl (Willige et al., 2013; Zourelidou et al., 2014), it does not appear that they play a role in primary root gravity response. If these genes were regulating PIN activity in the root statocyte, it would be expected that the quadruple mutant would

have gravitropic defects. However, our results do not support such a role for D6PKs in the primary root (Figure 4.7).

Much more work has to be done to elucidate which phosphatases are mediating PIN localisation in the primary root. It is important to keep in mind that this model of antagonistic phosphorylation controlling subcellular targeting was proposed after experiments involving the cortex and the epidermis. While it is likely that the gravity-sensing cells have a similar mechanism to the cortex and the epidermis, it is possible that the mechanism differs slightly in the gravity-sensing cells.

The role of the cytoskeleton, while implicated in several aspects of gravity response, is still relatively unknown. It could be argued that it is not a necessary part of gravity response since inhibiting the actin cytoskeleton actually increases gravity response (Hou et al., 2004) (Figure 4.8). One possibility, taken together with the fact that the roots treated with latrunculin B respond faster, is that the actin cytoskeleton is not necessary for initial gravity perception and response, but is more important for dampening the gravity response. It is interesting that cytochalasin D does not affect root gravitropism kinetics, indicating that new polymerisation of the actin cytoskeleton is not necessary for gravity response. Further, exciting work could include studying statolith dynamics and interaction with the cytoskeleton during gravity response.

From the results of this chapter, we have gained some insights into the possible mechanism that controls the angle-dependent auxin asymmetries formed during root gravity response. From previously published work and these results, auxin gradients are likely mediated by angle-dependent subcellular localisations of PIN3 and PIN7, with possibly differing roles for these two PINs. However, since auxin transport is so vital in gravity response and development, it is regulated at many levels. Much more work has to be done to further elucidate the control of auxin transport in the statocytes and how it affects primary root gravitropism. Furthermore, there are many transcriptional feedback loops of auxin response during growth that could contribute to gravity response in the root (and/or shoot). This transcriptional regulation is the focus of Chapter 5.

Chapter 5
The Role of Auxin Signalling in Root and Shoot Gravitropism

5 The Role of Auxin Signalling in Root and Shoot Gravitropism

5.1 Introduction

In plants, gravity perception and response are physically separated in different tissues. In roots, gravity perception occurs in the columella and the growth response occurs in the elongation zone of the epidermis (Swarup et al., 2001). In shoots, gravity perception occurs in the endodermis and the growth response occurs in the epidermis (Baldwin et al., 2013). Mutants that have obvious defects in gravitropism often have mutations in either auxin transport or in the signal transduction pathway that controls auxin response. However, a disruption in the auxin signalling cascade may affect either the gravity-sensing cells or the elongation zone cells.

Changes in auxin levels within the cell induce a wide range of cellular responses (reviewed in (Weijers and Wagner, 2016)). Auxin response is controlled in a cell- and tissue-type specific manner by two protein families: the Aux/IAAs and the ARFs. The Aux/IAAs are short lived nuclear proteins. They are not known to bind DNA directly, but alter gene expression through dimerisation with the ARF family of transcription factors (Tiwari et al., 2001). The ARFs bind DNA at specific auxin response elements (AuxRes) in auxin early response genes (Guilfoyle and Hagen, 2007). In low auxin concentrations, the Aux/IAAs interact with the ARFs, blocking their activity. In high auxin concentrations, the degradation of Aux/IAAs in the 26S proteasome is promoted, freeing the ARFs to regulate auxin response genes (reviewed in (Del Bianco and Kepinski, 2010; Weijers and Wagner, 2016)), summarised in Figure 1.6.

Transgenic plants harbouring mutations in the auxin signalling pathway often show developmental and, most relevant to this work, gravitropic defects. For example, the loss-of-function mutants of *arf10* and *arf16* (Wang et al., 2005), *arf7* and *arf19* (Okushima et al., 2007) both show gravitropic defects. Also, quadruple mutants of the auxin F-box receptors *tir1 arf1 afb2 afb3* show gravitropic defects (Dharmasiri et al., 2005) . Furthermore, stabilised versions of the Aux/IAAs corepressors, which cannot be degraded in

response to auxin, such as *axr2/iaa7* (Wilson et al., 1990), *axr3/iaa17* (Rouse et al., 1998), and *slr/iaa14* (Kato et al., 2002), show gravitropic defects in the root, with *axr2* also showing gravitropic defects in the shoot. All of these mutants are thought to affect auxin's control of differential growth, which occurs in the epidermis (Swarup et al., 2005; Kutschera and Niklas, 2007). However, work has been published that demonstrates a role of auxin signalling in the gravity-sensing cells of shoots (Sato et al., 2014). It has recently been shown that expressing a dominant form of *AXR2* in the gravity-sensing cell of the shoot using the endodermis specific promoter *SCR* (Di Laurenzio et al., 1996) causes gravitropic defects in the shoot (Sato et al., 2014).

Due to anatomical differences, it is likely that the mechanisms controlling root and shoot gravitropism are different. For example, shoots bend entirely along the axis of the stem, which results in them often overshooting, and then bending back towards, the vertical. This so-called autotropic process appears to be part of the normal gravitropic response of dicotyledonous shoots and has been recently modelled in several species, including Arabidopsis (Bastien et al., 2013). Owing to these differences, it is therefore likely that there is an additional control, on top of the auxin signalling mechanisms, that contributes to gravity response in the shoot. The *LAZY1* gene was first identified in maize with a phenotype that was "indifferent to gravity" (Jenkins and Gerhardt, 1931; Van Overbeek, 1936). In Arabidopsis, *lazy1* mutants have a very horizontal branch phenotype and have a slower gravity response (Yoshihara et al., 2013), similar the phenotype of *SCR::bdl* plants (Roychoudry et al., 2013). *LAZY1* is thought to play a signalling role between gravity perception and the processes that redirect auxin transport (Sasaki and Yamamoto, 2015). Recent work also indicates that *LAZY1* may interact with microtubules (Sasaki and Yamamoto, 2015), although its molecular function is still under investigation. Another gene that has been found in the same clade, *TAC1,* shows a very vertical branch angle (Dardick et al., 2013), hinting, again, at a role in the gravity signalling pathway. In addition, the gene *Deep Rooting 1* (*DRO1*) has been found to be similar to *Tiller Angle Control 1* (*TAC1*) and *LAZY,* but is expressed mainly in roots (Uga et al., 2011). *DRO1* seems to mirror the action of *LAZY* in roots (Hollender and Dardick, 2014). These genes represent a possible additional mechanism that works with the auxin signalling pathway to control shoot gravitropism.

In previous chapters, experiments focused on the formation of auxin asymmetries in the primary root tip and how those auxin asymmetries were regulated. This chapter seeks to explore the role of the auxin signalling framework during gravity response and identify the specific cell types in which auxin signalling plays a significant role in regulating gravity response. To do this, experiments were performed with the aim to affect auxin signalling in a cell-type specific manner. Transgenic lines expressing different versions of *AXR3* and *ARF7* in either the statocytes or the epidermis of roots and shoots were generated and their gravity response kinetics tested.

5.2 Results

To first quantify how auxin signalling affects gravity response, kinetics experiments were done with various mutants that affect auxin response. In particular, plants harbouring a double loss-of-function mutation in the activating *ARF* genes, *ARF7* and *ARF19*, were analysed (*arf7 arf19*). Moreover, plants with single loss-of-function mutations in AXR3/IAA17 (*axr3-10*) and the receptor TIR1 (*tir1-1*) were also included in the analysis. While *arf7 arf19* and *tir1-1* mutants should have a dampened auxin response and concomitantly gravity response, the *axr3-10* mutant should have an enhanced auxin response and concomitantly gravity response.

Five-day-old primary roots were reoriented by 90° in the dark and measured at 1-hour intervals for 6 hours (Figure 5.1A–C). It appears that the double loss-of-function mutant *arf7 arf19* has the most severe gravitropic defect. It was also found that the loss of *Aux/IAA AXR3* (*axr3-10*) also causes a slower gravity response. A single loss-of-function mutation of *TIR1* has the mildest effect. While the individual gravitropic defects are not surprising based on previously published works, as a whole the results are difficult to interpret. To further understand the role auxin signalling plays in the mechanisms of gravity response, experiments were devised to evaluate the possible distinct contributions of auxin signal transduction in both the tissues responsible for gravity perception and the tissues responsible for gravity response.

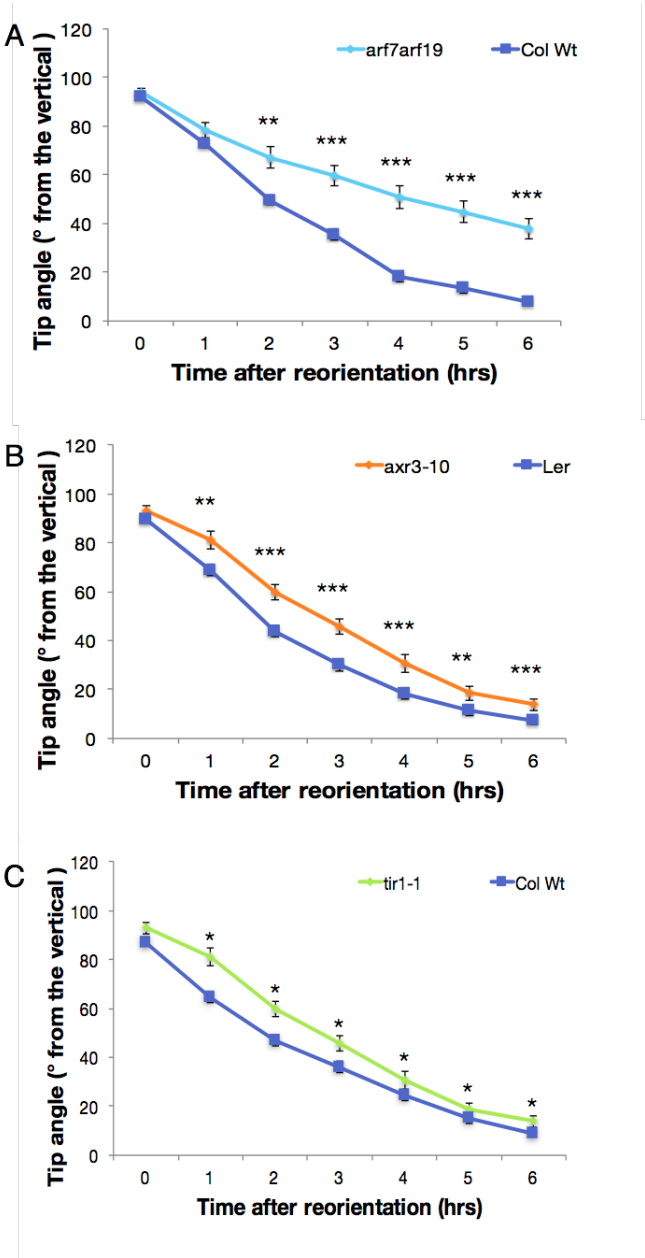

Figure 5.1 Gravity response of auxin signalling mutants.
Gravity response assays of mutants following reorientation by 90°. (A) *arf7arf19,* n ≥ 16 each genotype, (B) *axr3-10,* n ≥ 21 each genotype, and (C) *tir1-1*, n ≥ 34 each genotype. Bars represent s.e.m, stars represent $p < 0.05$, Student's t-test.

5.2.1 Modulating auxin signalling components in the gravity-sensing cells of the root has moderate effects on gravity response

To investigate auxin response within the gravity-sensing cells, we first sought to identify a promoter that could drive expression in the Arabidopsis columella cells. We selected the promoter of the *ARL2* gene that has been shown to be expressed in the columella (Harrison and Masson, 2007). The *ARL2 (ARG1-LIKE2*) is a J-domain protein that is required for normal root gravitropism and in the root is expressed specifically in the statocyte (Harrison and Masson, 2007). Previously in this project, a transcriptional reporter was made to confirm columella specificity (Figure 4.6).

To alter auxin signalling in the gravity-sensing cell, mutated versions of the *Aux/IAA* gene *AXR3* and the *ARF* gene *ARF7* were expressed from the *ARL2* promoter (Harrison and Masson, 2007) (Figure 4.5). For *ARF7*, two mutated versions were generated: *ARF7–SRDX and arf7delete. ARF7–SRDX* is a dominant-negative variant of *ARF7* with a short peptide containing an ERF-associated amphiphilic repression (EAR) motif, similar to that found in *Aux/IAA*s, fused to the full length protein. The EAR motif acts as a repression domain, blocking transcription of the targeted gene (Hiratsu et al., 2003). *arf7delete* is a version that is truncated in the c-terminal domain that, therefore, cannot interact with *Aux/IAA*s. In the case of *AXR3*, the *axr3-1* mutant version of the gene was expressed. The axr3-1 protein carries a mutation in the degron motif that makes AXR3 insensitive to auxin induced degradation (Dreher et al., 2006). This stabilised version of the protein has previously been used to disrupt auxin signalling (Swarup et al., 2005).

These transgenic plants were reoriented in the dark for 6 hours and root tip angles measured every hour. The data suggests that expression of a Aux/IAA-insensitive version of *ARF7* (*ARL2::arf7delete*) causes only very mild gravitropic defects. In addition, the expression of a transcriptionally repressing version of *ARF7* (*ARL2::ARF7–SRDX*) actually speeds up root gravitropic response (Figure 5.2, $p < 0.05$, Student's t-test). Moreover, it appears that expressing the stabilised version *axr3-1* in the gravity-sensing cell does not cause defects in gravitropism. This is surprising because the qualitatively similar *ARL2::ARF7–SRDX* has a measurable phenotype. In particular, it is not simply the case that the expressed axr3-1 protein is non-

functional, because the *ARL2::axr3-1* has a lateral root GSA phenotype (S. Rouchoudry and S. Kepinski unpublished).

The *ARL2::arf7delete*, *ARL2::ARF7–SRDX*, and *ARL2::axr3-1* transgenic lines were characterised further to try to explain the mechanism in which they alter gravity response. While it has been recently published that expressing *axr2 and bdl/IAA12* in the gravity-sensing cells of shoots causes gravitropic defects (Sato et al, 2014; Roychoudry et al., 2013), it is unclear how affecting auxin signal transduction in the gravity-sensing cell affects gravity response. To investigate how expressing a dominant-negative version of *ARF7* in the statocyte speeds up gravitropism, growth profiles were made of these transgenic lines. Each of these transgenic lines had a normal growth rate when compared to wild type, with *ARL2::ARF7–SRDX* being slightly reduced (Figure 5.3). Since the growth rates were not responsible for the changes in gravity response, further analysis was required. A possible explanation for altered gravity response is that auxin signalling is affecting the expression or localisation of PIN proteins. To test this hypothesis, a RT-qPCR analysis of *PIN* expression was performed. The relative expression levels of *PIN3*, *PIN4*, and *PIN7* in the root tips of *ARL2::axr3-1*, *ARL2::ARF7–SRDX*, and *ARL2::arf7delete* were quantified. It appears that only *ARL2::ARF7–SRDX* has any significant differences in PIN expression, with increased expression in *PIN3*, *PIN4*, and *PIN7* (Figure 5.3). This could explain the faster gravitropic response phenotype of this mutant, as a higher abundance of PIN3 and PIN7 could lead to more auxin being moved out of the lower side of the columella during gravity response.

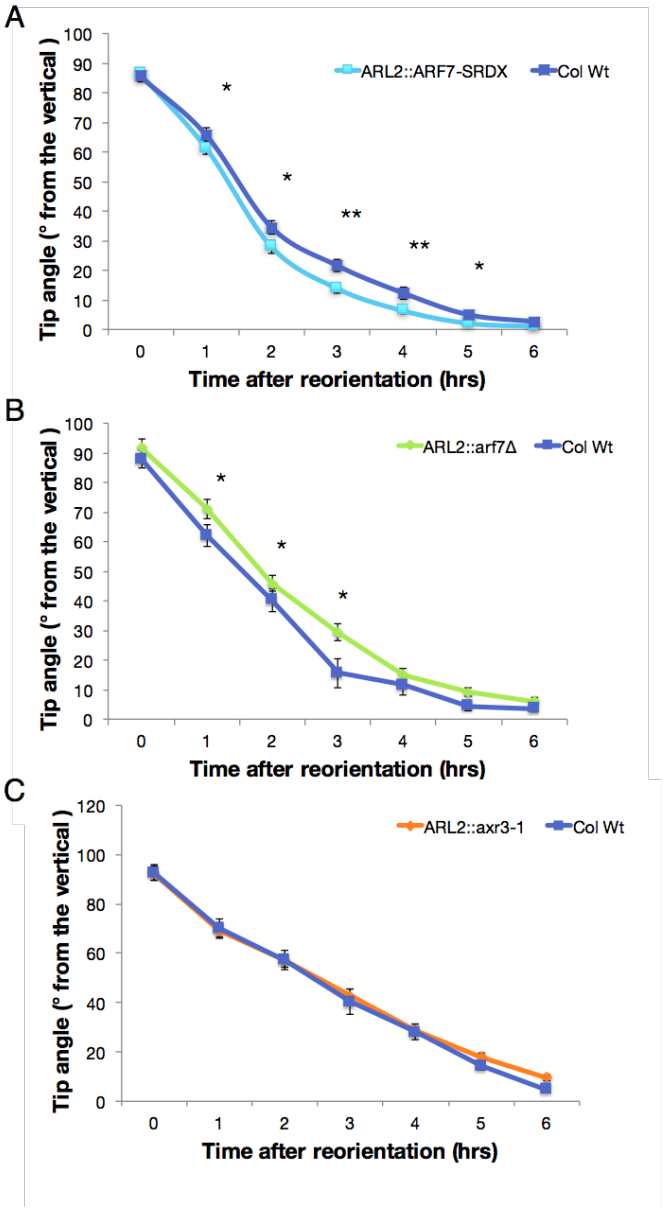

Figure 5.2 Gravity response assays of transgenic lines with altered auxin signalling in the gravity-sensing cells.
Gravity response assays of mutants following reorientation by 90°. (A) *ARL2::ARF7–SRDX*, n ≥ 66 each genotype, (B) *ARL2::arf7delete,* n ≥ 32 each genotype, and (C) *ARL2::axr3-1,* n ≥ 47 each genotype. Bars represent s.e.m., stars represent $p < 0.05$, Student's t-test.

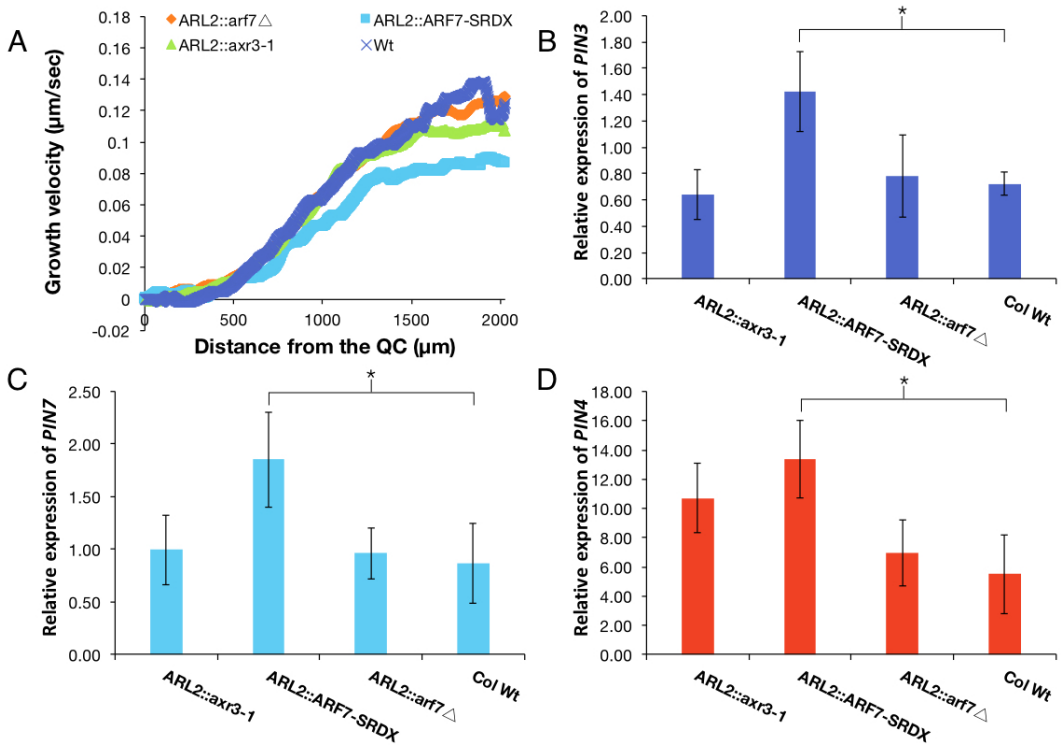

Figure 5.3 Characterisation of mutants with altered auxin signalling in the gravity-sensing cell of the root.
(A) Velocity profiles of *ARL2::axr3-1*, *ARL2:arf7delete*, *ARL2::ARF7–SRDX*, n ≥ 6 each genotype measured by Stripflow (see Methods 2.5.7). (B-D) Relative expression of *PIN3*, *PIN4*, and *PIN7* in the primary root tip of each genotype, as quantified by RT-qPCR. The final results were expressed as the ratio between the gene of interest and the housekeeping gene (GAPDH) arbitrary units. Two technical and four replicates were analysed for each genotype and primer pair. Stars represent $p < 0.05$, 1-way ANOVA, Tukey's HSD test between indicated pairs.

5.2.2 Effects in the epidermis of the root

To investigate the effects of modulating auxin signalling specifically within the root epidermis the UAS/GAL4 expression system was used. This two-component system allows for targeted expression of a chosen gene (Haseloff, 1999). A set of constructs were generated in which the coding sequences for *axr3-1*, its milder allele *axr3-3*, and *ARF7–SRDX* were placed downstream of the Upstream Activation Sequence (UAS) element. The resulting transgenic lines were crossed to the enhancer trap line J0951, which drives expression of the *GAL4–VP16* gene specifically in the lateral root cap and root epidermis. GAL4, a modular yeast protein, activates expression of the target genes placed downstream of the UAS element, due to the action of the viral activator domain VP16 (Haseloff, 1999).

Primary roots of these transgenic lines were reoriented by 90° and measured every hour (Figure 5.4). As expected, the J0951-driven expression of *axr3-1* and *axr3-3* show root gravitropic defects, as do *ARF7*–SRDX. However, these gravitropic defects are mild compared to previously published reports. For example, it has been previously shown that expressing *axr3-1* in the epidermis blocks gravitropism (Swarup et al., 2005). Here, we report a much milder defect. It is interesting that expressing a dominant-negative form of *ARF7* in the gravity-sensing cell speeds up gravitropism, while expressing it in the epidermis slows down gravitropism. From this experiment, it is likely that *ARF7* has a primary role affecting auxin-based differential growth in the epidermis; when a dominant-negative form is expressed in the elongation zone, it mimics, to a lesser extent, the gravity defects of the mutant *arf7 arf19* (Figure 5.1).

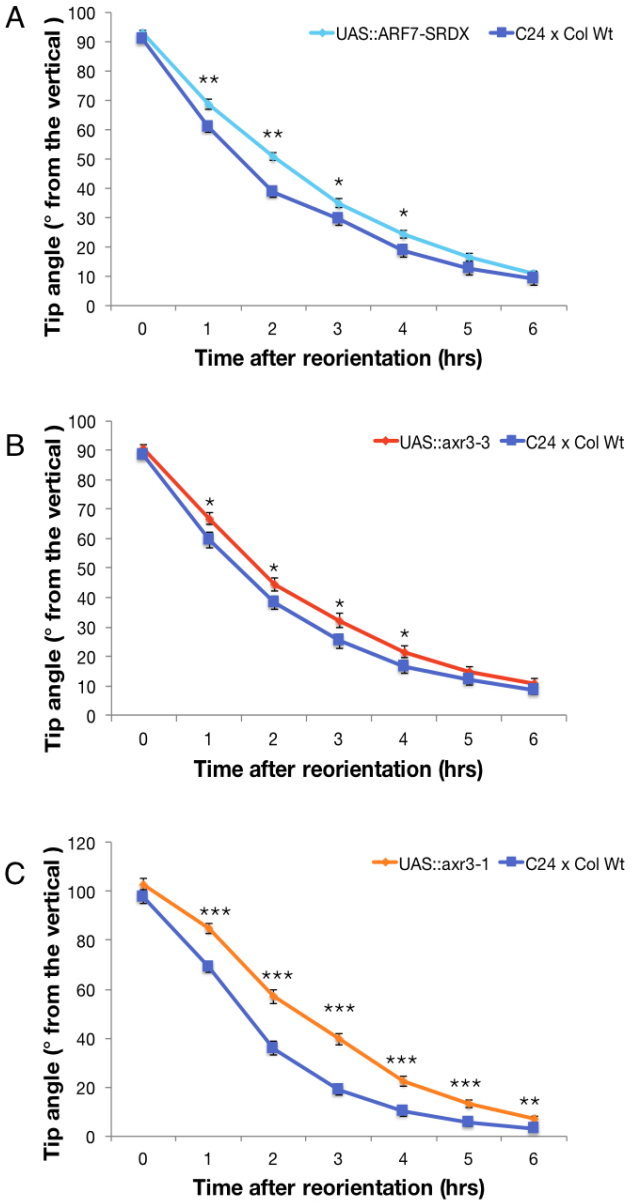

Figure 5.4 Gravity response assays of transgenic lines with altered auxin signalling expressed in the root epidermis.
Gravity response assays of mutants following reorientation by 90°. (A) *UAS::ARF7–SRDX* x *J0951,* n ≥ 76 each genotype, (B) *UAS::axr3-3 x J0951,* n ≥ 36 each genotype, (C) *UAS::axr3-1 x J0951*, n ≥ 26 each genotype. Bars represent s.e.m., stars represent $p < 0.05$, Student's t-test.

5.2.3 Auxin signalling components in the gravity-sensing and epidermal cells of shoots

To further investigate the effect of modulating auxin signalling specifically within the gravity-sensing cells (i.e., the endodermis) or the tropic growth tissues (i.e., the epidermis), two different promoters were identified. To drive expression in shoot gravity-sensing cells, the *SCARECROW* (*SCR*) promoter was used (Wysocka-Diller et al., 2000), and the *ARABIDOPSIS MERISTEM LAYER 1* (*ATML1)* promoter (Sessions et al., 1999) was used to target the epidermis. To investigate the role of auxin signalling in the shoot, we expressed the truncated, Aux/IAA-insensitive version of *ARF7*. *ARF7* was chosen as it is already known to play a role in shoot gravitropism (Harper et al., 2000). Moreover, for the study of the role of auxin response in the epidermis, we used an artificial microRNA (see Methods 2.3.14) to reduce expression of *ARF3* and *ARF4*. *ARF3* and *ARF4* are highly upregulated (Figure 7.6) in the shoot and their reduction should increase the capacity for auxin response in the shoot.

Kinetics experiments were carried out on these lines. Shoots were reoriented in the dark using the infrared imaging system (see Methods 2.5.2) and the primary shoot angle was measured. For these experiments, the gravity response curve was plotted at ten-minute intervals. Next, a scatter plot was made of the shoot tip angles, and a line of best fit was fitted. From the slope of the line of best fit, a maximum bending rate was calculated to obtain a quantitative measure of shoot gravity response, a method adapted from (Sato et al., 2014). Our results show that *ATML1::arf7delete* shoots have a slower maximum bending rate and their final shoot angle is lower than wild type (Figure 5.6). The presence of the *SCR::arf7delete* construct does not seem to have an effect on shoot gravitropism (Figure 5.5). From these experiments, it is not clear that *ARF7* has a role in gravity response in the statocytes of the shoot (Figure 5.5), as expressing a truncated, Aux/IAA-insensitive form of *arf7* in the statocytes did not create defects in gravity response. However, gravitropic defects were observed in a transgenic line expressing the form of *arf7* in the epidermis (Figure 5.6). These results also suggest that downregulating the expression of *ARF*s *3* and *4* in the epidermis does not affect gravity response.

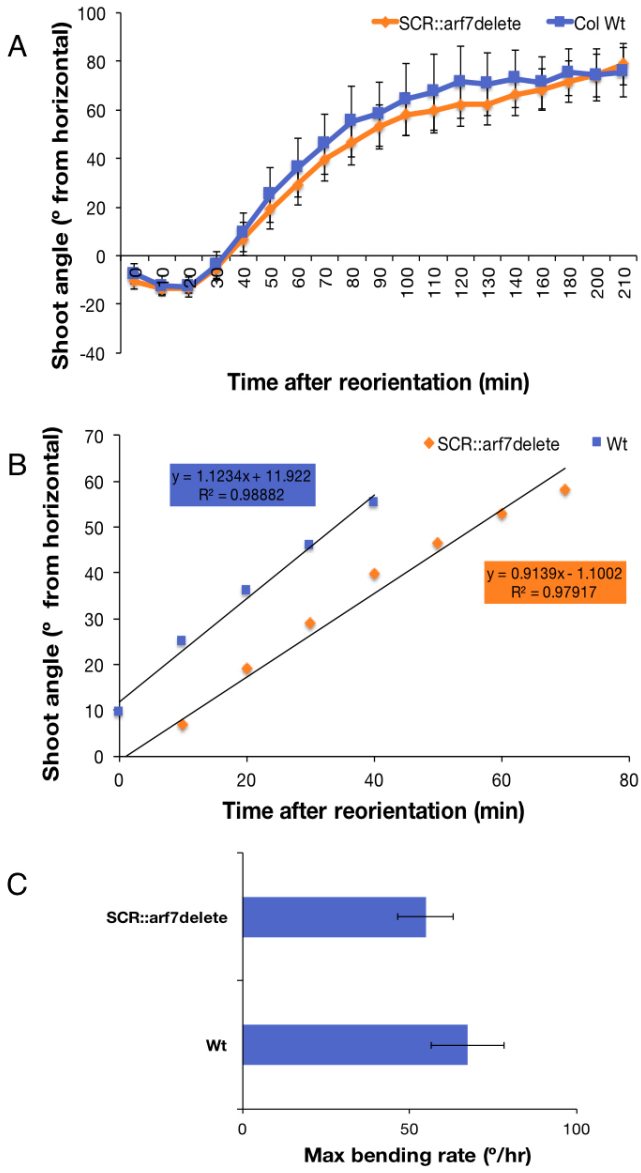

Figure 5.5 Gravity response assays of transgenic lines with altered auxin signalling expressed in the endodermis of the shoot.
(A) Gravity response curve of *SCR::arf7delete*, n = 8 each genotype. (B) Scatterplot of the average primary shoot tip angle during the linear phase of gravity response of Col-0 WT and *SCR::arf7delete*. The line represents a line of best fit with the formula highlighted in the corresponding colour. (C) The maximum bending rate of each genotype. Bars represent s.e.m.

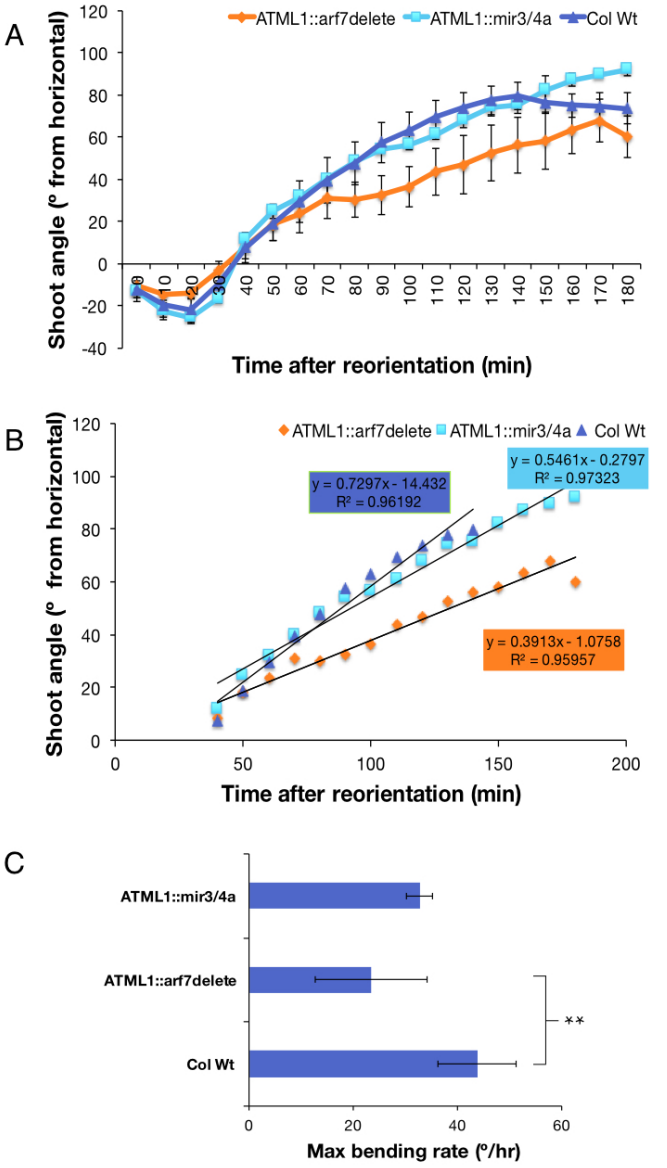

Figure 5.6 Gravity response assays of transgenic lines with altered auxin signalling expressed in the shoot epidermis.
Gravity response curves of *ATML1::arf7delete*, *ATML1::mir3/4a*, and Col-0 WT, n = 6 each genotype. (B) Scatterplot of the average primary shoot tip angle during the linear phase of gravity response of shoots. The line represents a line of best fit with the formula highlighted in the corresponding colour. (C) The maximum bending rate of each genotype, stars represent $p < 0.01$, 1-way ANOVA, Tukey HSD test between pair. Bars represent s.e.m.

5.2.4 Differences in the gravitropic mechanism between the root and shoot

Previous research has shown that there is likely an additional mechanism that works either on top of, or in conjunction with, the auxin signalling system to control shoot gravity response. These genes possibly include *LAZY1* and *TAC1.* Loss-of-function mutants of *LAZY1* have been found to have a lateral organ with nearly horizontal GSA. *LAZY1*-dependent control of shoot gravitropism is likely upstream of reorientation-induced auxin gradients. It is currently unknown if *LAZY1* is independent of auxin signalling events. A related gene, *TAC1,* is known to regulate GSA of lateral organs, with a loss-of-function mutation causing a nearly vertical angle phenotype (Dardick et al., 2013).

To explore the role of these genes in primary shoot gravity response, shoot gravity response was examined for the loss-of-function mutants of *tac1-1* and *lazy1.* Our experiments show that the effect of the loss-of-function of the *LAZY1* gene reduced the overall maximum bending rate, and led to a flattened gravity response profile (Figure 5.7A). The maximum bending rate of *tac1-1* shoots was largely increased and reached a higher final shoot angle (Figure 5.7A and B).

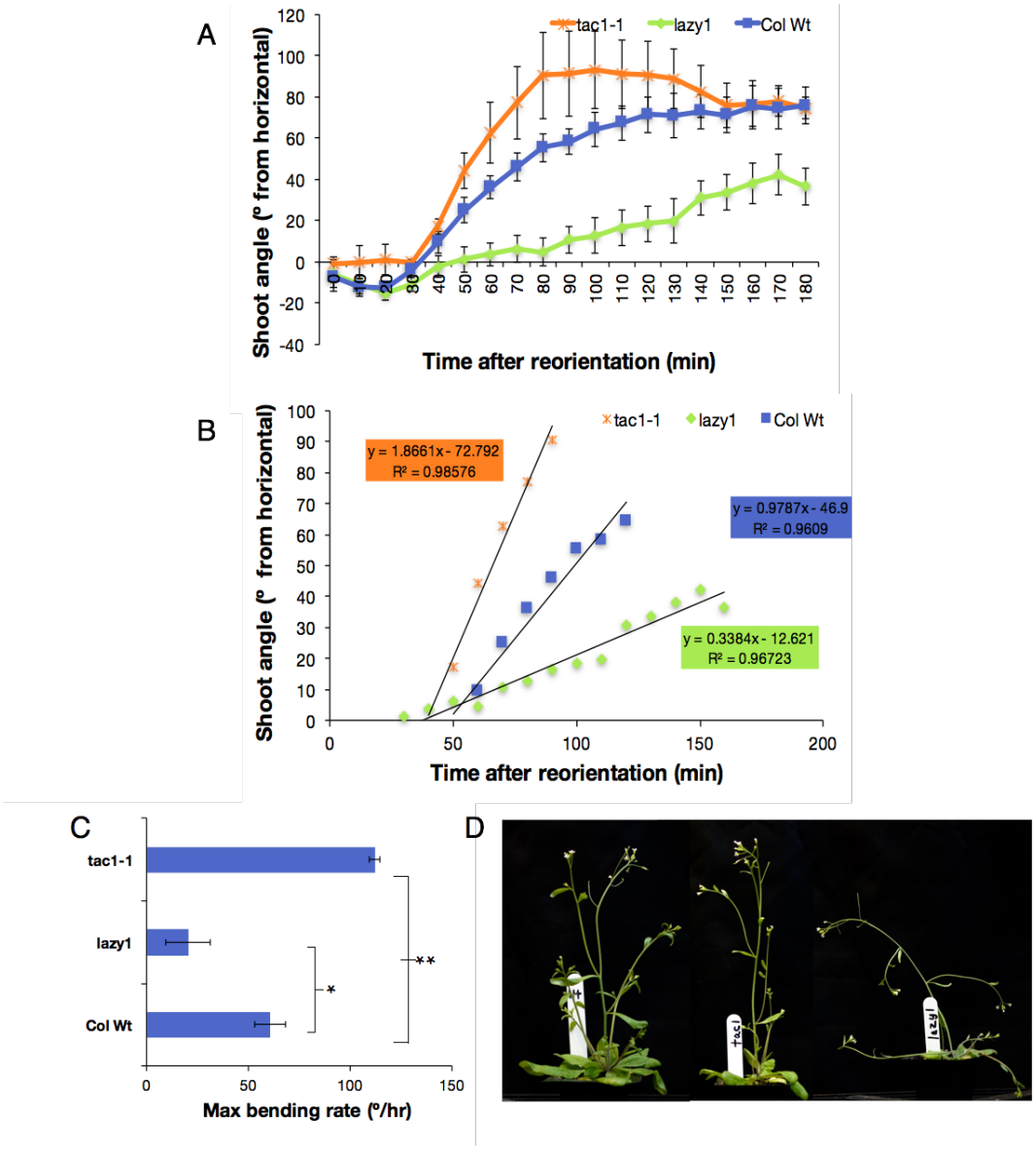

Figure 5.7 Gravity response assays of *tac1-1* and *lazy1.*
Gravity response curves of *tac1-1*, *lazy1*, and Col-0 WT, n = 6 each genotype. (B) Scatterplot of the average primary shoot tip angle during the linear phase of gravity response of shoots. The line represents a line of best fit with the formula highlighted in the corresponding colour. (C) The maximum bending rate of each genotype, stars represent $p < 0.05$, Student's t-test. Bars represent s.e.m. (D) Typical phenotypes of Col-0 WT (left), t*ac1-1* (middle*)*, and *lazy1* (right) shoots.

Discussion

In this chapter, the role of the auxin signalling transcriptional framework in the gravity response in roots and shoots was investigated. To do this, various loss- and gain-of-function mutants were analysed for gravitropic defects. Mutants with gravity response defects, generally, could have problems with either gravity perception (occurring in the statocytes) or the generation of differential growth (occurring in the epidermis). Therefore, efforts were made towards trying to understand which of these tissues were affected by auxin signalling manipulation, in both roots and shoots.

From the analysis of the mutants, it appears that the double loss-of-function mutant *arf7 arf19* has the most severe defect. *ARF7* and *ARF19* are both activating *ARF*s (Tiwari et al., 2003) and their loss should lead to an attenuated auxin response. Furthermore, *ARF7* is known to regulate tropic growth, so it is expected that a loss-of-function mutant of ARF7 leads to gravitropic defects (Harper et al., 2000). It was also found that the AXR3 loss-of-function mutant*, axr3-10,* has a slower gravitropic response. Interestingly, previous work has shown that the stabilized version of *AXR3* is also agravitropic. A single loss-of-function mutation of *TIR1* appears to have the mildest effect. This is likely explained by the redundancy within the TIR1/AFB family (Parry et al., 2009). While these individual gravitropic defects are not surprising based on previously published work, as a whole the results are somewhat difficult to interpret. It appears that removing elements that either activate or repress auxin response causes gravitropism to be slowed in the root.

To further understand the role of auxin signalling in the mechanism of gravity response, experiments were devised to evaluate the possible distinct contributions of auxin signal transduction in both the tissues responsible for gravity perception and gravity response. When transgenic lines affecting the gravity-sensing cells of roots were tested, it was found that expressing an *Aux/IAA*-insensitive version (*arf7delete*) and a dominant-negative version (*ARF7–SRDX*) of *ARF7* both affected gravity response (Figure 5.2). *ARL2::arf7delete* roots display slower gravitropism, although not as extreme as the loss-of-function of a*rf7 arf19* expressed everywhere in the plant (Figure 5.1). Surprisingly, *ARL2::ARF7–SRDX* roots display faster gravity response. This transgenic line should instead be more phenotypically similar

to a loss-of-function mutant of *ARF7*, because the genes that *ARF7* control should be repressed due to the addition of the SRDX domain.

We found that expressing *axr3-1* in the gravity-sensing cell with the *ARL2* promoter has no effect on primary roots (Figure 5.2). This confirms a previously published report using the UAS/GAL4 system that describes AXR3 as necessary in the epidermis and not in the columella for root gravitropism (Swarup et al., 2001). However, the *ARL2::axr3-1* line was found to have a more vertical GSA in the lateral roots (S. Roychoudry, pers. comm), while none of the other *ARL2* lines had a lateral root phenotype, demonstrating that the transgene was functional.

In an attempt to understand the mechanisms that lead to the gravity response phenotypes in the ARL2-misexpression lines, the mRNA levels of *PIN*s were analysed. It was found that the *ARL2::ARF7–SRDX* line has increased expression in *PIN3*, *PIN4,* and *PIN7* (Figure 5.3). Also, it appears that *PIN4* might be upregulated in the *ARL2::axr3-1* line. This is in contrast with evidence that shows that *PIN*s are upregulated by auxin (Vieten et al., 2005). However, abundance of PINs is only one of the many ways auxin transport is regulated during gravity response. An interesting way to explore the interaction between auxin signalling and the *PIN*s would be to cross PIN translational reporters into these transgenic lines to see if PIN localisation is affected.

The transcriptional control of auxin signalling in the epidermis during gravity response was also investigated. It was expected that affecting auxin signalling in the epidermis causes gravity defects. However, we report a milder effect of expressing *axr3-1* in the epidermis on gravity response in comparison to a previously published work (Swarup et al., 2005). It was reported that *axr3-1* when expressed in the epidermis blocked gravitropism (Swarup et al., 2005), but in that report gravitropism was recorded by characterising a root as gravitropic once it had achieved 45º of reorientation. In the experiments in this thesis, the root tip angle was recorded every 30 minutes following reorientation. This difference in method could explain the differences between our results and the previously published finding. It was also found that expressing *ARF7–SRDX* in the epidermis slows down gravity response (Figure 5.4). This result fits with the loss-of-function gravity

response of *arf7* and revealed a role for *ARF7* in the regulation of auxin-mediated gravity response in the expanding cells of the root.

We found that auxin signalling has a minor role in the gravity sensing cell of the root. This result is incongruous with previously published work showing that auxin signalling in the gravity-sensing cells is necessary for shoot gravitropism (Sato et al., 2014; Roychoudhry et al., 2013). In addition to anatomical differences, shoot and root gravitropism differ due to differences in auxin sensitivity; auxin is growth inhibiting in root tissues, but growth promoting in shoot tissues (Thimann, 1956). While the gravity perception and the initial mechanism of gravity response is similar, there are likely differences in context specificity and response.

These differences were explored by expressing modulated auxin signalling components in the statocyte (using the *SCR* promoter) and the epidermis (using the *ATML1* promoter), and analysing their gravity response. While previously published reports show that expressing *axr2-1* (Sato et al., 2014) yields significant gravitropic and phototropic defects, the effect of expressing an Aux/IAA-insensitive version of *ARF7 (arf7delete)* in the gravity-sensing cells of shoots seems to have no effect (Figure 5.5). This is interesting because we found that expressing *arf7delete* in the epidermis of the shoot leads to a slower gravity response (Figure 5.6). While there is published evidence that the auxin signalling system has a role in the gravity-sensing cell in the shoot (Sato et al., 2014; Roychoudhry et al., 2013), from our results it appears that *ARF7* only has a role in the epidermis (Figure 5.6). It seems that only constitutively repressing auxin response in the shoot gravity-sensing cells affects gravity response, as both transgenic lines with gravitropic defects are stabilised *Aux/IAA*s (Sato et al., 2014; Roychoudhry et al., 2013).

In summary, expressing an Aux/IAA-insensitive version of *ARF7* in the epidermis of the root and shoot leads to a slower gravity response. In the root, expressing a dominant negative form of *ARF7* in the gravity-sensing cells leads to a faster gravity response. It was found that expressing this Aux/IAA-insensitive version of *ARF7* in the gravity-sensing cell of the shoot had no effect. From the results of this thesis, and previously published work, it appears that only repressing auxin response via stabilised *Aux/IAA*s in the

shoot gravity-sensing cells seems to have an effect. Interestingly, expressing the stabilised version of AXR3 in the root gravity-sensing cell had no effect. While the results of this research have uncovered a role for auxin signalling in the gravity-sensing cells of roots, there are still some unanswered questions. It is puzzling that repressing *ARF7* in the gravity-sensing cell of the root increases the speed of the gravity response, but the speed of gravity response decreases when repressing *ARF7* in the epidermis or the whole plant. This highlights the need for more work to tease apart what role auxin signalling has in the gravity-sensing cell of the root. The regulation of auxin signalling is complex and there are many possible ways auxin signalling could affect gravity response, including modulating known downstream effectors.

Shoot gravity response is further complicated by the possible existence of other mechanisms involving the *LAZY1* and *TAC1* genes. In this chapter, a brief investigation into how these genes affect gravitropism in shoots was given. The data presented in Figure 5.7A and B show that *lazy1* shoots have a reduced overall maximum bending rate and a flattened gravity response profile, while the maximum bending rate of *tac1-1* was largely increased and reached a higher final shoot angle. It has previously been shown that *lazy1* maize coleoptiles have increased auxin transport rates (Dong et al., 2013), yet are defective in creating the auxin gradients necessary for adequate gravity response (Dong et al., 2013). It is likely that the role of *LAZY1* lies between amyloplast sedimentation and the formation of auxin gradients, as rice *lazy1* mutants were found to have normal amyloplast sedimentation (Abe et al., 1994). The *LAZY1* gene also seems to be a conserved gene across several species (Dong et al., 2013; Yoshihara et al., 2013; Van Overbeek, 1936). Future work could include targeted expression of the *lazy*1 gene in epidermal and endodermal cell types to locate its method of action in gravity response. This could shed further light on how gravitropic response is regulated in shoots. The *TAC1* gene could also be further investigated, as it has been identified to affect the GSA of the lateral organs in many species (Yu et al., 2007; Ku et al., 2011; Dardick et al., 2013). Moreover, the role of *DRO1* (Hollender and Dardick, 2014) should be further investigated to understand whether a similar mechanism is involved in root gravitropism.

The inherent complexity of the auxin signalling system and the anatomical differences between roots and shoots makes understanding and identifying the role of auxin signalling in the gravity-sensing cells difficult. More work is required to tease apart the exact roles of specific *Aux/IAA*s and *ARF*s in regulating auxin response and the possibility of further mechanisms involving the *LAZY1* and *TAC1* genes in the shoot and *DRO1* in the root. The results of this chapter seem to raise more questions about how gravity response is specified in the response phase of gravitropism than to provide answers.

Chapter 6
General Discussion

6 General Discussion

6.1 Gravitropism in Arabidopsis Roots is Angle-Dependent and is Governed by Auxin Asymmetry

A unified model of gravitropism taking into account the full physiology and kinetics of root gravitropism has yet to be put forward. Previously, a “tipping-point” model (Band et al., 2012) has been proposed based on the observation that auxin asymmetries appear to be lost at ~48° from the vertical. It is further suggested by this model that there is possibly a secondary, non-Cholodny-Went based, mechanism that exists for angles of stimulation below that threshold. However, this model is incompatible with the observed kinetics of primary root gravitropic response, as roots at 20° respond to gravity (Mullen et al., 2000).

The results presented here demonstrate previously unreported quantifiable auxin asymmetries at stimulation angles greater than 30° in gravity responding primary roots. Angle-dependent auxin gradients were quantified in this thesis with more sensitive reporters, such as *DR5v2* and the ratiometric reporter *R2D2,* that have recently become available. Moreover, with measurements using the *R2D2* reporter, more auxin was found in non-hair cells than hair cells when roots were growing vertically. In our analysis, only the same cell types were used to quantify the auxin asymmetry at each angle. Auxin gradients at angles below 48° could have previously been missed due to inherent differences between hair and non-hair cell types. Understandably, this could have obscured small auxin gradients at lower angles of stimulation. The results from the *DR5v2* auxin response reporter demonstrate the need for an even more sensitive reporter to measure differences in auxin gradients at lower stimulation angles, as even this newer, more sensitive reporter can only distinguish between stimulation angles more than 30° apart. However, if Cholodny-Went theory is indeed correct, auxin asymmetries at stimulation angles below 30° are likely to exist, since the minimum angle of stimulation of Arabidopsis roots is 20° (Mullen et al., 2000).

The observation that non-hair cells contain more auxin than hair cells of the epidermis suggests the possibility of a cell-type specific contribution to gravity response. These data also corroborate the finding that *AUX1* is preferentially expressed in non-hair cells over hair cells (Jones et al., 2008), suggesting that auxin is being transported preferentially in those cells. The cell-type specific contribution to gravity response is complicated further by the observation that hair and non-hair cells may have different capacities for auxin response, as measured by the *DR5v2* reporter (M. Kieffer, pers. comm.). Furthermore, *CAPRICE* and *TRYPTYCHON (cpc try)* loss-of-function mutants have roots that are made up of all non-hair cells (Schellmann et al., 2002) that are less sensitive to auxin (M. Kieffer, pers. comm.), and may respond faster to gravity (Löfke et al., 2015). Conversely, roots with more hair cells, such as the *wer myb23* loss-of-function mutant (Lee and Schiefelbein, 1999), are more sensitive to auxin (M. Kieffer, pers. comm.), but are gravitropically normal (Löfke et al., 2015). Future work might include further experiments investigating how cell-type identity affects both the amount of auxin and the auxin sensitivity of cells in the epidermis.

The sine law of gravitropism seems to be a good description of gravity response in the shoot and coleoptile of many species such as oat (Galland, 2002), rice, and maize (Iino et al., 2005). However, the sine law is less well described in roots. In Chapter 3, we confirmed that root gravitropism in Arabidopsis is angle-dependent. Indeed, gravity response assays, and experiments in which the gravity vector was randomised after gravity experiments, showed that gravity response in Arabidopsis is angle-dependent. These data are in agreement with other published results on Arabidopsis roots (Mullen et al., 2000) and other species such as lentil roots (Perbal, 1974) and cress roots (Iversen and Rommelhoff, 1978; Larsen, 1969). During the course of this thesis, two other species, bean and wheat were tested. According to our results, the gravitropic response of bean and wheat did not appear to be angle-dependent. Instead, at each angle of stimulation, the roots of bean and wheat underwent a rapid elongation during the first hour and then the rate of gravity response plateaued. This result is similar to previously published findings in maize roots (Barlow et al., 1993)

Differences in anatomy of gravity perceiving organs between species may explain why some species do not exhibit angle-dependent gravitropism. For example, the number of statocytes, the number of statoliths per cell, and the

relative size of statoliths compared to the volume of the cell might affect angle-dependent gravitropism. While this is currently an unanswered question, there is some evidence that the number of statocytes may affect gravity response. Studies in bean indicate that gravity response is correlated with tissue size, with a greater number of statocytes increasing the capacity for gravity response (Moore, 1985). Additionally, it is possible that distances between the statocytes and the elongation zone might contribute to differences in gravitropism between species. In all species, the size of the auxin molecule remains constant, and auxin must be transported along the lower side of the root to inhibit cell elongation in the epidermis. However, the distance or number of cells auxin must travel to affect change in the epidermis may affect angle-dependent gravitropism. It is possible that analysis of these differences in the anatomy of the gravity sensing cells between species might further elucidate the mechanism of angle-dependent gravitropism.

The results from this thesis indicate that 135° is the stimulation angle that yields the fastest gravity response when roots are allowed to freely respond. This is consistent with previous data gathered from cress (Iversen and Rommelhoff, 1978; Larsen, 1969) and lentil roots (Perbal, 1974). However, previously published work on Arabidopsis using a constant feedback system (ROTATO) found that the angle that led to the greatest response was ~90° (Mullen et al., 2000). Moreover, when further ROTATO experiments at higher angles greater than 120° were carried out for work in this thesis, it appeared that the roots no longer responded in an angle-dependent manner. These differences cannot rely on different conditions since in both our research and the ROTATO experiments plants were analysed at similar developmental stage. Since our data from roots allowed to respond freely to gravity stimulation are in agreement with other previously published works, it is likely that angle-dependence is maintained at these higher angles. To better understand what may be occurring at these higher angles, auxin gradients could be quantified at angles greater than 120°. If auxin gradients dictate angle-dependent gravity response and Cholodny-Went theory is correct, then one would expect that the magnitude of the auxin asymmetry decreases after 135°.

Future work could explore the difference between these two methods of gravistimulation (constrained vs free response), as this could be revealing of

mechanisms of gravity perception and response. It is possible that when both roots constrained on ROTATO and roots allowed to respond freely are stimulated, all of the statoliths arrive on the new lower side wall and the output is the same. However, when gravistimulated on ROTATO, the gravitropic response is measured after the response has reached a linear phase. With this method, it is possible that the differences between angles could be missed. To test this hypothesis, the lag time between stimulation and response could be further studied to determine if roots constrained on ROTATO stimulated at higher angles have a shorter lag time.

The mechanism of gravity response and GSA maintenance of lateral roots was also explored in this thesis. Angle-dependent variation in gravity response is a key component of a recently proposed model of lateral root and shoot GSAs (Roychoudhry et al., 2013) In this thesis, it was found that auxin gradients were not present in lateral roots that were growing at their GSA, but gradients were present in upbending and downbending lateral roots. This result confirms that the regulation of auxin distribution is necessary for the maintenance of GSA in lateral roots, and is entirely consistent with Cholodny-Went theory. Furthermore, these data provide further mechanistic insight into the kinetics of reorienting lateral roots, as downbending lateral roots were found to have a stronger auxin asymmetry than upbending lateral roots. This finding fits with both Cholodny-Went theory and the kinetics of reoriented lateral roots (S. Roychoudry, pers. comm.), and demonstrates that gravity response in primary and lateral roots follow the same rules.

6.2 Mechanisms Generating and Maintaining Auxin Asymmetry During Gravity Response

Previously published work and the data in this thesis indicate that PIN proteins are primarily responsible for auxin efflux during gravity response (Friml et al., 2002). Microscopy data show *PIN*s relocalising to the lower side of columella cells upon gravistimulation, and the mutant *pin3-3* has been described as gravitropically defective (Friml et al., 2002). In this thesis, gravity response kinetics of plants with a confirmed loss-of-function mutation in *pin3* and *pin4* were found to have a weak agravitropic phenotype in both their primary and the lateral roots. These data on their own suggest that

*PIN*s may not be primarily responsible for auxin efflux following gravity stimulation. However, *PIN*s are known to be functionally redundant, and it has been recently shown that *PIN1* is ectopically expressed in the columella of the loss-of-function *pin3-3* mutant (Omelyanchuk et al., 2016). This ectopic expression could explain the mild phenotype of the loss-of-function *pin3 pin4* mutant. Despite evidence for functional redundancy and ectopic expression of *PIN*s, its molecular basis is not currently known.

In Chapter 4, the localisation and expression patterns of *PIN3* and *PIN7* were studied to determine their role in governing auxin asymmetries created during gravity response. The results suggest that PIN3 and PIN7 localise in an angle-dependent manner, as the data show that *PIN3* is targeted to the lower side of the plasma membrane to a greater extent as stimulation angle increases at 45° and above. It was further found that PIN7 was only differentially targeted to the lower side of the columella PM following a 90° and 135° stimulation, but not at angles around 45°. This could suggest that PIN3 is more important for moving auxin out of the gravity-sensing cells at lower angles, while PIN7 becomes more important at higher angles. Previous ROTATO experiments show that the loss-of-function *pin7-2* mutant responds to gravity stimulation much slower at stimulation angles 90° and 120° (C. Wolverton, unpublished results). Moreover, laser ablation studies have shown that different cells of the columella contribute differently to gravitropism, with the flanking cells potentially contributing more to gravitropism at higher angles (Blancaflor et al., 1998). Therefore, the expression patterns of *PIN3* and *PIN7* were analysed, and, while *PIN3* expression was limited more to the central columella cells, *PIN7* could also be found more diffusely in the flanking cells. Taken together, these data indicate a possible, specific role for different *PIN*s during auxin-dependent gravity response. Much research could be done to further understand PIN specificity and redundancy.

The mechanism that targets PINs within the gravity-sensing cells is not currently known. However, a current model, based on data gathered from Arabidopsis cortex cells, predicts that dephosphorylated PINs are more likely to enter the basally targeted pathway than phosphorylated PINs. This process seems to be modulated by the phosphatases RCN1 and the PID/WAG1/WAG2 family of kinases (Kleine-Vehn et al., 2009). The role of *RCN1* and *WAG2* was investigated in the root by expressing *RCN1* and

WAG2 in the gravity-sensing cell using the *ARL2* promoter. Expressing *RCN1* in the gravity-sensing cells increased the speed of gravity response in the primary root. This is in accordance with an increase in dephosphorylated, basal-targeted PINs in the columella. This result aligns with some previously published reports of a loss-of-function *pid wag1 wag2* triple mutant leading to a hypertropic growth in hypocotyls (Rakusová et al., 2011). While this increase in dephosphorylated PINs is likely, it is possible that *RCN1* has other downstream targets that could be affecting gravity response in the root columella. It has been shown that *RCN1* is capable of dephosphorylating PINs, but its particular role in PIN phosphorylation during gravity response has yet to be demonstrated.

The results in this thesis suggest that *WAG2* has no gravitropic effects when expressed in the columella. However, it is possible that the amount of kinase in those cells is not the limiting factor and increasing it does not affect gravity response. PINOID was not investigated, because, even though the loss-of-function *pid* mutant phenotypically has a collapsed root (Friml et al., 2004), *PID* is not preferentially expressed in the root tip (Benjamins et al., 2001). Our experiments did not find a suitable kinase to act antagonistically to RCN1 in root statocytes. We also analysed the D6PK kinases, which are known to affect PIN activity during hypocotyl gravity response (Willige et al., 2013), but they also did not have an effect on root gravitropism. Further work is necessary to discover which kinase, possibly not yet identified, is responsible for phosphorylating PINs in the columella.

In this thesis, we also investigated the possible contribution of the cytoskeleton to angle-dependent gravity response. From our experiments, the cytoskeleton does not appear to be necessary for gravity response, as treatment with the cytoskeleton depolymerizing drug, latrunculin B, actually increases the rate of gravity response in roots. However, the cytoskeleton was not dismissed as it has been implicated in several aspects of gravitropism. Previously published work has found that the cytoskeleton interacts with PIN localisation components (Löfke et al., 2013). In addition, other cytoskeleton inhibiting drugs such as cytochalasin D, an inhibitor of actin polymerisation, has been found to reduce polar auxin transport in zucchini (Butler et al., 1998). Another study shows that latrunculin-treated roots had an increased gravitropic response after rotation on a clinostat, which should randomize the gravitropic field perceived by the roots after

gravistimulation (Hou et al., 2004). These data suggest that the cytoskeleton is not necessary for the primary gravity response, but could be important in regulating the magnitude of gravity response. Indeed, the cytoskeleton could act as a dampener or a way to reset the gravity response machinery. Moreover, it has been found that saltatory movements of statoliths in the columella are significantly reduced with treatment of latrunculin B (Hou et al., 2004). An attractive hypothesis might be that latrunculin B-treated roots are more sensitive to gravity because the cytoskeleton is important for sensing saltatory movements that allow the plant to distinguish between background noise and statolith sedimentation due to displacement. The cytoskeleton's role in gravity response is an interesting avenue to explore, and would be greatly helped by a fluorescent statolith marker paired with vertical imaging. This would allow one to visualize the fall of statoliths and analyse their interaction with the cytoskeleton.

6.3 The Role of Auxin Signalling in the Gravity-Sensing Cells of Roots and Shoots During Gravity Response

It has recently been shown that the Aux/IAA-ARF signalling system has a role in the gravitropism of shoots (Sato et al., 2014; Roychoudhry et al., 2013). In Chapter 5, we aimed to investigate to which extent auxin signalling in the gravity-sensing cells and in the epidermis contribute to gravity response. To do this, auxin response was perturbed in either the gravity-sensing cells or the epidermis of roots, using the *ARL2* promoter and a UAS/GAL4 system, respectively.

It was found that expressing a truncated, Aux/IAA insensitive version of *ARF7* in the gravity-sensing cell slowed down gravitropic response, while expressing a dominant-negative version of *ARF7* increased the rate of gravity response in the root. Furthermore, the expression of a stabilised Aux/IAA, *axr3-1*, in the gravity-sensing cells did not induce a primary root phenotype. This is in contrast to our previous results, since the expression of *axr3-1* should have a similar effect as the dominant-negative form of *ARF7*. These results show that auxin signalling is necessary in the gravity-sensing cells. However, its role is not straightforward as dampening the auxin response in the gravity-sensing cell slows down gravity response.

A role for auxin signalling in the root gravity-sensing cell is interesting although its mechanism is currently unknown. To investigate how auxin signalling might affect the rate of gravity response in the primary roots, the mRNA expression of three *PIN*s that are known to affect gravity response in primary root were quantified. It was found that *PIN3* and *PIN7* were upregulated in the gravity-sensing cells of the transgenic line *ARL2::ARF7–SRDX.* This result contrasts with previously published work. Indeed, it would be expected that dampening auxin response would lead to a downregulation of *PIN*s, since most PINs are positively regulated by auxin (Vieten et al., 2005). It is possible that repressing *ARF7* in the gravity-sensing cell affects the abundance or activity of other Aux/IAAs and/or possible downstream effectors that could be upregulating *PIN*s. There is evidence that other transcription factors affect *PIN* expression, such as FOUR LIPS (FLP) and its paralogue MYB88 (Wang et al., 2015).

Expressing the stabilised version of AXR3/IAA17 in the gravity-sensing cells did not affect primary root gravitropism, yet the lateral roots showed a more vertical GSA. This is interesting as *axr3-1* and *ARF7–SRDX* are qualitatively similar mutations that should be repressing auxin response in the gravity-sensing cells. It is possible that either of these genes affect only the primary or the lateral organs, and have a context specific role. This pattern was also observed in several other transgenic lines, as some had mutations that affected either just the primary organs (*ARL2::ARF7–SRDX, ARL2::arf7delete, ATML1::arf7delete*), just the lateral organs (*ARL2::axr3-1*, *SCR::arf7delete*), or both (*ARL2::RCN1, tac1, lazy1*). This context-specificity could be further explored to probe the differences between primary and lateral organ gravitropism.

To understand the specific contributions of auxin signalling in the tissue responsible for gravity-induced cell elongation in the primary root, transgenic lines affecting auxin signalling in the root epidermis were made using the UAS/GAL4 system. Again, the same dominant-negative form of *ARF7* and AXR3/IAA17 (*axr3-1*, and the milder allele) were used. Expressing the dominant-negative form of *ARF7* (*ARF7–SRDX)* in the epidermis slowed down root gravity response. This result fits with the loss-of-function mutant of ARF7 showing a slower root gravity response when expressed in the whole plant. However, this is in contrast to the phenotype of faster gravity response that occurs when *ARF7–SRDX* was expressed in the gravity-sensing cells.

These data suggest that *ARF7* could have different roles in gravity response: one as a positive regulator of cell expansion in the epidermis, and another as a negative regulator in the gravity-sensing cell. *axr3-1* and *axr3-3* also showed gravitropic defects when expressed in the epidermis, in agreement with a previously published report (Swarup et al., 2005), although we report milder defects. These results taken together, suggest that dampening auxin response in the root epidermis by increasing the stability of *Aux/IAA* corepressors or repressing an activating *ARF* slow down gravity response, while dampening the auxin response in the gravity-sensing cell is possibly more complex. Much more work is needed to understand the context-specific differences between these tissues that are the basis of these effects. Further work may include a study of tissue-specific auxin signalling networks and the interacting binding pairs between *Aux/IAA*s and *ARF*s, as the transcriptional control of auxin response is complex and not fully understood.

A role for auxin signalling in the gravity-sensing cell was first observed in the shoot (Sato et al., 2014; Roychoudhry et al., 2013). These works demonstrate that expressing stabilised versions of *Aux/IAA*s in the gravity-sensing cells, thereby likely repressing auxin response in those cells, causes defects in gravity response in the shoot. In this thesis, the role of auxin signalling in gravity-sensing cells and in the tissue responsible for gravity-induced cell elongation, the epidermis, of the shoot was investigated by increasing auxin response in those cells. Shoot gravitropism experiments were carried out with transgenic lines expressing an *Aux/IAA*-irrepressible version of *ARF7 (arf7delete)* in either the epidermis or the gravity-sensing cells of the shoot.

The data indicate that increasing the capacity for auxin response in the gravity-sensing cell does not have an effect. However, it has been shown that expressing stabilised versions of Aux/IAAs in the gravity-sensing cells of the shoot leads to an agravitropic phenotype (Roychoudhry et al., 2013; Sato et al., 2014). It is possible that only repressing auxin signalling in the gravity-sensing cell of the shoot causes gravity defects. However, it was found that expressing *arf7delete* in the epidermis slows down gravity response. Further work is needed to clarify the role of *ARF7* in the shoot epidermis. It appears that expressing an irrepressible version of *ARF7* has a similar phenotype to a loss-of-function mutant of *ARF7* (Okushima et al.,

2005). It is also possible that *ARF7* is part of a feedback loop that is involved differently in the gravity response of roots and shoots.

It is possible that there is an additional regulatory mechanism in the shoot that either interacts with the auxin efflux carriers or the auxin signalling system. Genes such as *LAZY1* and *TAC1,* which are part of the same family, could either interact with the auxin efflux carriers or the auxin signalling system or are part of a possible second mechanism of gravity perception and response. Loss-of-function *lazy1* plants are gravitropically defective across many species, meaning it is likely a fundamental protein is involved in gravitropism (Yoshihara et al., 2013). Furthermore, *lazy1* maize coleoptiles have been found to have increased auxin transport rates but are defective in creating an auxin gradient that is necessary for gravity response (Dong et al., 2013). A similar gene, *TAC1* has been found to regulate GSA of lateral branches in maize, rice, and peach trees (Yu et al., 2007; Ku et al., 2011; Dardick et al., 2013). In Chapter 5, we briefly investigated the gravity response of the primary shoots of a loss-of-function mutant of *TAC1.* The primary *tac1* shoots bend faster than wild type and overshoot before returning to 90º. *lazy1* shoots appear to be phenotypically similar to *SCR::bdl* shoots, displaying a very horizontal lateral phenotype and gravitropic defects in the primary. An interesting possibility is that *TAC1* and *LAZY1* affect gravitropism by interacting with the auxin signalling framework. It has been found, using a yeast two-hybrid system, that LAZY1 may interact with IAA17 and a putative kinase (Dong et al., 2013). These data suggest that it is possible that LAZY is interacting with either the auxin efflux carriers to modulate lateral auxin transport or the *Aux/IAA*s to regulate auxin signalling. Both mechanisms could be happening, since LAZY1 was found to be localised to both the nucleus and the plasma membrane, however its method of action is believed to be at the plasma membrane (Yoshihara et al., 2013). More work needs to be done to understand the possible interactions between *LAZY1*/*TAC1* and Aux/IAAs and/or auxin efflux carriers. These experiments could include expression analysis of *LAZY1* and *TAC1* in the gravity-sensing cells of agravitropic mutants such as *SCR::bdl*. Another possible avenue of research is to explore the role of *DRO1,* which is thought to have a similar function as *LAZY1* in the root (Uga et al., 2011).

6.4 Concluding Remarks

The aim of this thesis project was to understand the molecular basis for the auxin-mediated sine law of root gravitropism. Our results allow us to conclude that there are angle-dependent auxin asymmetries that likely regulate the magnitude of gravity response in Arabidopsis. The mechanism that confers angle-dependent auxin asymmetries was further investigated. Our results indicate that the subcellular localisation of PINs is angle-dependent and is likely one of the mechanisms that generate and maintain angle-dependent auxin asymmetries. Moreover, we suggest that different *PIN*s may have some angle-specific role. Since there are many ways in which auxin response is regulated, this thesis also investigated the interesting idea that auxin signalling might have a role in the gravity-sensing cells during root gravity response. The results from this thesis do indicate that TIR1-AFB-Aux/IAA mediated-auxin signalling is involved in the gravity-sensing cells during root gravity response, although more work is necessary to elucidate its role.

Understanding how angle-dependent gravitropism is mediated by auxin fundamentally furthers the knowledge of plant gravitropism. Lateral roots must continually monitor and maintain their nonvertical growth pattern. In addition, the mechanism in which primary roots mediate angle-dependent responses might also explain how lateral roots maintain their GSA. The maintenance of lateral root GSA is auxin-dependent (Roychoudhry et al., 2013) and is maintained by both a gravitropic component and an anti-gravitropic offset. Key to understanding the anti-gravitropic offset is deciphering how plants can respond to gravity with a variable magnitude. Understanding how a primary root can respond with a variable magnitude might further explain the anti-gravitropic offset that controls lateral root GSA. Fundamental knowledge of the mechanism governing GSA in plants is important as GSA is required for plants to change the growth patterns of lateral roots and shoots to interact with their environment (reviewed in (Jung and McCouch, 2013)). Furthermore, GSA is known to affect crop yields (Lynch, 2013; Pierik and Testerink, 2014).

While the majority of this work was performed on the model species Arabidopsis, sine law has been described in many other species. Here, we identified some differences between Arabidopsis and other species that will

likely be the subject of a new project. The differences in gravitropism between species presents an important research question and could provide more mechanistic insight.

In addition to application of fundamental knowledge to crop species, Arabidopsis root gravitropism can be used as a model of mechanosensing and signal transduction. There is strong evidence for the starch-statolith theory of gravity perception, but how the physical signal of statolith sedimentation becomes a chemical signal is still relatively unknown. Understanding gravity perception also provides a good model for mechanosensing in other systems. Furthermore, because gravity perception and gravity response are spatially separated in the Arabidopsis primary root, the study of the gravity response provides a good model for auxin signal transduction along the root meristem.

The results of this thesis provide a better understanding of angle-dependent gravitropism. However, there are still many open questions. An aspect of gravitropism that requires further study, and may yield lots of insight, is how statoliths provide information about both the direction of the gravitropic change and how far an organ has been displaced from its GSA (Toyota et al., 2013). The ability to live-image statoliths in the root during sedimentation would allow us to further understand how the physical signal is transduced into angle-dependent auxin gradients. While many pieces of the gravitropism puzzle have been uncovered, further work is required to understand how these pieces fit together to regulate the complete process of gravity response.

7 Appendix

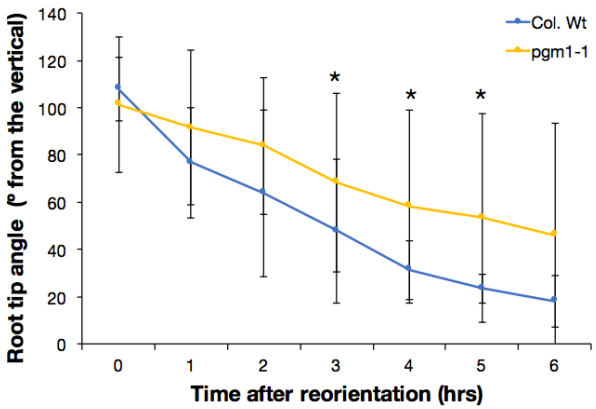

Figure 7.1 Gravity response kinetics of *pgm1-1* mutants.
N > 10, stars represent a p value of < 0.05, Student's t-test. Bars represent s.d.

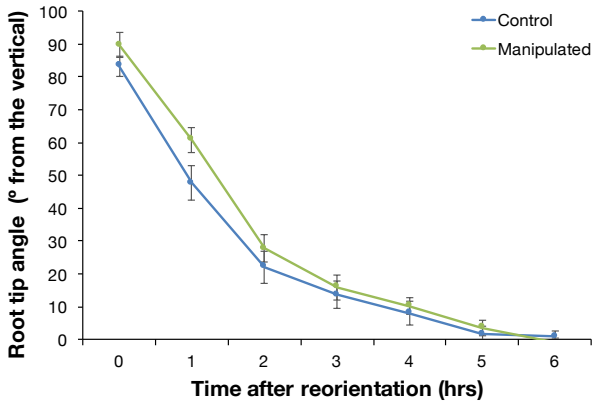

Figure 7.2 The effect of physical manipulation on 5-day-old primary roots. Roots were moved with forceps gently 1 hour prior to gravistimulation. N = 24 roots each condition, spread over 2 plates. Bars represent s.e.m.

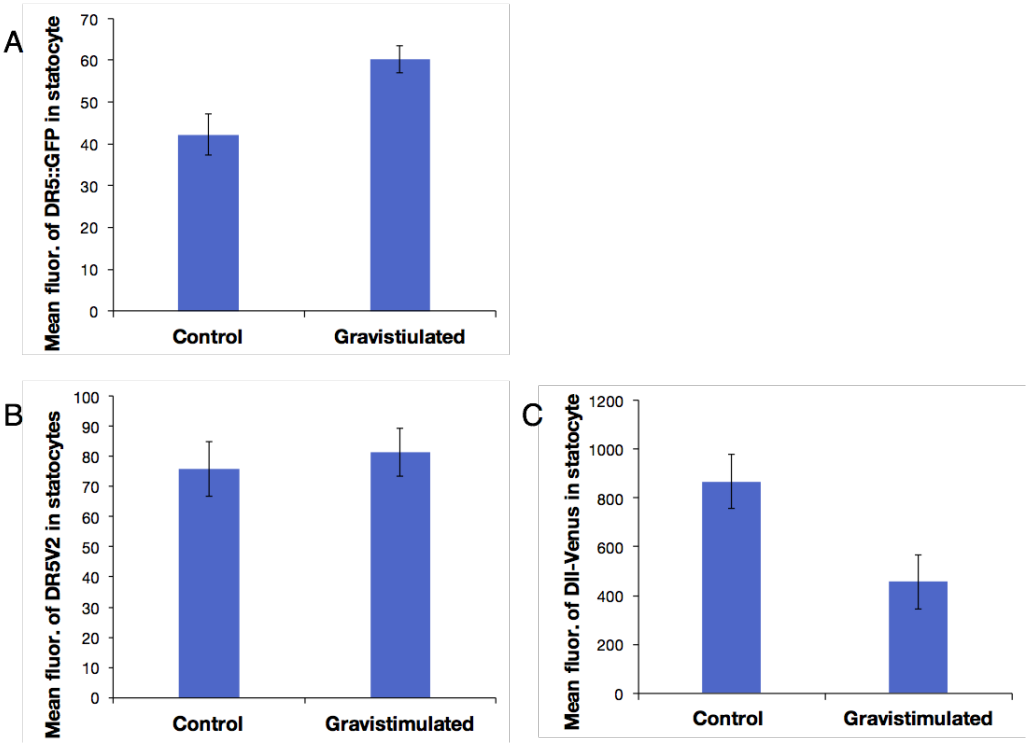

Figure 7.3 Investigating overall amount of auxin in the root statocytes.
(A) Inferred amount of auxin in the primary root columella after gravistimulation using the *DR5::GFP* reporter, n = 6, $p < 0.01$, Student's t-test. (B) Inferred auxin amount in the primary root gravistimulation using the *DR5v2* auxin reporter, n = 6. (C) Inferred auxin amount in the primary root after gravistimulation using the *DII-VENUS* reporter, n = 5. All bars represent s.e.m.

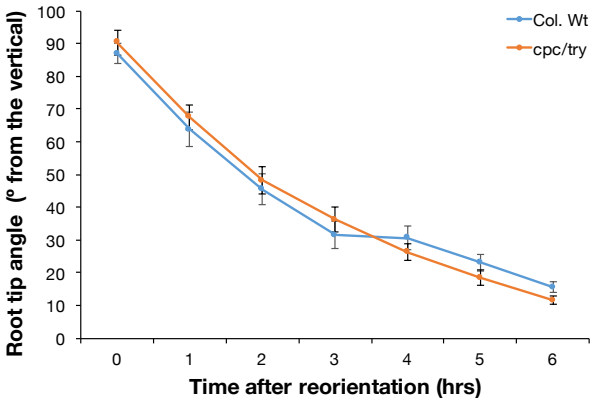

Figure 7.4 Gravity response kinetics of *cpc try* mutants.
N = 38, spread across two plates. Bars represent s.e.m.

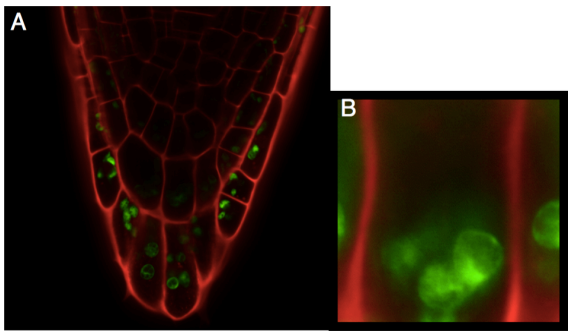

Figure 7.5 Images of plastid marker *pt-yk* (Nelson et al., 2007). Images taken using LSM880 with Airy Scan.

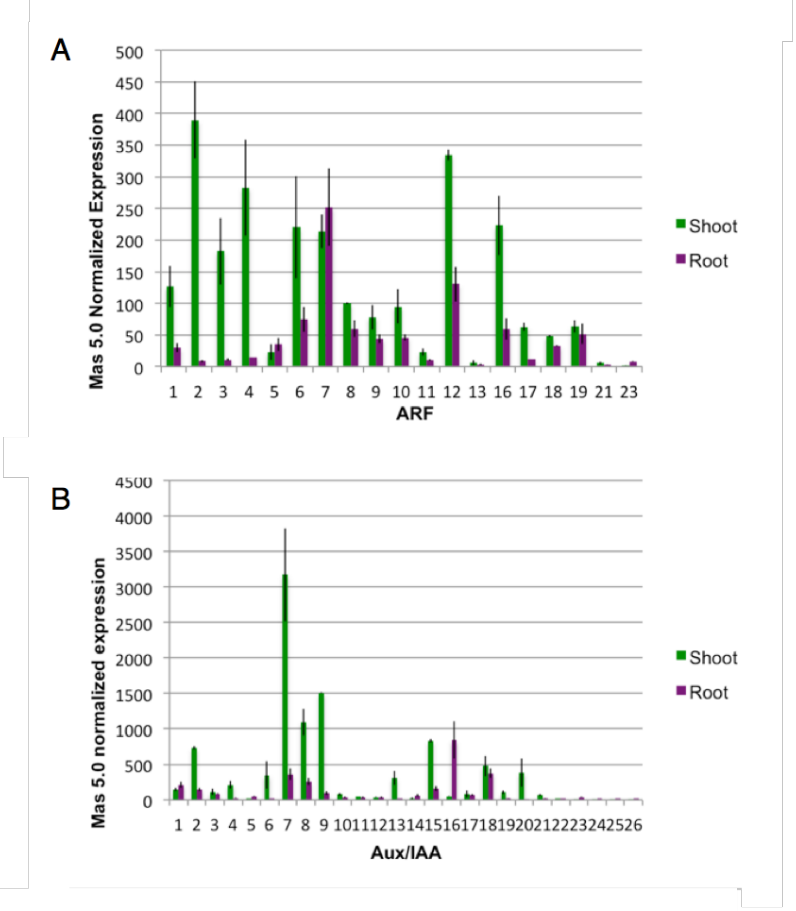

Figure 7.6 Differential expression of *ARF* and *Aux/IAA* genes in the epidermal layer of Arabidopsis roots and shoots.
Mas 50.0 normalised data from a previously published paper on the epidermal layer of shoots (Suh et al., 2005) was compared to unpublished root epidermal tissue data from the Kepinski lab.

Table 7.1 List of primers used in this project.

Name	Sequence	Type
ARL2b1b5r	GGG GAC AAC TTT TGT ATA CAA AGT TGT TGT TCA ATA ACA GGT TTT TGT TTC CCA GTT TG	cloning
ARL2b1f	GGG GAC AAG TTT GTA CAA AAA AGC AGG CTT TTT AAA CTG ATT ACA AAA ATC TTA TAT AC	cloning
UASB1f	GGG GAC AAG TTT GTA CAA AAA AGC AGG CTG CGG CCG CGG ATC GAT CC	cloning
UASB5r	GGG GAC AAC TTT TGT ATA CAA AGT TGT GGC GGC CGC TCT AGC CCA TC	cloning
atml1reverseB5r	GGG GAC AAC TTT TGT ATA CAA AGT TGT ATG ATG ATG GAT GCC TAT CAA TT	cloning
frwdatml1prgtway	GGG GAC AAG TTT GTA CAA AAA AGC AGG CTT CGC CTC GAC TGG CCA ATT TTT AAT	cloning
mir393aB5f	GGG GAC AAC TTT GTA TAC AAA AGT TGC TAC GTA CCC ATC ATG AAC ACT GTG	cloning
mir393aReB2	GGG GAC AAG TTT GTA CAA AAA AGC AGG CTC TAC GTA CCC ATC ATG AAC ACT GTG	cloning
pARL2B2	GGG GAC CAC TTT GTA CAA GAA AGC TGG GTT TGT TCA ATA ACA GGT TTT TGT TTC CCA GTT TG	cloning
B3NLS	GGG GAC AAC TTT GTA TAA TAA AGT TGT AAT GGT GAG CAA GGG CGA GGA GC	cloning

B4	GGG GAC AAC TTT GTA TAG AAA AGT TGG GTG GAC AAA TTC GAT CGC ACA AAC T	cloning
B5 NLS	GGG GAC AAC TTT GTA TAC AAA AGT TGT AAT GGT GAG CAA GGG CGA GGA GC	cloning
DII28UBI10B4	GGG GAC AAC TTT GTA TAG AAA AGT TGG GTG GTT TCT CCG GGA TGA TCT C	cloning
DII28UBI10nestedprimer	GTT TCT CCG GGA TGA TCT CAC CGG CGG CCA TCC CAC CAC TGG AGC TAC CTC AAC CCT GTT ATT CTG TTA ATC AGA AAA ACT CAG ATT	cloning
DIIIAA28UBI10Fusionb5r new	GGG GAC AAC TTT TGT ATA CAA AGT TGT GTT TCT CCG GGA TGA TCT C	cloning
GFPNLSnestedprimerHa seloff	ATG TTG CAG CCT AAG AAG AAG AGA AAG GTT GGA GGA TCA AAG GGA GAG GAA CTT TTC AC	cloning
GFPhaseloffB2	GGG GAC CAC TTT GTA CAA GAA AGC TGG GTT TCA CTT ATA CAA CTC ATC CAT TCC	cloning
GFPmrgeneB2	GGG GAC CAC TTT GTA CAA GAA AGC TGG GTT TTA TTT GTA TAG TTC ATC CAT GCC	cloning
IAA17LB3R	GGG GAC AAC TTT ATT ATA CAA AGT TGT CGC CGC CGC CTC CGG GCC	cloning
IAA17LB4r	GGG GAC AAC TTT TCT ATA CAA AGT TGT AAT GAT GGG CAG TGT CGA GC	cloning
VenusB2	GGG GAC CAC TTT GTA CAA GAA AGC TGG GTT CTT GTA CAG CTC GTC CAT GC	cloning
VenusNLSnestedprimer	ATG TTG CAG CCT AAG AAG AAG AGA AAG GTT GGA GGA GTG AGC AAG GGC GAG G	cloning

pUBI10B4	GGG GAC AAC TTT GTA TAG AAA AGT TGG GTG CTG TTA ATC AGA AAA ACT CAG	cloning
pUBI10B54	GGG GAC AAC TTT TGT ATA CAA AGT TGT CTG TTA ATC AGA AAA ACT CAG	cloning
CSSpin7102CF450	GAT TGA AGT TAG ATC CTC TTG	genotyping
CSpin4101Mt12	CAT TTG GAC GTG AAT GTA GAC AC	genotyping
CSpin4101WTF	CAA CGC CGT TAA ATA TGG	genotyping
CSpin4101WtRCF448	TTA TTC AGC CCT GCT GTA GC	genotyping
CSpin4101gabiLB	CAT TTG GAC GTG AAT GTA GAC AC	genotyping
CSpin7102CF449tdna	TGA TCA CAT GGC ACG ACC	genotyping
CSpin7102WtF	GGT CGT CAT GTG TTT GCT GT	genotyping
CSpin7102gabLB	GGC AAT CAG CTG TTG CCC GTC TCA CTG GTG	genotyping
En8130pin71en	GAG CGT CGG TCC CCA CAC TTC TAT AC	genotyping
JFpin42WTF	GGC CTT CGA ATC TTA CCG GA	genotyping

JFpin42WTR	TCA GAT TGT TCC GTT GCC AC	genotyping
JFpin7enMTR	TAG CTC TTT AGG GTT TAG CTC	genotyping
JFpin7enWTF	GGT CGT CAT GTG TTT GCT GT	genotyping
Pin33JF	GGA GCT CAA ACG GGT CAC CCG	genotyping
Pin33JFR	GCT GGA TGA GCT ACA GCT ATA TTC	genotyping
SALKLBa1	TGG TTC ACG TAG TGG GCC ATC G	genotyping
TBpin43MandWtF	CAA CGC CGT TAA ATA TGG	genotyping
TBpin43MtR	TGC AGC AAA ACC CAC ACT TTT ACT TC	genotyping
TBpin43WTR	TTC CCA CTA CAA TTA TTC C	genotyping
TBpin71enRP2	CCA CAT CCC ACC TTC ATA TC	genotyping
TBpin72LP	TCC TCG TCC GTC TAA TCT	genotyping
TBpin72MtR	ATT TTG CCG ATT TCG GAA C	genotyping

TBpin72MtandWtF	TTT ACT TGA ACA ATG GCC ACA C	genotyping
TBpin72WtR	GGT AAA GGA AGT GCC TAA CGG	genotyping
En8130pin71en	GAG CGT CGG TCC CCA CAC TTC TAT AC	genotyping
PIN4 RT 88 R	CAGCCCTGCTGTAGCTTTCT	RT-qPCR
PIN4 RT 88 F	TCAACCTCGAAAGAGTGGTG	RT-qPCR
PIN7 RT 81 R	CCGTTCATCGGACCAGCATT	RT-qPCR
PIN7 RT 81 F	CGGAAAATCCGATCAAGGCG	RT-qPCR
PIN3 RT 175 R	CTCGGGGCTTTCATAACCGA	RT-qPCR
PIN3 RT 175 F	AGTTCAGGCCGCATTACCTC	RT-qPCR
GAPHDH F	AGGCTGCTGAAGGACCATTGAA G	RT-qPCR
GAPDH R	CCATTCGTTATCGTACCAGGCT ACA	RT-qPCR

List of References

Abas, L., Benjamins, R., Malenica, N., Paciorek, T., Wiřniewska, J., Moulinier Anzola, J.C., Sieberer, T., Friml, J. and Luschnig, C. 2006. Intracellular trafficking and proteolysis of the Arabidopsis auxin-efflux facilitator PIN2 are involved in root gravitropism. *Nature Cell Biology*. **8**(3),pp.249–256.

Abe, K., Takahashi, H. and Suge, H. 1994. Localisation of cells containing sedimented amyloplasts in the shoots of normal and lazy rice seedlings. *Biological Sciences in Space*. **8**(4),pp.221–225.

Abel, S., Oeller, P.W. and Theologis, A. 1994. Early auxin-induced genes encode short-lived nuclear proteins. *Proceedings of the National Academy of Sciences*. **91**(1),pp.326–330.

Audus, L.J. 1964. Geotropism and the modified sine rule; an interpretation based on the amyloplast statolith theory. *Physiologia Plantarum*. **17**(3),pp.737–745.

Baldwin, K.L., Strohm, A.K. and Masson, P.H. 2013. Gravity Sensing and Signal Transduction in Vascular Plant Primary Roots. *American Journal of Botany*. **100**(1),pp.126–142.

Band, L.R., Wells, D.M., Larrieu, A., Sun, J., Middleton, A.M., French, A.P., Brunoud, G., Sato, E.M., Wilson, M.H. and Péret, B. 2012. Root gravitropism is regulated by a transient lateral auxin gradient controlled by a tipping-point mechanism. *Proceedings of the National Academy of Sciences*. **109**(12),pp.4668–4673.

Barbosa, I.C.R., Zourelidou, M., Willige, B.C., Weller, B. and Schwechheimer, C. 2014. D6 PROTEIN KINASE Activates Auxin Transport-Dependent Growth and PIN-FORMED Phosphorylation at the Plasma Membrane. *Developmental Cell*. **29**(6),pp.674–685.

Barlow, P.W., Parker, J.S., Butler, R. and Brain, P. 1993. Gravitropism of primary roots of Zea mays L. at different displacement angles. *Annals of Botany*. **71**(1),pp.383–388.

Baskin, T.I., Wilson, J.E., Cork, A. and Williamson, R.E. 1994. Morphology and microtubule organization in Arabidopsis roots exposed to oryzalin or taxol. *Plant & cell physiology*. **35**(6),pp.935–942.

Baster, P.L., Robert, S.E.P., Kleine-Vehn, J.U.R., Vanneste, S., Kania, U., Grunewald, W., De Rybel, B., Beeckman, T. and Friml, J.R.I. 2012. - auxin signalling regulates PIN vacuolar trafficking and auxin fluxes during root gravitropism. *The EMBO Journal*. **32**(2),pp.260–274.

Bastien, R., Bohr, T., Moulia, B. and Douady, S. 2013. Unifying model of shoot gravitropism reveals proprioception as a central feature of posture control in plants. *Proceedings of the National Academy of Sciences*. **110**(2),pp.755–760.

Benjamins, R., Quint, A., Weijers, D., Hooykaas, P. and Offringa, R. 2001. The PINOID protein kinase regulates organ development in Arabidopsis by enhancing polar auxin transport. *Development*. **128**(20),pp.4057–4067.

Benkova, E., Michniewicz, M., Sauer, M. and Teichmann, T. 2003. Local, efflux-dependent auxin gradients as a common module for plant organ formation. *Cell*.pp.1–12.

Bensmihen, S., To, A., Lambert, G., Kroj, T., Giraudat, J. and Parcy, F. 2004. Analysis of an activated ABI5allele using a new selection method for transgenic Arabidopsis seeds. *FEBS Letters*. **561**(1-3),pp.127–131.

Blakeslee, J.J., Zhou, H.W., Heath, J.T., Skottke, K.R., Barrios, J.A.R., Liu, S.Y. and DeLong, A. 2007. Specificity of RCN1-Mediated Protein Phosphatase 2A Regulation in Meristem Organization and Stress Response in Roots. *Plant Physiology*. **146**(2),pp.539–553.

Blancaflor, E.B., and Masson, P.H. 2003. Plant Gravitropism. Unraveling the Ups and Downs of a Complex Process. *Plant Physiology*. **133**(4),pp.1677–1690.

Blancaflor, E.B., Fasano, J.M. and Gilroy, S. 1998. Mapping the functional roles of cap cells in the response of Arabidopsis primary roots to gravity. *Plant Physiology*. **116**(1),pp.213–222.

Boer, D.R., Freire-Rios, A., van den Berg, W.A.M., Saaki, T., Manfield, I.W., Kepinski, S., López-Vidrieo, I., Franco-Zorrilla, J.M., de Vries, S.C., Solano, R., Weijers, D. and Coll, M. 2014. Structural Basis for DNA Binding Specificity by the Auxin-Dependent ARF Transcription Factors. *Cell*. **156**(3),pp.577–589.

Brunoud, G., Wells, D.M., Oliva, M., Larrieu, A., Mirabet, V., Burrow, A.H., Beeckman, T., Kepinski, S., Traas, J., Bennett, M.J. and Vernoux, T. 2012. A novel sensor to map auxin response and distribution at high spatio-temporal resolution. *Nature*. **482**(7383),pp.103–106.

Butler, J.H., Hu, S., Brady, S.R., Dixon, M.W. and Muday, G.K. 1998. In vitro and in vivo evidence for actin association of the naphthylphthalamic acid-binding protein from zucchini hypocotyls. *The Plant Journal*. **13**(3),pp.291–301.

Calderon-Villalobos, L.I.A., Lee, S., De Oliveira, C., Ivetac, A., Brandt, W., Armitage, L., Sheard, L.B., Tan, X., Parry, G., Mao, H., Zheng, N., Napier, R., Kepinski, S. and Estelle, M. 2012. A combinatorial

TIR1/AFB–Aux/IAA co-receptor system for differential sensing of auxin. *Nature Chemical Biology*. **8**(5),pp.477–485.

Causier, B., Ashworth, M., Guo, W. and Davies, B. 2012. The TOPLESS Interactome: A Framework for Gene Repression in Arabidopsis. *Plant Physiology*. **158**(1),pp.423–438.

Chen, R., Rosen, E. and Masson, P.H. 1999. Gravitropism in higher plants. *Plant Physiology*. **120**(2),pp.343–350.

Christensen, S.K., Dagenais, N., Chory, J. and Weigel, D. 2000. Regulation of auxin response by the protein kinase PINOID. *Cell*. **100**(4),pp.469–478.

Dardick, C., Callahan, A., Horn, R., Ruiz, K.B., Zhebentyayeva, T., Hollender, C.A., Whitaker, M., Abbott, A. and Scorza, R. 2013. PpeTAC1 promotes the horizontal growth of branches in peach trees and is a member of a functionally conserved gene family found in diverse plants species. *The Plant journal : for cell and molecular biology*. **75**(4),pp.618–630.

Darwin, C. and F. 1880. The Power of Movement in Plants. John Murray. London.

Del Bianco, M. and Kepinski, S. 2010. Context, Specificity, and Self-Organization in Auxin Response. *Cold Spring Harbor Perspectives in Biology*. **3**(1),pp.a001578–a001578.

Deruère, J., Jackson, K., Garbers, C., Söll, D. and DeLong, A. 1999. The RCN1-encoded A subunit of protein phosphatase 2A increases phosphatase activity in vivo. *The Plant journal : for cell and molecular biology*. **20**(4),pp.389–399.

Dharmasiri, N., Dharmasiri, S. and Estelle, M. 2005. The F-box protein TIR1 is an auxin receptor. *Nature Cell Biology*. **435**(7041),pp.441–445.

Dharmasiri, N., Dharmasiri, S., Weijers, D., Lechner, E., Yamada, M., Hobbie, L., Ehrismann, J.S., Jürgens, G. and Estelle, M. 2005. Plant Development Is Regulated by a Family of Auxin Receptor F Box Proteins. *Developmental Cell*. **9**(1),pp.109–119.

Dhonukshe, P., Aniento, F., Hwang, I., Robinson, D.G., Mravec, J., Stierhof, Y.-D. and Friml, J. 2007. Clathrin-Mediated Constitutive Endocytosis of PIN Auxin Efflux Carriers in Arabidopsis. *Current Biology*. **17**(6),pp.520–527.

Dhonukshe, P., Huang, F., Galvan-Ampudia, C.S., Mahonen, A.P., Kleine-Vehn, J., Xu, J., Quint, A., Prasad, K., Friml, J., Scheres, B. and Offringa, R. 2010. Plasma membrane-bound AGC3 kinases phosphorylate PIN auxin carriers at TPRXS(N/S) motifs to direct apical PIN recycling. *Development*. **137**(19),pp.3245–3255.

Di Laurenzio, L., Wysocka-Diller, J., Malamy, J.E. and Pysh, L. 1996. The SCARECROW gene regulates an asymmetric cell division that is essential for generating the radial organization of the Arabidopsis root. *Cell*. **86**(3),pp.423–433.

Digby, J. and Firn, R.D. 1995. The gravitropic set-point angle (GSA): the identification of an important developmentally controlled variable governing plant architecture. **18**(12),pp.1434–1440.

Dolan, L., Janmaat, K., Willemsen, V., Linstead, P., Poethig, S., Roberts, K. and Scheres, B. 1993. Cellular organisation of the Arabidopsis thaliana root. *Development*. **119**(1),pp.71–84.

Dong, Z., Jiang, C., Chen, X., Zhang, T., Ding, L., Song, W., Luo, H., Lai, J., Chen, H., Liu, R., Zhang, X. and Jin, W. 2013. Maize LAZY1 Mediates Shoot Gravitropism and Inflorescence Development through Regulating Auxin Transport, Auxin Signaling, and Light Response. *Plant Physiology*. **163**(3),pp.1306–1322.

Dreher, K.A., Brown, J., Saw, R.E. and Callis, J. 2006. The Arabidopsis Aux/IAA protein family has diversified in degradation and auxin responsiveness. *The Plant Cell*. **18**(3),pp.699–714.

Dubrovsky, J.G., Sauer, M., Napsucialy-Mendivil, S., Ivanchenko, M.G., Friml, J., Shishkova, S., Celenza, J. and Benková, E. 2008. Auxin acts as a local morphogenetic trigger to specify lateral root founder cells. *Proceedings of the National Academy of Sciences*. **105**(25),pp.8790–8794.

Ferrell K, Wilkinson CR, Dubiel W, Gordon C (2000) Regulatory subunit interactions of the 26S proteasome, a complex problem. Trends Biochem Sci **25**(2):83–88

Fasano, J.M., Swanson, S.J., Blancaflor, E.B., Dowd, P.E., Kao, T.H. and Gilroy, S. 2001. Changes in root cap pH are required for the gravity response of the Arabidopsis root. *The Plant Cell*. **13**(4),pp.907–921.

Friml, J., Wiśniewska, J., Benková, E., Mendgen, K. and Palme, K. 2002. Lateral relocation of auxin efflux regulator PIN3 mediates tropism in Arabidopsis. *Nature*. **415**(6873),pp.806–809.

Friml, J., Yang, X., Michniewicz, M., Weijers, D., Quint, A., Tietz, O., Benjamins, R., Ouwerkerk, P.B.F., Ljung, K., Sandberg, G., Hooykaas, P.J.J., Palme, K. and Offringa, R. 2004. A PINOID-dependent binary switch in apical-basal PIN polar targeting directs auxin efflux. *Science*. **306**(5697),pp.862–865.

Fujihira, K., Kurata, T., Watahiki, M.K., Karahara, I. and Yamamoto, K.T. 2000. An agravitropic mutant of Arabidopsis, endodermal-amyloplast less 1, that lacks amyloplasts in hypocotyl endodermal cell layer. *Plant &*

cell physiology. **41**(11),pp.1193–1199.

Fukaki, H., Wysocka-Diller, J., Kato, T., Fujisawa, H., Benfey, P.N. and Tasaka, M. 1998. Genetic evidence that the endodermis is essential for shoot gravitropism in Arabidopsis thaliana. *The Plant journal : for cell and molecular biology*. **14**(4),pp.425–430.

Galland, P. 2002. Tropisms of Avena coleoptiles: sine law for gravitropism, exponential law for photogravitropic equilibrium. *Planta.* **215**(5),pp.779–784.

Galland, P., Wallacher, Y., Finger, H., Hannappel, M., Tröster, S., Bold, E. and Grolig, F. 2002. Tropisms in Phycomyces : sine law for gravitropism, exponential law for photogravitropic equilibrium. *Planta.* **214**(6),pp.931–938.

Garbers, C., DeLong, A., Deruère, J., Bernasconi, P. and Söll, D. 1996. A mutation in protein phosphatase 2A regulatory subunit A affects auxin transport in Arabidopsis. *The EMBO Journal*. **15**(9),pp.2115–2124.

Gälweiler, L., Guan, C., Müller, A., Wisman, E., Mendgen, K., Yephremov, A. and Palme, K. 1998. Regulation of polar auxin transport by AtPIN1 in Arabidopsis vascular tissue. *Science*. **282**(5397),pp.2226–2230.

Geldner, N., Anders, N., Wolters, H., Keicher, J., Kornberger, W., Muller, P., Delbarre, A., Ueda, T., Nakano, A. and Jürgens, G. 2003. The Arabidopsis GNOM ARF-GEF mediates endosomal recycling, auxin transport, and auxin-dependent plant growth. *Cell*. **112**(2),pp.219–230.

Geldner, N., Friml, J., Stierhof, Y.D., Jurgens, G. and Palme, K. 2001. Auxin transport inhibitors block PIN1 cycling and vesicle trafficking. *Nature*. **413**(6854),pp.425–428.

Gray, W.M., del Pozo, J.C., Walker, L., Hobbie, L., Risseeuw, E., Banks, T., Crosby, W.L., Yang, M., Ma, H. and Estelle, M. 1999. Identification of an SCF ubiquitin-ligase complex required for auxin response in Arabidopsis thaliana. *Genes & Development*. **13**(13),pp.1678–1691.

Gray, W.M., Kepinski, S., Rouse, D., Leyser, O. and Estelle, M. 2001. Auxin regulates SCFTIR1-dependent degradation of AUX/IAA proteins. *Nature*. **414**(6861),pp.271–276.

Grieneisen, V.A., Xu, J., Marée, A.F.M., Hogeweg, P. and Scheres, B. 2007. Auxin transport is sufficient to generate a maximum and gradient guiding root growth. *Nature*. **449**(7165),pp.1008–1013.

Grunewald, W. and Friml, J.R.I. 2010. Focus ReviewThe march of the PINs: developmental plasticity by dynamic polar targeting in plant cells. *The EMBO Journal*. **29**(16),pp.2700–2714.

Guilfoyle, T.J. and Hagen, G. 2007. Auxin response factors. *Current Opinion*

in Plant Biology. **10**(5),pp.453–460.

Harper, R.M., Stowe-Evans, E.L., Luesse, D.R., Muto, H., Tatematsu, K., Watahiki, M.K., Yamamoto, K. and Liscum, E. 2000. The NPH4 locus encodes the auxin response factor ARF7, a conditional regulator of differential growth in aerial Arabidopsis tissue. *The Plant Cell*. **12**(5),pp.757–770.

Harrison, B.R. and Masson, P.H. 2007. ARL2, ARG1 and PIN3 define a gravity signal transduction pathway in root statocytes. *The Plant Journal*. **53**(2),pp.380–392.

Haseloff, J. 1999. GFP variants for multispectral imaging of living cells. *Methods Cell Biology*. **58**,pp.139–151.

Hiratsu, K., Matsui, K., Koyama, T. and Ohme-Takagi, M. 2003. Dominant repression of target genes by chimeric repressors that include the EAR motif, a repression domain, in Arabidopsis. *The Plant journal : for cell and molecular biology*. **34**(5),pp.733–739.

Hollender, C.A. and Dardick, C. 2014. Molecular basis of angiosperm tree architecture. *New Phytologist*. **206**(2),pp.541–556.

Hou, G., Kramer, V.L., Wang, Y.-S., Chen, R., Perbal, G., Gilroy, S. and Blancaflor, E.B. 2004. The promotion of gravitropism in Arabidopsisroots upon actin disruption is coupled with the extended alkalinization of the columella cytoplasm and a persistent lateral auxin gradient. *The Plant Journal*. **39**(1),pp.113–125.

Iino, M., Tarui, Y. and Uematsu, C. 2005. Gravitropism of maize and rice coleoptiles: dependence on the stimulation angle. **19**(10),pp.1160–1168.

Iversen, T. and Rommelhoff, A. 1978. The starch statolith hypothesis and the interaction of amyloplasts and endoplasmic reticulum in root geotropism. *Journal of Experimental Botany*. **29**(113),pp.1319–1328.

Jenkins, M.T. and Gerhardt, F. 1931. *Gene Influencing The Composition Of The Culm In Maize*.

Jones, A.R., Kramer, E.M., Knox, K., Swarup, R., Bennett, M.J., Lazarus, C.M., Leyser, H.M.O. and Grierson, C.S. 2008. Auxin transport through non-hair cells sustains root-hair development. *Nature Cell Biology*. **11**(1),pp.78–84.

Jung, J. and McCouch, S. 2013. Getting to the roots of it: genetic and hormonal control of root architecture. *Frontiers in Plant Science*.

Kato, T. Morita, M., Fukaki, H., Yamauchi, Y., Uehara, M., Nihama, M., and Tasaka, M. 2002. SGR2, a Phospholipase-Like Protein, and ZIG/SGR4, a SNARE, Are Involved in the Shoot Gravitropism of Arabidopsis. *The Plant Cell Online*. **14**(1),pp.33–46.

Kepinski, S. 2007. The anatomy of auxin perception. *BioEssays*. **29**(10),pp.953–956.

Kepinski, S. and Leyser, O. 2005. The Arabidopsis F-box protein TIR1 is an auxin receptor. *Nature*. **435**,pp.446–451.

Kiss, J.Z., Wright, J.B. and Caspar, T. 1996. Gravitropism in roots of intermediate-starch mutants of Arabidopsis. *Physiologia Plantarum*. **97**(2),pp.237–244.

Kleine-Vehn, J., Dhonukshe, P., Sauer, M., Brewer, P.B., Wiśniewska, J., Paciorek, T., Benková, E. and Friml, J. 2008. ARF GEF-Dependent Transcytosis and Polar Delivery of PIN Auxin Carriers in Arabidopsis. *Current Biology*. **18**(7),pp.526–531.

Kleine-Vehn, J., Dhonukshe, P., Swarup, R., Bennett, M. and Friml, J. 2006. Subcellular Trafficking of the Arabidopsis Auxin Influx Carrier AUX1 Uses a Novel Pathway Distinct from PIN1. *The Plant Cell*. **18**(11),pp.3171–3181.

Kleine-Vehn, J., Huang, F., Naramoto, S., Zhang, J., Michniewicz, M., Offringa, R. and Friml, J. 2009. PIN auxin efflux carrier polarity is regulated by PINOID kinase-mediated recruitment into GNOM-independent trafficking in Arabidopsis. *The Plant Cell*. **21**(12),pp.3839–3849.

Kleine-Vehn, J., Leitner, J., Zwiewka, M., Sauer, M., Abas, L., Luschnig, C. and Friml, J. 2008. Differential degradation of PIN2 auxin efflux carrier by retromer-dependent vacuolar targeting. *Proceedings of the National Academy of Sciences*. **105**(46),pp.17812–17817.

Knight, T.A. 1806. On the direction of the radicle and germen during the vegetation of seeds. *Transactions of the Royal Society of London*. **96**,pp.99–108.

Korasick, D.A., Westfall, C.S., Lee, S.G., Nanao, M.H., Dumas, R., Hagen, G., Guilfoyle, T.J., Jez, J.M. and Strader, L.C. 2014. Molecular basis for AUXIN RESPONSE FACTOR protein interaction and the control of auxin response repression. *Proceedings of the National Academy of Sciences*. **111**(14),pp.5427–5432.

Ku, L., Wei, X., Zhang, S., Zhang, J., Guo, S. and Chen, Y. 2011. Cloning and characterization of a putative TAC1 ortholog associated with leaf angle in maize (Zea mays L.). *PLoS ONE*. **6**(6),p.e20621.

Kutschera, U. and Niklas, K.J. 2007. The epidermal-growth-control theory of stem elongation: An old and a new perspective. *Journal of Plant Physiology*. **164**(11),pp.1395–1409.

Landy, A. 1989. Dynamic, structural, and regulatory aspects of lambda site-specific recombination. *Annual review of biochemistry*. **58**,pp.913–949.

Larsen, P. 1969. The optimum angle of geotropic stimulation and its relation to the starch statolith hypothesis. *Physiologia Plantarum*. **22**(3),pp.469–488.

Lee, M.M. and Schiefelbein, J. 1999. WEREWOLF, a MYB-related protein in Arabidopsis, is a position-dependent regulator of epidermal cell patterning. *Cell*. **99**(5),pp.473–483.

Leitz, G., Kang, B.H., Schoenwaelder, M.E.A. and Staehelin, L.A. 2009. Statolith Sedimentation Kinetics and Force Transduction to the Cortical Endoplasmic Reticulum in Gravity-Sensing Arabidopsis Columella Cells. *The Plant Cell Online*. **21**(3),pp.843–860.

Liao, C.-Y., Smet, W., Brunoud, G., Yoshida, S., Vernoux, T. and Weijers, D. 2015. Reporters for sensitive and quantitative measurement of auxin response. **12**(3),pp.207–210.

Lincoln, C., Britton, J.H. and Estelle, M. 1990. Growth and development of the axr1 mutants of Arabidopsis. *The Plant Cell*. **2**(11),pp.1071–1080.

Lino, M. and Briggs, W.R. 1984. Growth distribution during first positive phototropic curvature of maize coleoptiles. *Plant, cell & environment*. **7**(2),pp.97–104.

Livak, K.J. and Schmittgen, T.D. 2001. Analysis of Relative Gene Expression Data Using Real-Time Quantitative PCR and the 2−ΔΔCT Method. *Methods*. **25**(4),pp.402–408.

Löfke, C., Luschnig, C. and Kleine-Vehn, J. 2013. Posttranslational modification and trafficking of PIN auxin efflux carriers. *Mechanisms of Development*. **130**(1),pp.82–94.

Löfke, C., Scheuring, D., Dünser, K., Schöller, M., Luschnig, C. and Kleine-Vehn, J. 2015. Tricho- and atrichoblast cell files show distinct PIN2 auxin efflux carrier exploitations and are jointly required for defined auxin-dependent root organ growth. *Journal of Experimental Botany*. **66**(16),pp.5103–5112.

Luschnig, C., Gaxiola, R.A. and Grisafi, P. 1998. EIR1, a root-specific protein involved in auxin transport, is required for gravitropism inArabidopsis thaliana. *Genes & Development*. **12**(14),pp.2175–2187.

Lynch, J.P. 2013. Steep, cheap and deep: an ideotype to optimize water and N acquisition by maize root systems. *Annals of Botany*. **112**(2),pp.347–357.

Marchant, A., Kargul, J., May, S.T., Muller, P., Delbarre, A., Perrot-Rechenmann, C. and Bennett, M.J. 1999. AUX1 regulates root gravitropism in Arabidopsis by facilitating auxin uptake within root apical tissues. *The EMBO Journal*. **18**(8),pp.2066–2073.

Men, S., Boutté, Y., Ikeda, Y., Li, X., Palme, K., Stierhof, Y.-D., Hartmann, M.-A., Moritz, T. and Grebe, M. 2008. Sterol-dependent endocytosis mediates post-cytokinetic acquisition of PIN2 auxin efflux carrier polarity. *Nature Cell Biology*. **10**(2),pp.237–244.

Michniewicz, M., Zago, M.K., Abas, L., Weijers, D., Schweighofer, A., Meskiene, I., Heisler, M.G., Ohno, C., Zhang, J., Huang, F., Schwab, R., Weigel, D., Meyerowitz, E.M., Luschnig, C., Offringa, R. and Friml, J. 2007. Antagonistic regulation of PIN phosphorylation by PP2A and PINOID directs auxin flux. *Cell*. **130**(6),pp.1044–1056.

Monshausen, G.B., Miller, N.D., Murphy, A.S. and Gilroy, S. 2010. Dynamics of auxin-dependent Ca2+ and pH signaling in root growth revealed by integrating high-resolution imaging with automated computer vision-based analysis. *The Plant Journal*. **65**(2),pp.309–318.

Moon, J., Parry, G., and Estelle, M. 2004. The Ubiquitin-Proteasome Pathway and Plant Development. *The Plant Cell Online*. **16**(12),pp.3181–3195.

Moore, R. 1985. Dimensions of root caps and columella tissues of primary roots of Ricinus communis characterised by differing degrees of graviresponsiveness. *Annals of Botany*. **55**,pp.375–380.

Morita, M.T. and Tasaka, M. 2004. Gravity sensing and signaling. *Current Opinion in Plant Biology*. **7**(6),pp.712–718.

Mravec, J., Skůpa, P., Bailly, A., Hoyerová, K., Křeček, P., Bielach, A., Petrášek, J., Zhang, J., Gaykova, V., Stierhof, Y.-D., Dobrev, P.I., Schwarzerová, K., Rolčík, J., Seifertová, D., Luschnig, C., Benková, E., Zažímalová, E., Geisler, M. and Friml, J. 2009. Subcellular homeostasis of phytohormone auxin ismediated by the ER-localised PIN5 transporter. *Nature*. **459**(7250),pp.1136–1140.

Mullen, J.L., Wolverton, C., Ishikawa, H. and Evans, M.L. 2000. Kinetics of constant gravitropic stimulus responses in Arabidopsis roots using a feedback system. *Plant Physiology*. **123**(2),pp.665–670.

Müller, A., Guan, C., Gälweiler, L., Tänzler, P., Huijser, P., Marchant, A., Parry, G., Bennett, M., Wisman, E. and Palme, K. 1998. AtPIN2 defines a locus of Arabidopsis for root gravitropism control. *The EMBO Journal*. **17**(23),pp.6903–6911.

Nelson, B.K., Cai, X. and Nebenführ, A. 2007. A multicolored set of in vivo organelle markers for co-localisation studies in Arabidopsis and other plants. *The Plant Journal : for cell and molecular biology*. **51**(6),pp.1126–1136.

Oh, E., Zhu, J.-Y., Bai, M.-Y., Arenhart, R.A., Sun, Y. and Wang, Z.-Y. 2014. Author response. *eLife*. **3**,p.601.

Okada, K., Ueda, J., Komaki, M.K., Bell, C.J. and Shimura, Y. 1991. Requirement of the Auxin Polar Transport System in Early Stages of Arabidopsis Floral Bud Formation. *The Plant Cell*. **3**(7),pp.677–684.

Okushima Y, Overvoorde P., Arima K., Alonso J., Chan A., Chang C., Ecker J., Hughes B., Lui A., Nguyen D., Onodera C., Quach H., Smith A., Yu G., and Theologis A. 2005. Functional genomic analysis of the AUXIN RESPONSE FACTOR gene family members in Arabidopsis thaliana: unique and overlapping functions of ARF7 and ARF19. *The Plant Cell* 17(2):444–463.

Okushima, Y., Fukaki, H., Onoda, M., Theologis, A. and Tasaka, M. 2007. ARF7 and ARF19 Regulate Lateral Root Formation via Direct Activation of LBD/ASL Genes in Arabidopsis. *The Plant Cell*. **19**(1),pp.118–130.

Omelyanchuk, N.A., Kovrizhnykh, V.V., Oshchepkova, E.A., Pasternak, T., Palme, K. and Mironova, V.V. 2016. A detailed expression map of the PIN1 auxin transporter in Arabidopsis thaliana root. *BMC Plant Biology*.pp.1–12.

Orbovic, V. and Poff, K.L. 1993. Growth Distribution during Phototropism of Arabidopsis thaliana Seedlings. *Plant Physiology*. **103**(1),pp.157–163.

Ottenschläger, I., Wolff, P., Wolverton, C., Bhalerao, R.P., Sandberg, G., Ishikawa, H., Evans, M. and Palme, K. 2003. Gravity-regulated differential auxin transport from columella to lateral root cap cells. *Proceedings of the National Academy of Sciences of the United States of America*. **100**(5),pp.2987–2991.

Ouellet, F., Overvoorde, P.J. and Theologis, A. 2001. IAA17/AXR3: biochemical insight into an auxin mutant phenotype. *The Plant Cell*. **13**(4),pp.829–841.

Paciorek, T., Zažímalová, E., Ruthardt, N., Petrášek, J., Stierhof, Y.-D., Kleine-Vehn, J., Morris, D.A., Emans, N., Jürgens, G., Geldner, N. and Friml, J.R.Í. 2005. Auxin inhibits endocytosis and promotes its own efflux from cells. *Nature Cell Biology*. **435**(7046),pp.1251–1256.

Parry, G., Calderon-Villalobos, L.I., Prigge, M., Peret, B., Dharmasiri, S., Itoh, H., Lechner, E., Gray, W.M., Bennett, M. and Estelle, M. 2009. Complex regulation of the TIR1/AFB family of auxin receptors. *Proceedings of the National Academy of Sciences of the United States of America*. **106**(52),pp.22540–22545.

Perbal, G. 1974. L'action des statolithes dans la reponse geotropique des racines de Lens culinaris. *Planta*. **116**(2),pp.153–171.

Petrasek, J. and Friml, J. 2009. Auxin transport routes in plant development. *Development*. **136**(16),pp.2675–2688.

Pickett, F.B., Wilson, A.K. and Estelle, M. 1990. The aux1 Mutation of

Arabidopsis Confers Both Auxin and Ethylene Resistance. *Plant Physiology*. **94**(3),pp.1462–1466.

Pierik, R. and Testerink, C. 2014. The Art of Being Flexible: How to Escape from Shade, Salt, and Drought. *Plant Physiology*. **166**(1),pp.5–22.

Rakusová, H., Gallego-Bartolomé, J., Vanstraelen, M., Robert, H.S., Alabadí, D., Blazquez, M.A., Benková, E. and Friml, J. 2011. Polarization of PIN3-dependent auxin transport for hypocotyl gravitropic response in Arabidopsis thaliana. *The Plant Journal*. **67**(5),pp.817–826.

Rosquete, M.R., Wangenheim, von, D., Marhavý, P., Barbez, E., Stelzer, E.H.K., Benková, E., Maizel, A. and Kleine-Vehn, J. 2013. An Auxin Transport Mechanism Restricts Positive Orthogravitropism in Lateral Roots. *Current Biology*. **23**(9),pp.817–822.

Rouse, D., Mackay, P., Stirnberg, P., Estelle, M. and Leyser, O. 1998. Changes in auxin response from mutations in an AUX/IAA gene. *Science*. **279**(5355),pp.1371–1373.

Roychoudhry, S., Del Bianco, M., Kieffer, M. and Kepinski, S. 2013. Auxin Controls Gravitropic Setpoint Angle in Higher Plant Lateral Branches. *Current Biology*. **23**(15),pp.1497–1504.

Sachs, J. Vorlesungen über Pflanzen-Physiologie. 1882. W. Engelmann Leipzig.

Sachs, T. 1981. The Control of the Patterned Differentiation of Vascular Tissues *In*: H. W. Woolhouse, ed. *Advances in Botanical Research*. Advances in Botanical Research. Advances in Botanical Research, pp. 151–262.

Sack, F.D., MM, S. and AC, L. 1985. Amyloplast sedimentation kinetics in gravistimulated maize roots. *Planta*. **165**,pp.295–300.

Saito, C., Morita, M.T., Kato, T., and Tasaka, M. 2005. Amyloplasts and Vacuolar Membrane Dynamics in the Living Graviperceptive Cell of the Arabidopsis Inflorescence Stem. *The Plant Cell*. **17**(2),pp.548–558.

Santos Maraschin, dos, F., Memelink, J. and Offringa, R. 2009. Auxin-induced, SCF TIR1-mediated poly-ubiquitination marks AUX/IAA proteins for degradation. *The Plant Journal*. **59**(1),pp.100–109.

Sasaki, S. and Yamamoto, K.T. 2015. Arabidopsis LAZY1 is a peripheral membrane protein of which the carboxy-terminal fragment potentially interacts with microtubules. *Plant Biotechnology*. **32**(1),pp.103–108.

Sato, A., Sasaki, S., Matsuzaki, J. and Yamamoto, K.T. 2014. Light-dependent gravitropism and negative phototropism of inflorescence stems in a dominant Aux/IAA mutant of Arabidopsis thaliana, axr2. *Journal of Plant Research*. **127**(5),pp.627–639.

Sato, E.M., Hijazi, H., Bennett, M.J., Vissenberg, K. and Swarup, R. 2015. New insights into root gravitropic signalling. *Journal of Experimental Botany*. **66**(8),pp.2155–2165.

Sauer, M., Balla, J., Luschnig, C., Wisniewska, J., Reinohl, V., Friml, J. and Benkova, E. 2006. Canalization of auxin flow by Aux/IAA-ARF-dependent feedback regulation of PIN polarity. *Genes & Development*. **20**(20),pp.2902–2911.

Scarpella, E., Barkoulas, M. and Tsiantis, M. 2010. Control of Leaf and Vein Development by Auxin. *Cold Spring Harbor Perspectives in Biology*. **2**(1),pp.a001511–a001511.

Schellmann, S., Schnittger, A., Kirik, V., Wada, T., Okada, K., Beermann, A., Thumfahrt, J., Jurgens, G. and Hülskamp, M. 2002. TRIPTYCHON and CAPRICE mediate lateral inhibition during trichome and root hair patterning in Arabidopsis. *The EMBO Journal*. **21**(19),pp.5036–5046.

Scott, A.C. and Allen, N.S. 1999. Changes in cytosolic pH within Arabidopsis root columella cells play a key role in the early signaling pathway for root gravitropism. *Plant Physiology*. **121**(4),pp.1291–1298.

Sessions, A., Weigel, D. and Yanofsky, M.F. 1999. The Arabidopsis thaliana MERISTEM LAYER 1 promoter specifies epidermal expression in meristems and young primordia. *The Plant journal : for cell and molecular biology*. **20**(2),pp.259–263.

Sieberer, T., Seifert, G.J., Hauser, M.T., Grisafi, P. and Fink, G.R. 2000. Post-transcriptional control of the Arabidopsis auxin efflux carrier EIR1 requires AXR1. *Current Biology*. **10**(24),pp.1595–1598.

Staves, M.P., Wayne, R. and Leopold, A.C. 1992. Hydrostatic pressure mimics gravitational pressure in characean cells. *Protoplasma*. **168**(3-4),pp.141–152.

Staves, M.P., Wayne, R. and Leopold, A.C. 1997. The effect of the external medium on the gravitropic curvature of rice (Oryza sativa, Poaceae) roots. *American Journal of Botany*. **84**(11),pp.1522–1529.

Steinmann, T., Geldner, N., Grebe, M., Mangold, S., Jackson, C.L., Paris, S., Gälweiler, L., Palme, K. and Jurgens, G. 1999. Coordinated polar localisation of auxin efflux carrier PIN1 by GNOM ARF GEF. *Science*. **286**(5438),pp.316–318.

Suh, M.C., Samuels, A.L., Jetter, R., Kunst, L., Pollard, M., Ohlrogge, J., and Beisson, F. 2005. Cuticular Lipid Composition, Surface Structure, and Gene Expression in Arabidopsis Stem Epidermis. *Plant Physiology*. **139**(4),pp.1649–1665.

Sukumar, P., Edwards, K.S., Rahman, A., DeLong, A. and Muday, G.K. 2009. PINOID Kinase Regulates Root Gravitropism through Modulation

of PIN2-Dependent Basipetal Auxin Transport in Arabidopsis. *Plant Physiology*. **150**(2),pp.722–735.

Swarup, K., Benková, E., Swarup, R., Casimiro, I., Péret, B., Yang, Y., Parry, G., Nielsen, E., De Smet, I., Vanneste, S., Levesque, M.P., Carrier, D., James, N., Calvo, V., Ljung, K., Kramer, E., Roberts, R., Graham, N., Marillonnet, S., Patel, K., Jones, J.D.G., Taylor, C.G., Schachtman, D.P., May, S., Sandberg, G., Benfey, P., Friml, J., Kerr, I., Beeckman, T., Laplaze, L. and Bennett, M.J. 2008. The auxin influx carrier LAX3 promotes lateral root emergence. *Nature Cell Biology*. **10**(8),pp.946–954.

Swarup, R., Friml, J., Marchant, A., Ljung, K., Sandberg, G., Palme, K. and Bennett, M. 2001. Localisation of the auxin permease AUX1 suggests two functionally distinct hormone transport pathways operate in the Arabidopsis root apex. *Genes & Development*. **15**(20),pp.2648–2653.

Swarup, R., Kramer, E.M., Perry, P., Knox, K., Leyser, H.M.O., Haseloff, J., Beemster, G.T.S., Bhalerao, R. and Bennett, M.J. 2005. Root gravitropism requires lateral root cap and epidermal cells for transport and response to a mobile auxin signal. *Nature Cell Biology*. **7**(11),pp.1057–1065.

Szemenyei, H., Hannon, M. and Long, J.A. 2008. TOPLESS Mediates Auxin-Dependent Transcriptional Repression During Arabidopsis Embryogenesis. *Science*. **319**(5868),pp.1384–1386.

Tan, X., Calderon-Villalobos, L.I.A., Sharon, M., Zheng, C., Robinson, C.V., Estelle, M. and Zheng, N. 2007. Mechanism of auxin perception by the TIR1 ubiquitin ligase. *Nature*. **446**(7136),pp.640–645.

Tanaka, H., Kitakura, S., De Rycke, R., DenbspGroodt, R. and Friml, J. 2009. Fluorescence Imaging-Based Screen Identifies ARF GEF Componentof Early Endosomal Trafficking. *Current Biology*. **19**(5),pp.391–397.

Teale, W.D., Paponov, I.A. and Palme, K. 2006. Auxin in action: signalling, transport and the control of plant growth and development. *Nature Reviews Molecular Cell Biology*. **7**(11),pp.847–859.

Thimann, K.V. 1939. Auxins and the inhibition of plant growth. *Biological Reviews*.

Thimann, K.V. 1956. Promotion and inhibition: twin themes of physiology. *American Naturalist*.pp.145–162.

Tiwari, S.B., Hagen, G. and Guilfoyle, T. 2003. The roles of auxin response factor domains in auxin-responsive transcription. *The Plant Cell*. **15**(2),pp.533–543.

Tiwari, S.B., Wang, X.J., Hagen, G. and Guilfoyle, T.J. 2001. AUX/IAA

proteins are active repressors, and their stability and activity are modulated by auxin. *The Plant Cell*. **13**(12),pp.2809–2822.

Toyota, M., Furuichi, T., Sokabe, M. and Tatsumi, H. 2013. Analyses of a Gravistimulation-Specific Ca2+ Signature in Arabidopsis using Parabolic Flights. *Plant Physiology*. **163**(2),pp.543–554.

Uga, Y., Okuno, K. and Yano, M. 2011. Dro1, a major QTL involved in deep rooting of rice under upland field conditions. *Journal of Experimental Botany*. **62**(8),pp.2485–2494.

Ulmasov, T., Hagen, G. and Guilfoyle, T.J. 1999. Activation and repression of transcription by auxin-response factors. *Proceedings of the National Academy of Sciences of the United States of America*. **96**(10),pp.5844–5849.

Ulmasov, T., Hagen, G. and Guilfoyle, T.J. 1997. ARF1, a transcription factor that binds to auxin response elements. *Science*. **276**(5320),pp.1865–1868.

van der Weele, C.M., Jiang, H.S., Palaniappan, K.K., Ivanov, V.B., Palaniappan, K., and Baskin, T.I. 2003. A New Algorithm for Computational Image Analysis of Deformable Motion at High Spatial and Temporal Resolution Applied to Root Growth. Roughly Uniform Elongation in the Meristem and Also, after an Abrupt Acceleration, in the Elongation Zone. *Plant Physiology*. **132**(3),pp.1138–1148.

Van Overbeek, J. 1936. “LAZY,” An a-geotropic form of maize “gravitational indifference” rather than structural weakness accounts for prostrate growth-habit of this form. *Journal of Heredity*. **27**(3),pp.93–97.

Vieten, A., Sauer, M., Brewer, P.B. and Friml, J. 2007. Molecular and cellular aspects of auxin-transport-mediated development. *Trends in plant science*. **12**(4),pp.160–168.

Vieten, A., Vanneste, S., Wisniewska, J., Benkova, E., Benjamins, R., Beeckman, T., Luschnig, C. and Friml, J. 2005. Functional redundancy of PIN proteins is accompanied by auxin-dependentcross-regulation of PIN expression. *Development*. **132**(20),pp.4521–4531.

Viotti, C., Bubeck, J., Stierhof, Y.-D., Krebs, M., Langhans, M., van den Berg, W., van Dongen, W., Richter, S., Geldner, N., Takano, J., Jürgens, G., de Vries, S.C., Robinson, D.G. and Schumacher, K. 2010. Endocytic and Secretory Traffic in ArabidopsisMerge in the Trans-Golgi Network/Early Endosome, an Independent and Highly Dynamic Organelle. *The Plant Cell*. **22**(4),pp.1344–1357.

Wang, H-Z., Yang K-Z., Zou J-J., Zhu L-L., Xie Z.D., Morita M.T., Tasaka M, Friml J, Grotewold E, Beeckman T, Vanneste S, Sack F, and Le J. 2015. Transcriptional regulation of PIN genes by FOURLIPS and MYB88

during Arabidopsis rootgravitropism. *Nature Communications* 6:1–9.

Wang, J-W., Wang, L-J., Mao, Y-B., Cai, W-J., Xue, H-W., and Chen, X-Y. 2005. Control of root cap formation by MicroRNA-targeted auxin response factors in Arabidopsis. *The Plant Cell* 17(8):2204–2216.

Weijers, D. and Wagner, D. 2016. Transcriptional Responses to the Auxin Hormone. *Annual Review of Plant Biology*. **67**(1),pp.539–574.

Went, F.W. and Thimann, K.V. 1937. *Phytohormones.* MacMillan. New York.

Willemsen, V., Friml, J., Grebe, M., van den Toorn, A., Palme, K., and Scheres, B. 2003. Cell Polarity and PIN Protein Positioning in Arabidopsis Require STEROL METHYLTRANSFERASE1 Function. *The Plant Cell Online*. **15**(3),pp.612–625.

Willige, B.C. and Chory, J. 2015. A current perspective on the role of AGCVIII kinases in PIN-mediated apical hook development. *Frontiers in Plant Science*. **6**(767),pp.1–7.

Willige, B.C., Ahlers, S., Zourelidou, M., Barbosa, I.C.R., Demarsy, E., Trevisan, M., Davis, P.A., Roelfsema, M.R.G., Hangarter, R., Fankhauser, C. and Schwechheimer, C. 2013. D6PK AGCVIII Kinases Are Required for Auxin Transport and Phototropic Hypocotyl Bending in Arabidopsis. *The Plant Cell*. **25**(5),pp.1674–1688.

Wilson, A.K., Pickett, F.B., Turner, J.C. and Estelle, M. 1990. A dominant mutation in Arabidopsis confers resistance to auxin, ethylene and abscisic acid. *Molecular & general genetics : MGG*. **222**(2-3),pp.377–383.

Wisniewska, J., Xu, J., Seifertová, D., Brewer, P.B., Ruzicka, K., Blilou, I., Rouquié, D., Benková, E., Scheres, B., and Friml, J. 2006. Polar PIN Localisation Directs Auxin Flow in Plants. *Science*. **312**(5775),pp.883–883.

Wolverton, C., Paya, A.M. and Toska, J. 2011. Root cap angle and gravitropic response rate are uncoupled in the Arabidopsis pgm-1 mutant. *Physiologia Plantarum*. **141**(4),pp.373–382.

Wysocka-Diller, J.W., Helariutta, Y., Fukaki, H., Malamy, J.E. and Benfey, P.N. 2000. Molecular analysis of SCARECROW function reveals a radial patterning mechanism common to root and shoot. *Development*. **127**(3),pp.595–603.

Yang, H. and Murphy, A.S. 2009. Functional expression and characterization of Arabidopsis ABCB, AUX 1 and PIN auxin transporters in Schizosaccharomyces pombe. *The Plant Journal*. **59**(1),pp.179–191.

Yoshihara, T., Spalding, E.P. and Iino, M. 2013. AtLAZY1 is a signaling component required for gravitropism of the Arabidopsis thaliana

inflorescence. *The Plant Journal*. **74**(2),pp.267–279.

Yu, B., Lin, Z., Li, H., Li, X., Li, J., Wang, Y., Zhang, X., Zhu, Z., Zhai, W., Wang, X., Xie, D. and Sun, C. 2007. TAC1, a major quantitative trait locus controlling tiller angle in rice. *The Plant Journal*. **52**(5),pp.891–898.

Zazimalova, E., Křeček, P., Skůpa, P., Hoyerova, K. and Petrasek, J. 2007. Polar transport of the plant hormone auxin – the role of PIN-FORMED (PIN) proteins. *Cellular and Molecular Life Sciences*. **64**(13),pp.1621–1637.

Zazimalova, E., Murphy, A.S., Yang, H., Hoyerova, K. and Hosek, P. 2010. Auxin Transporters--Why So Many? *Cold Spring Harbor Perspectives in Biology*. **2**,p.a001552.

Zhang, J., Nodzynski, T., Pencik, A., Rolcik, J. and Friml, J. 2010. PIN phosphorylation is sufficient to mediate PIN polarity and direct auxin transport. *Proceedings of the National Academy of Sciences*. **107**(2),pp.918–922.

Zourelidou, M., Absmanner, B., Weller, B., Barbosa, I.C., Willige, B.C., Fastner, A., Streit, V., Port, S.A., Colcombet, J., la Fuente van Bentem, de, S., Hirt, H., Kuster, B., Schulze, W.X., Hammes, U.Z. and Schwechheimer, C. 2014. Auxin efflux by PIN-FORMED proteins is activated by two different protein kinases, D6 PROTEIN KINASE and PINOID. *eLife*. **3**(0),p.e02860.